

Dynamics and Control of Electric Power Systems

Lectures 35–528, ITET ETH

Göran Andersson
EEH - Power Systems Laboratory
ETH Zürich

March 2003



Eidgenössische Technische Hochschule Zürich
Swiss Federal Institute of Technology Zurich

Contents

Preface	v
1 Introduction	1
1.1 Control Theory Basics - A Review	2
1.1.1 Simple Control Loop	2
1.1.2 State Space Formulation	5
1.2 Control of Electric Power Systems	5
2 Frequency Control in Electric Power Systems	9
2.1 System Model	9
2.2 Model of Frequency Control	12
2.2.1 Frequency Dependency of Loads	13
3 Primary Frequency Control	17
3.1 Introduction	17
3.2 Turbine Control	22
3.2.1 Turbine Models	22
3.2.2 Turbine Controllers	31
3.3 Role of Speed Droop	33
4 Load Frequency Control	41
4.1 Automatic Generation Control - Static Model	41
4.2 Dynamic Model	44
4.2.1 One Node System	44
4.2.2 Two Area System	52
5 Model of the Synchronous Machine	57
5.1 Park's Transformation	57
5.2 The Inductances of the Synchronous Machine	61
5.3 Voltage Equations for the Synchronous Machine	63
5.4 Synchronous, Transient, and Subtransient Inductances, and Time Constants.	66
5.5 Simplified Models of the Synchronous Machine	71

6	The Excitation System of the Synchronous Machine	75
6.1	Construction of the Excitation System	75
6.2	Compensation Equipment	76
6.3	DC Excitation Systems	77
6.4	AC Excitation Systems	78
6.5	Static Excitation Systems	78
7	Damping in Power Systems	81
7.1	General	81
7.2	Causes of Damping	82
7.3	Methods to Increase Damping	83
8	Load Modelling	85
8.1	The Importance of the Loads for System Stability	85
8.2	Load Models	86
8.2.1	Static Load Models	86
8.2.2	Motor Loads	87
8.2.3	Equivalent Dynamic Loads	88
	References	91
A	Connection between per unit and SI Units for the Swing Equation	93
B	Influence of Rotor Oscillations on the Curve Shape	95

Preface

These lectures notes are intended to be used in the *Systemdynamik und Leittechnik der elektrischen Energieversorgung* (Vorlesungsnummer ETH Zürich 35-528) lectures given at ETH in the eighth semester in electrical engineering.

The main topic covered is frequency control in power systems. The needed models are derived and the primary and secondary frequency control are studied. A detailed model of the synchronous machine, based on Park's transformation, is also included. The excitation and voltage control of synchronous machines are briefly described. An overview of load models are also given.

Zürich in March 2003

Göran Andersson

1

Introduction

In this chapter a general introduction to power systems control is given. Some basic results from control theory are reviewed, and an overview of the use of different kinds of power plants in a system is given.

The main topics of these lectures will be

- Power system dynamics
- Power system control
- Security and operational efficiency.

In order to study and discuss these issues the following tools are needed

- Control theory (particularly for linear systems)
- Modelling
- Simulation
- Communication technology.

The studied system comprises the subsystems *Electricity Generation, Transmission, Distribution, and Consumption (Loads)*, and the associated control system has a hierarchic structure. This means that the control system consists of a number of nested control loops that control different quantities in the system. In general the control loops on lower system levels, e.g. locally in a generator, are characterized by smaller time constants than the control loops active on a higher system level. As an example, the *Automatic Voltage Regulator (AVR)*, which regulates the voltage of the generator terminals to the reference (set) value, responds typically in a time scale of a second or less, while the *Secondary Voltage Control*, which determines the reference values of the voltage controlling devices, among which the generators, operates in a time scale of tens of seconds or minutes. That means that these two control loops are virtually de-coupled. This is also generally true for other controls in the systems, resulting in a number of de-coupled control loops operating in different time scales. A schematic diagram showing the different time scales is shown in Figure 1.1.

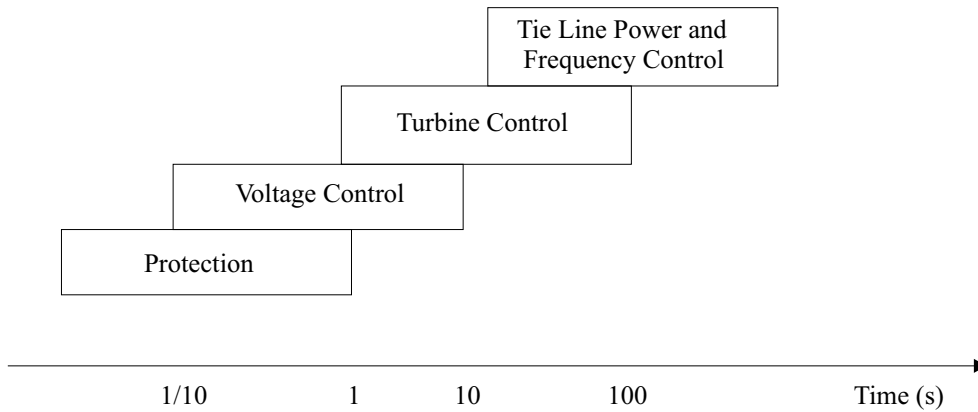


Figure 1.1. Schematic diagram of different time scales of power system controls.

The overall control system is very complex, but due to the de-coupling it is in most cases possible to study the different control loops individually. This facilitates the task, and with appropriate simplifications one can quite often use classical standard control theory methods to analyse these controllers. For a more detailed analysis, one has usually to resort to computer simulations.

A characteristic of a power system is that the load, i.e. the electric power consumption, varies significantly over the day and over the year. This consumption is normally uncontrolled. Furthermore, since substantial parts of the system is exposed to external disturbances, the possibility that lines etc. could be disconnected due to faults must be taken into account. The task of the different control systems of the power system is to keep the power system within acceptable operating limits such that security is maintained and that the quality of supply, e.g. voltage magnitudes and frequency, is within specified limits. In addition, the system should be operated in an economically efficient way. This has resulted in a hierarchical control system structure as shown in Figure 1.2.

1.1 Control Theory Basics - A Review

The de-coupled control loops described above can be analyzed by standard methods from the control theory. Just to refresh some of these concepts, and to explain the notation to be used, a very short review is given here.

1.1.1 Simple Control Loop

The control system in Figure 1.3 is considered. In this figure the block $G(s)$ represents the controlled plant and also possible controllers. From this figure

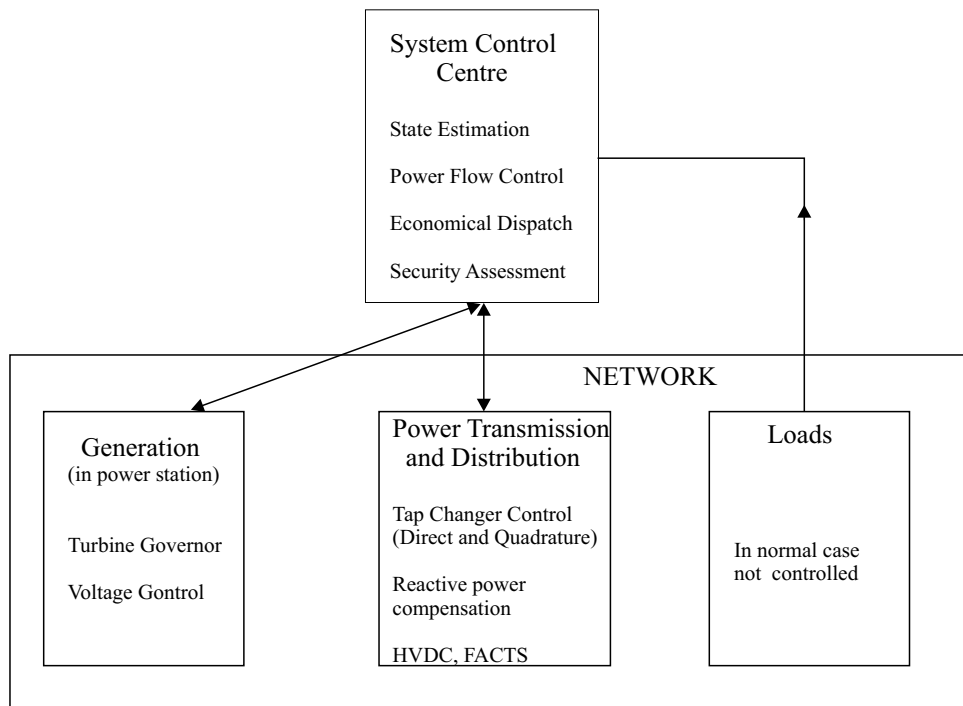


Figure 1.2. The structure of the hierarchical control systems of a power system.

the following quantities are defined ¹ :

- $r(t)$ = Reference (set) value (input)
- $e(t)$ = Control error
- $y(t)$ = Controlled quantity (output)
- $v(t)$ = Disturbance

Normally the controller is designed assuming that the disturbance is equal to zero, but to verify the robustness of the controller realistic values of v must be considered.

In principle two different problems are solved in control theory:

1. Regulating problem
2. Tracking problem

¹Here the quantities in the time domain are denoted by small letters, while the Laplace transformed corresponding quantities are denoted by capital letters. In the following this convention is not always adhered to, but it should be clear from the context if the quantity is expressed in the time or the s domain.

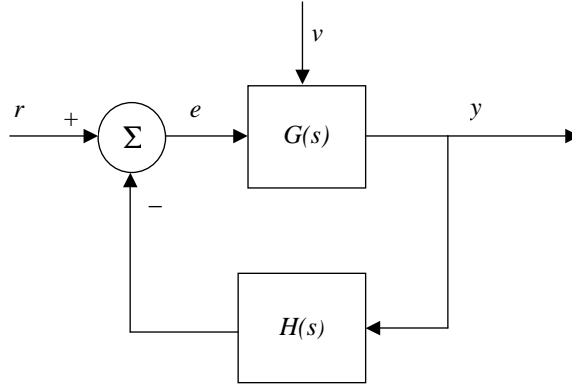


Figure 1.3. Simple control system with control signals.

In the regulating problem, the reference value r is normally kept constant and the task is to keep the output close to the reference value even if disturbances occur in the system. This is the most common problem in power systems, where the voltage, frequency and other quantities should be kept at the desired values irrespective of load variations, line switchings, etc.

In the tracking problem the task is to control the system so that the output y follows the time variation of the input r as good as possible. This is sometimes also called the servo problem.

The transfer function from the input, R , to the output, Y , is given by (in Laplace transformed quantities)

$$F(s) = \frac{Y(s)}{R(s)} = \frac{C(s)}{R(s)} = \frac{G(s)}{1 + G(s)H(s)} \quad (1.1)$$

In many applications one is not primarily interested in the detailed time response of a quantity after a disturbance, but rather the value direct after the disturbance or the stationary value when all transients have decayed. Then the two following properties of the Laplace transform are important:

$$g(t \rightarrow 0+) = \lim_{s \rightarrow \infty} sG(s) \quad (1.2)$$

and

$$g(t \rightarrow \infty) = \lim_{s \rightarrow 0} sG(s) \quad (1.3)$$

where G is the Laplace transform of g . If the input is a step function, Laplace transform = $1/s$, and $F(s)$ is the transfer function, the initial and stationary response of the output would be

$$y(t \rightarrow 0+) = \lim_{s \rightarrow \infty} F(s) \quad (1.4)$$

and

$$y(t \rightarrow \infty) = \lim_{s \rightarrow 0} F(s) \quad (1.5)$$

1.1.2 State Space Formulation

A linear and time-invariant controlled system is defined by the equations

$$\begin{cases} \dot{x} &= Ax + Bu \\ y &= Cx + Du \end{cases} \quad (1.6)$$

The vector $x = (x_1 \ x_2 \ \dots \ x_n)^T$ contains the states of the system, which uniquely describe the system. The vector u has the inputs as components, and the vector y contains the outputs as components. The matrix A , of dimension $n \times n$, is the system matrix of the uncontrolled system. The matrices B , C , and D depend on the design of the controller and the available outputs. In most realistic cases $D = 0$, which means that there is zero feedthrough, and the system is said to be strictly proper. The matrices A and B define which states that are controllable, and the matrices A and C which states that are the observable. A controller using the outputs as feedback signals can be written as $u = -Ky = -KCx$, assuming $D = 0$, where the matrix K defines the feedback control, the controlled system becomes

$$\dot{x} = (A - BKC)x \quad (1.7)$$

1.2 Control of Electric Power Systems

The overall control task in an electric power system is to maintain the balance between the electric power produced by the generators and the power consumed by the loads, including the network losses, at all time instants. If this balance is not kept, this will lead to frequency deviations that if too large will have serious impacts on the system operation. A complication is that the electric power consumption varies both in the short and in the long time scales. In the long time scale, over the year, the peak loads of a day are in countries with cold and dark winters higher in the winter, so called winter peak, while countries with very hot summers usually have their peak loads in summer time, summer peak. Examples of the former are most European countries, and of the latter Western and Southern USA. The consumption vary also over the day as shown in Figure 1.4. Also in the short run the load fluctuates around the slower variations shown in Figure 1.4, so called spontaneous load variations.

In addition to keeping the above mentioned balance, the delivered electricity must conform to certain quality criteria. This means that the *voltage magnitude*, *frequency*, and *wave shape* must be controlled within specified limits.

If a change in the load occurs, this is in the first step compensated by the kinetic energy stored in the rotating parts, rotor and turbines, of the

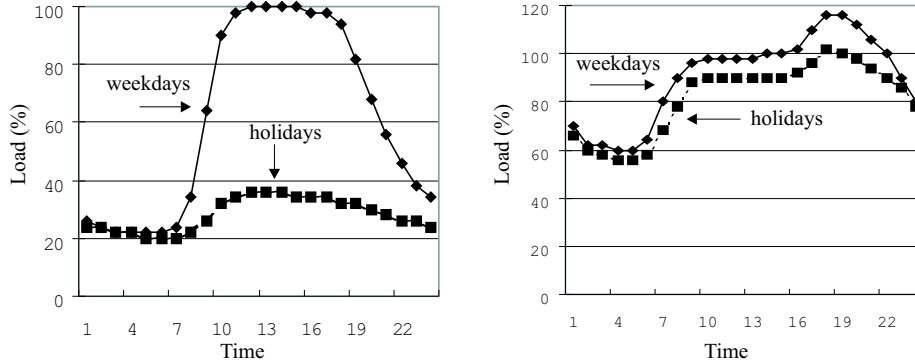


Figure 1.4. Typical load variations over a day. Left: Commercial load.; Right: Residential load.

generators resulting in a frequency change. If this frequency change is too large, the power supplied from the generators must be changed, which is done through the *frequency control* of the generators in operation. An unbalance in the generated and consumed power could also occur as a consequence of that a generating unit is tripped due to a fault. The task of the frequency control is to keep the frequency deviations within acceptable limits during these events.

To cope with the larger variations over the day and over the year generating units must be switched in and off according to needs. Plans regarding which units should be on line during a day are done beforehand based on *load forecasts*². Such a plan is called *unit commitment*. When doing such a plan, economic factors are essential, but also the time it takes to bring a generator on-line from a state of standstill. For hydro units and gas turbines this time is typically of the order of some minutes, while for thermal power plants, conventional or nuclear, it usually takes several hours to get the unit operational. This has an impact on the unit commitment and on the planning of reserves in the system³.

Depending on how fast power plants can be dispatched, they are classified as peak load, intermediate load, or base load power plants. This classification is based on the time it takes to activate the plants and on the

²With the methods available today one can make a load forecast a day ahead which normally has an error that is less than a few percent.

³In a system where only one company is responsible for the power generation, the unit commitment was made in such a way that the generating costs were minimized. If several power producers are competing on the market, liberalized electricity market, the situation is more complex. The competing companies are then bidding into different markets, pool, bi-lateral, etc, and a simple cost minimizing strategy could not be applied. But also in these cases a unit commitment must be made, but after other principles.

fuel costs and is usually done as below⁴. The classification is not unique and might vary slightly from system to system.

- **Peak load units**, operational time 1000–2000 h/a
 - Hydro power plants with storage
 - Pumped storage hydro power plants
 - Gas turbine power plants
- **Intermediate load units**, operational time 3000–4000 h/a
 - Fossil fuel thermal power plants
 - Bio mass thermal power plants
- **Base load units**, operational time 5000–6000 h/a
 - Run of river hydro power plants
 - Nuclear power plants

In Figure 1.5 the use of different power plants is shown in a load duration curve representing one years operation.

The overall goal of the unit commitment and the economic dispatch is the

- Minimization of costs over the year
- Minimization of fuel costs and start/stop costs

⁴The fuel costs should here be interpreted more as the “value” of the fuel. For a hydro power plant the “fuel” has of course no cost *per se*. But if the hydro plant has a storage with limited capacity, it is obvious that the power plant should be used during high load conditions when generating capacity is scarce. This means that the “water value” is high, which can be interpreted as a high fuel cost.

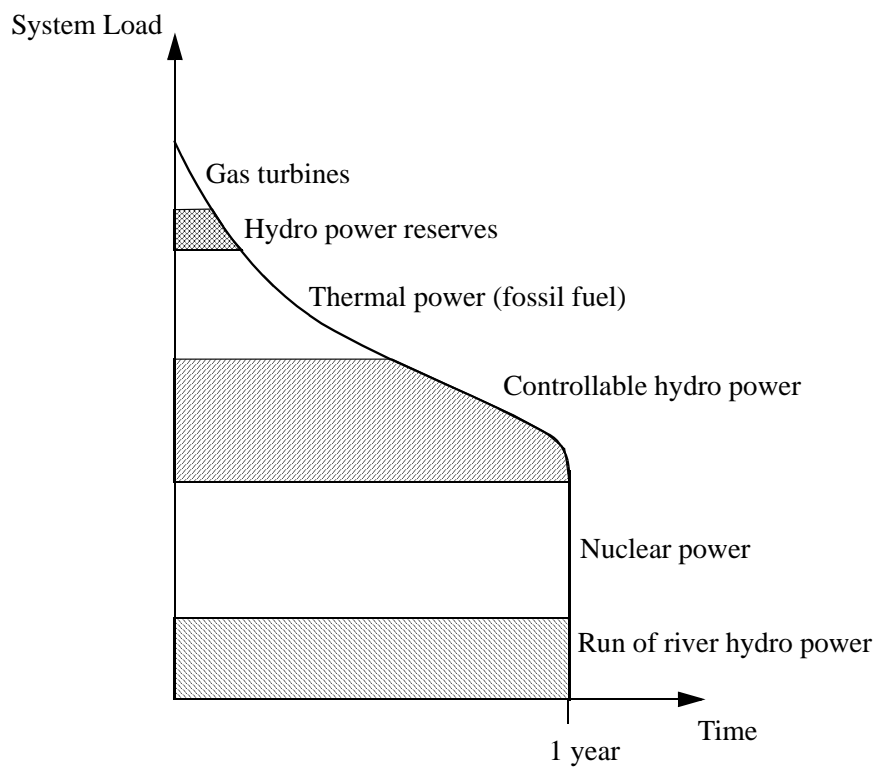


Figure 1.5. Duration curve showing the use of different kinds of power plants.

2

Frequency Control in Electric Power Systems

In this chapter, a model that can be used for studying frequency variations following a disturbance, like generator or load tripping, in an electric power system is developed. Models for the frequency dependency of loads are discussed.

2.1 System Model

It was discussed in chapter 1 that the system's frequency will deviate from the desired (or nominal) frequency if the balance between power generation and load consumption (including losses) is not maintained. Since the swing equations constitute a general model of the movement of the generators' rotors, these equations can be used for studying the variation of the system frequency.

After a disturbance, like loss of production, in the system, the frequency in different parts of the system will vary according to Figure 2.1. The frequencies of the different machines can be viewed as comparatively small variations over an average frequency in the system. This average frequency, called the system frequency in the following, is the frequency that can be defined for the so-called centre of inertia (COI) of the system.

We want to derive a model that is valid for reasonable frequency deviations, the exact version of swing equation will be used, i.e.

$$\Delta\dot{\omega}_i = \frac{\omega_0}{2H_i}(T_{mi}(p.u.) - T_{ei}(p.u.)) , \quad (2.1)$$

with the usual notation. The indices m and e denote mechanical (turbine) and electrical quantities respectively. $\Delta\omega_i$ is used here to denote the deviation in rotor angular frequency as compared with the nominal one ω_0 . (For rotor oscillations the frequency of $\Delta\omega_i$ is often of interest, while the amplitude of $\Delta\omega_i$ is the main concern in frequency control.) By extending the right hand side with the actual angular frequency and expressing the

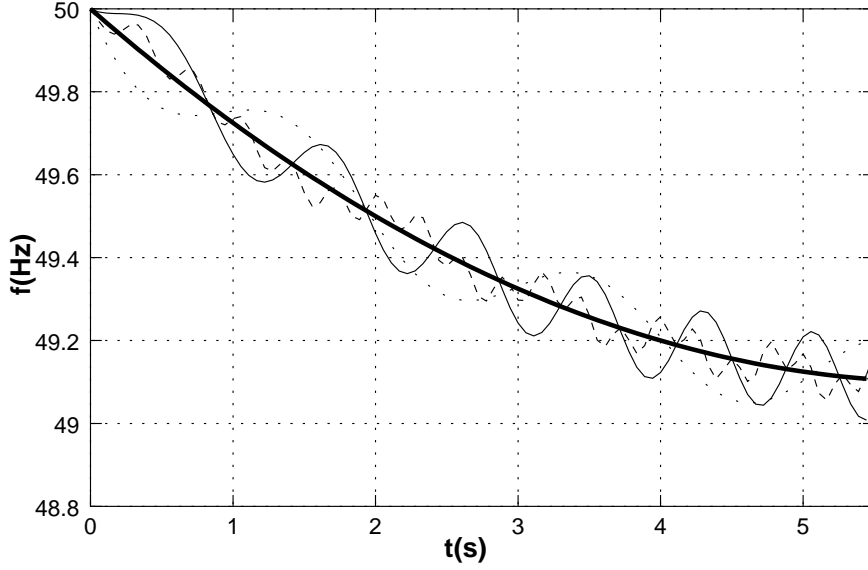


Figure 2.1. The frequency in different locations in an electric power system after a disturbance. The thicker solid curve indicates the average system frequency. Other curves depict the frequency of individual generators.

power in SI-units, like MW instead of p.u.,

$$2H_i S_i \Delta \dot{\omega}_i = \frac{\omega_0^2}{\omega_i} (P_{mi} - P_{ei}) \quad (2.2)$$

is obtained. P_{mi} and P_{ei} are now expressed in the same SI-unit as S_i , cf. Appendix A. Further, for every synchronous machine i

$$\omega_i = \omega_0 + \Delta \omega_i \quad , \quad (2.3)$$

and for the frequency in the centre of inertia (COI)

$$\omega = \omega_0 + \Delta \omega \quad . \quad (2.4)$$

The system frequency deviation $\Delta \omega$ (or ω) is now defined as

$$\sum_i H_i S_i \Delta \omega_i = H \Delta \omega \quad (2.5)$$

with

$$H = \sum_i H_i S_i \quad . \quad (2.6)$$

Adding eq. (2.2) for all generators in the system leads to

$$2H \Delta \dot{\omega} = \omega_0^2 \sum_i \frac{P_{mi} - P_{ei}}{\omega_i} \quad . \quad (2.7)$$

A very simple and useful model can be derived if some more assumptions are made.

The overall goal of our analysis is to derive an expression that gives the variation of $\Delta\omega$ after disturbance of the balance between $\sum P_{mi}$ and $\sum P_{ei}$. Therefore, we define

$$P_m = \sum_i P_{mi} = P_{m0} + \Delta P_m \quad , \quad (2.8)$$

where ΔP_m denotes a possible disturbance, like loss of a generator (turbine). The total generated power is consumed by the loads and the transmission system losses, i.e.

$$P_e = \sum_i P_{ei} = P_{load} + P_{loss} \quad , \quad (2.9)$$

which can, in the same way as in eq. (2.8), be written as

$$P_e = P_{e0} + \Delta P_{load} + \Delta P_{loss} \quad (2.10)$$

with

$$P_{e0} = P_{load0} + P_{loss0} \quad . \quad (2.11)$$

If the system is in equilibrium prior to the disturbance,

$$P_{m0} = P_{e0} \quad (2.12)$$

and

$$P_{m0} = P_{load0} + P_{loss0} \quad (2.13)$$

are valid.

The following assumptions are now made:

- The transmission losses after and before the disturbance are equal, i.e. $\Delta P_{loss} = 0$.
- All generator angular frequencies ω_i in the right hand side of eq. (2.7) are set equal to the system average angular frequency ω .

If neither the disturbance nor the oscillations in the transmission system are too large, these approximations are reasonable. Using these assumptions and eqs. (2.8) – (2.13), eq. (2.7) can now be written as

$$\Delta\dot{\omega} = \frac{\omega_0^2}{2H\omega} (\Delta P_m - \Delta P_{load}) \quad . \quad (2.14)$$

Eq. (2.14) can be represented by the block diagram in Figure 2.2.

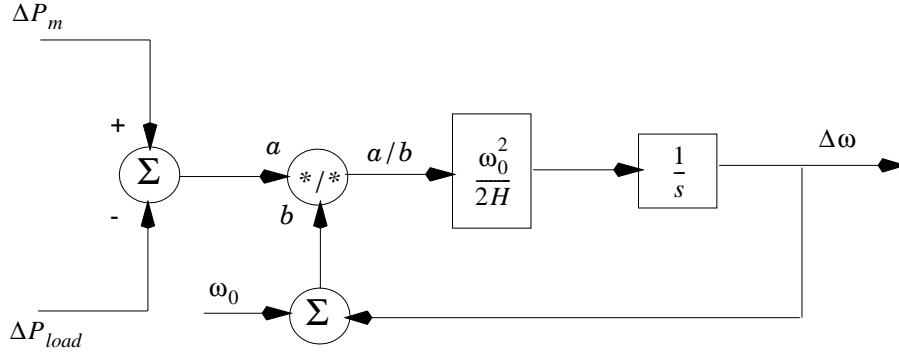


Figure 2.2. Block diagram of eq. (2.14).

2.2 Model of Frequency Control

Eq. (2.14) describes the variation of the system's average frequency when the balance between generated and demanded power is no longer preserved, i.e. when $\Delta P_m \neq \Delta P_{load}$. In the most common case $\Delta P_m - \Delta P_{load}$ is negative after a disturbance, like the tripping of a generator station. It is also possible that the frequency rises during a disturbance, for example when an area that contains much generation capacity is isolated. Since too large frequency deviations in a system are not acceptable, automatic frequency control, which has the goal of keeping the frequency during disturbances at an acceptable level, is used. The spontaneous load variations in an electric power system result in a minute-to-minute variation of up to 2%. This alone requires that some form of frequency control must be used in most systems.

There are at least two reasons against allowing the frequency to deviate too much from its nominal value. A non-nominal frequency in the system results in a lower quality of the delivered electrical energy. Many of the devices that are connected to the system work best at nominal frequency. Further, too low frequencies (lower than $\approx 47 - 48$ Hz) lead to damaging vibrations in steam turbines, which in the worst case have to be disconnected. This constitutes an even worse stress on the system and can endanger the system's security. (Hydro power plants are more robust and can normally cope with frequencies down to 45 Hz.)

The frequency after a disturbance thus depends on the parameters contained in eq. 2.14). In addition to the constant of inertia, H , the trajectory is determined by

- the frequency dependency of the loads,
- the control of the hydro turbines,

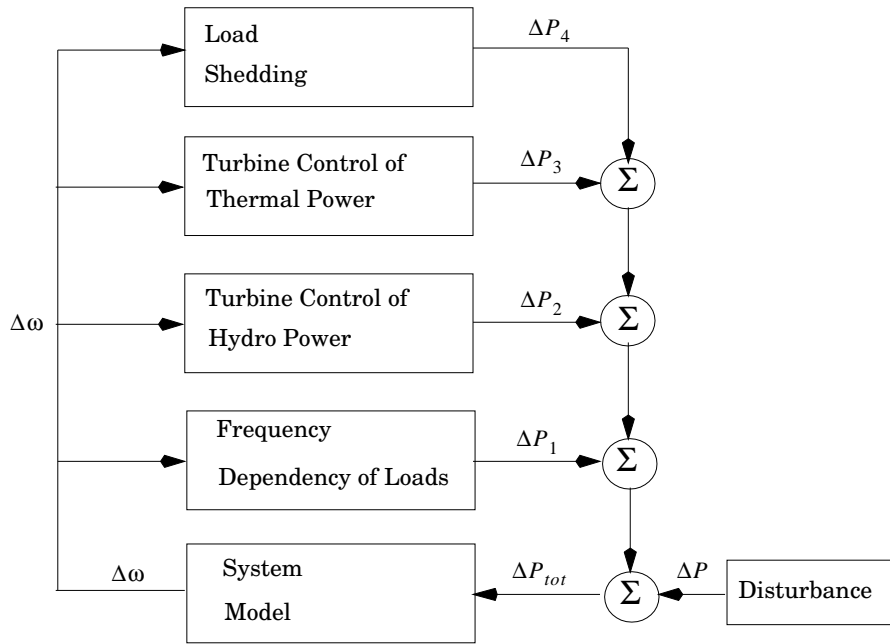


Figure 2.3. Block diagram of the frequency control in a power system.

- the control of the steam turbines, and
- load shedding.

This is summarized in the block diagram in Figure 2.3. Under frequency load shedding is a form of system protection.

In many systems, a rotating scheme for how load should be shed, if that is necessary, is devised. Such a scheme is often called rotating load shedding.

The frequency dependency of loads will be discussed in the next section, while the frequency control performed by generating units will be discussed in subsequent two chapters.

To give the reader a pre-view of how a typical frequency response would be in systems with different frequency controls, Figure 2.4 is included. We will revert to this figure when the models in the next chapter has been developed.

2.2.1 Frequency Dependency of Loads

In an electric power system, the power demand of the load varies with the frequency and the voltage. These variations are, as a rule, highly complicated and change during the day and over the year. For compound loads, such as a transformer station in the high-voltage net, the compound structure of the separate loads is difficult to represent in a simple way. Generally,

more or less simplified models have to be used. For the phenomenon studied here, the main influence is the frequency dependency of the loads, which, for small frequency variations, can be written as

$$P_{load} = P_{load0}(1 + D_l\Delta\omega) = P_{load0} + D\Delta\omega . \quad (2.15)$$

The parameter D_l changes of course, depending on the load type and composition, but typical values are in the interval 0–2% per % frequency variation. Since D_l is positive, the frequency dependency of the loads leads to natural stabilization of the frequency in the system. If that is the only stabilizing control in the system, an unbalance between generation and load power of ΔP leads to a value of $\Delta\omega = \Delta P/D$ for the remaining frequency deviation in the system.

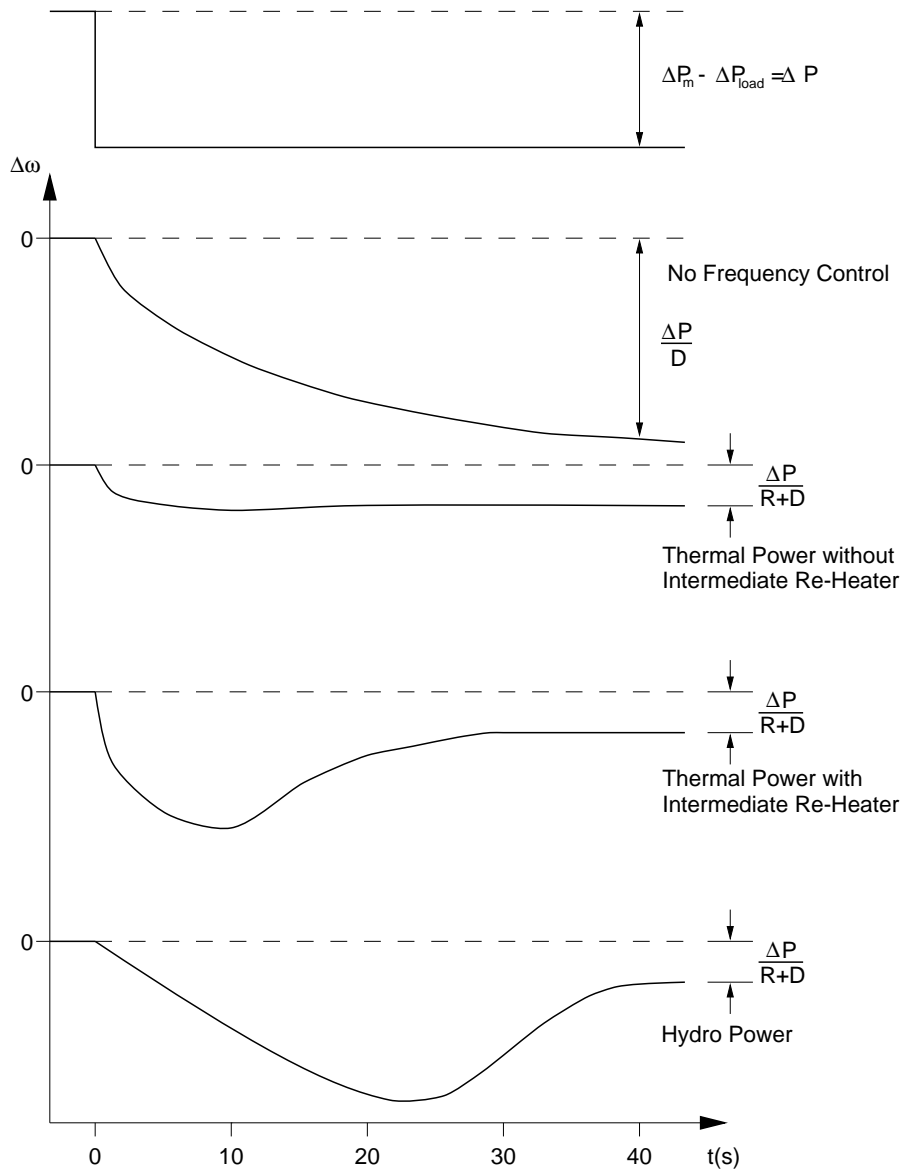


Figure 2.4. Frequency variation after a step in $\Delta P_m - \Delta P_{load}$. That step can, for example, be caused by loss of production in the system. D = frequency dependency of loads (see section 2.2.1). R = frequency control droop (see chapter 3)

3

Primary Frequency Control

In this chapter the part of the frequency control that is performed on the power plant level will be described. This is called the primary frequency control. The static, i.e. steady state, characteristics of this is described by the speed (or frequency) droop, which determines the permanent frequency deviation after the primary frequency control has acted. Turbine models are also derived.

3.1 Introduction

A schematic block diagram of the power and frequency control of a power plant is given in Figure 3.1. The control loop consists here of the turbine, generator, and the network.

The primary control indicates here the control actions that are done locally based on the set values for frequency (normally the nominal frequency) and the power. The actual values of these could be measured locally, and deviations from the set values will result in a signal that will influence the valves, gates, servos, etc, so that the desired active power output is delivered from the generating unit. In the primary frequency control the control task of priority is to bring the frequency back to (short term) acceptable values, and this control task is shared by all generators participating in the primary frequency control irrespective of what caused the control action.

In the secondary frequency control, also called *load frequency control*, the set values of the generator power is adjusted to compensate for undesired fluctuations introduced by the primary frequency control. These undesired fluctuations could be too large a frequency deviation during steady state or power flows on tie lines outside the scheduled values. In this control loop the cause of the control error is considered when the control action is determined. This control could be done automatically, and is then often called *Automatic Generation Control*, or it could be done manually. This is further discussed in chapter 4.

The tertiary control loop in Figure 3.1 concerns the unit commitment and economic dispatch problems and is done off line based on economic optimization. This will not be elaborated on in these lectures.

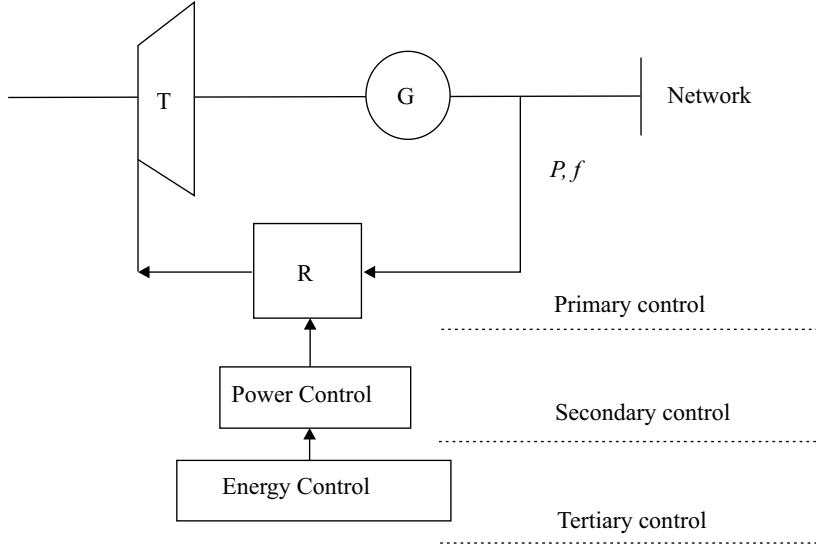


Figure 3.1. Schematic block diagram of the power and frequency control of a power plant. R = Controller. T = Turbine. G = Generator.

For a thermal unit the block diagram of the primary control is shown in Figure 3.2. The controller controls by use of a servomotor the valve through which the high pressure and high temperature steam flows from the boiler to the turbines. In the high pressure turbine part of the energy of the steam is converted into mechanical energy. Often the steam is then reheated before it is injected into a medium pressure or low pressure turbine, where more energy is extracted from the steam. (More about different steam turbines and their modelling can be found in subsection 3.2.1.) These turbine-generator systems can be very large. In a big thermal unit of rating 1000 MW, the total length of the turbine-generator shaft could be more than 50 m.

We will now make some simplified studies concerning the dynamics of the frequency response of the system in Figure 3.2. If the total inertia of the turbine-generator system is J , the mechanical torque from the turbine(s) is T_m , the electrical torque on the generator is T_e , then the equation of motion will be

$$J \frac{d\omega}{dt} = T_m - T_e \quad (3.1)$$

where both T_m and T_e are positive for a generator. If the frequency controller is implemented as a proportional controller, i.e. as $\Delta T_m = K \Delta \omega$, the block diagram of Figure 3.3 is obtained. This model can now be used to study the frequency response. The relationship between power and torque is given by:

$$T = \frac{P}{\omega} \quad (3.2)$$

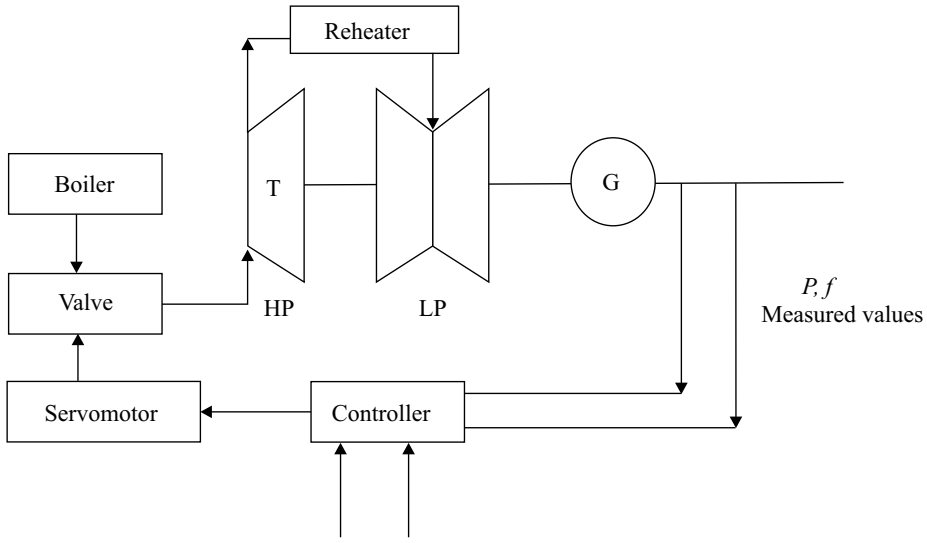


Figure 3.2. Block diagram of the primary control of a thermal unit. HP = High Pressure Turbine. LP = Low Pressure turbine.

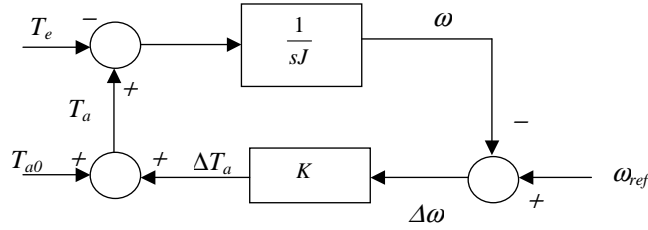


Figure 3.3. Block diagram of simple system with proportional frequency controller.

Two cases will be studied:

1. Change of the reference value of the frequency by a step.
2. Change of the active power load P_e with a step.

It is straightforward to derive the following relationship for case 1

$$\frac{\Delta\omega}{\Delta\omega_{ref}} = \frac{1}{s} \cdot \frac{1}{1 + s\tau} \quad (3.3)$$

and the following for the second case

$$\frac{\Delta\omega}{\Delta T_e} = -\frac{1}{s} \cdot \frac{1/K}{1 + s\tau} \quad (3.4)$$

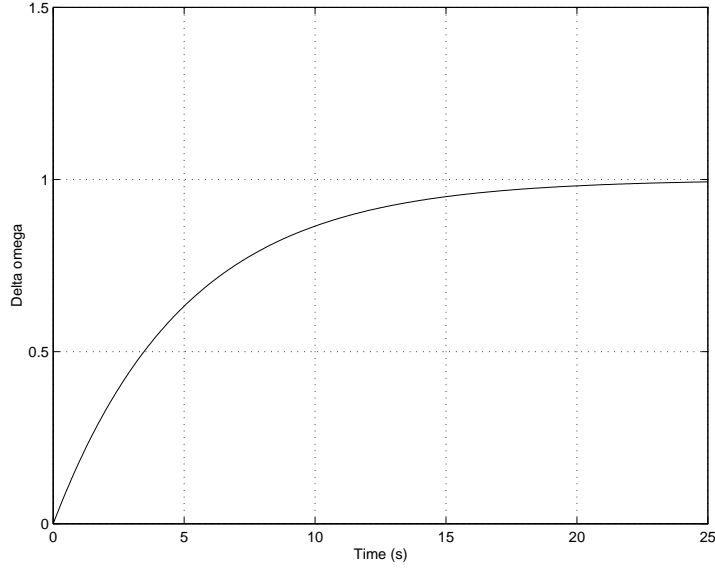


Figure 3.4. Step response in the frequency after a step change, $\Delta\omega_{ref}$, in the reference value of the frequency. (In per unit of $\Delta\omega_{ref}$) ($\tau = 5$ s)

The time constant τ is given by

$$\tau = \frac{J}{K} \quad (3.5)$$

These step responses are shown in Figures 3.4 and 3.5.

It is common to express the gain K of the controller in per unit:

$$K = \frac{\Delta T_m / T_N}{\Delta \omega / \omega_N} \quad (3.6)$$

where the value of K often is in the range

$$0.03 < 1/K < 0.1 \quad (3.7)$$

This means that a change in the frequency of 3 to 10 % will result in a change in the delivered electrical torque of 100 %. This is called the static *speed droop* of the controller, see Figure 3.6. For small deviations of the frequency, the per unit values of torque and power are almost identical.

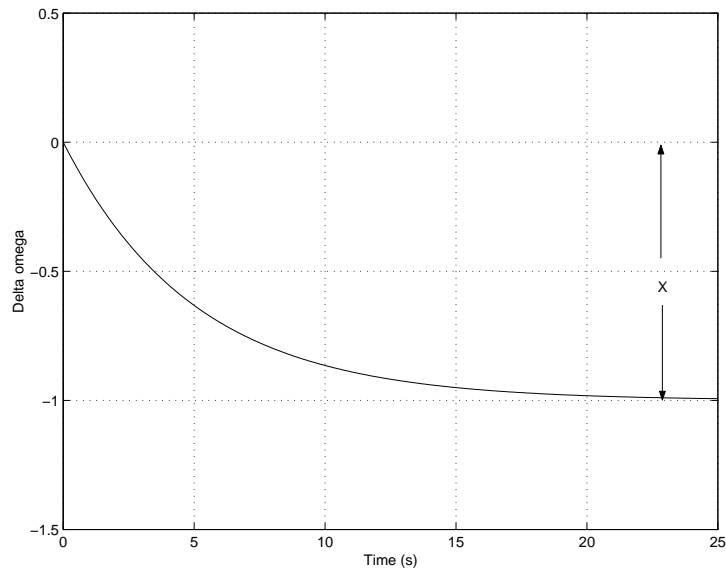


Figure 3.5. Step response in the frequency after a step change, ΔT_e in the active power load. ($X = \Delta T_e/K$, $T = 5$ s)

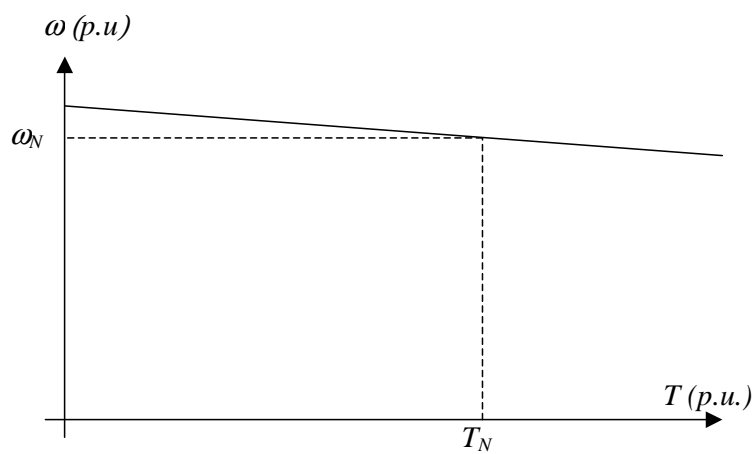


Figure 3.6. The speed droop of a frequency controller.

3.2 Turbine Control

This section gives an overview of the modelling of turbines, steam and hydro, and their controllers. Their characteristics and behaviour are also briefly discussed. The aim here is to give an understanding of the basic physical mechanisms behind these models that are very commonly used in simulation packages for the study of power systems dynamics. Figure 3.7 shows a block diagram how these turbine models are integrated in the overall system models.

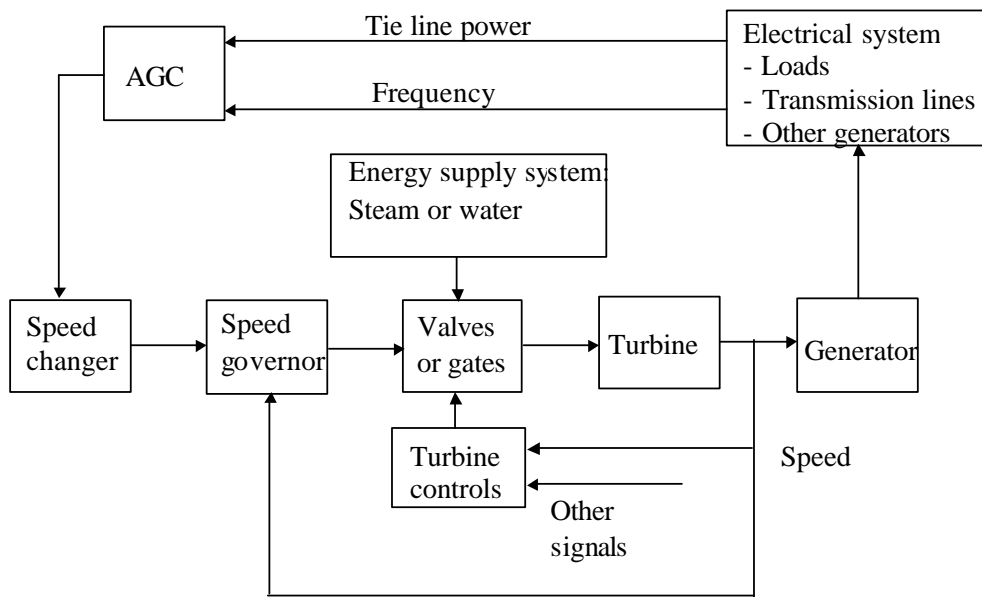


Figure 3.7. Functional block diagram of power generation and control system. AGC = Automatic Generation Control, see chapter 4 (From ref. [1])

3.2.1 Turbine Models

Steam Turbines

Figures 3.8 ,3.9, and 3.10 show the most common steam turbines and their models.

It is outside the scope of these lecture notes to give a detailed derivation and motivation of these models, only a brief qualitative discussion will be provided. In a steam turbine the stored energy of high temperature and high pressure steam is converted into mechanical (rotating) energy, which then is converted into electrical energy in the generator. The original source

of heat can be a furnace fired by fossil fuel (coal, gas, or oil) or biomass, or it can be a nuclear reactor.

The turbine can be either *tandem compound* or *cross compound*. In a tandem compound unit all sections are on the same shaft with a single generator, while a cross compound unit consists of two shafts each connected to a generator. The cross compound unit is operated as one unit with one set of controls. Most modern units are of tandem compound type, even if the crossover compound units are more efficient and has higher capacity. However, the costs are higher and could seldom be motivated.

The power outlet from the turbine is controlled through the position of the *Control Valves*, which control the flow of steam to the turbines. The delay between the different parts of the steam path is usually modelled by a first order filter as seen in Figures 3.8, 3.9, and 3.10. Certain fractions of the total power is extracted in the different turbines, and this is modelled by the factors F_{VHP} , F_{HP} , F_{IP} , F_{LP} in the models. Typical values of the time constant of the delay between the control valves and the high-pressure turbine, T_{CH} , is 0.1–0.4 s. If a re-heater is installed the time delay is larger, typically $T_{RH} = 4 - 11$ s. The time constant of delay between the intermediate pressure and the low pressure turbines, T_{CO} , is in the order 0.3–0.6 s.

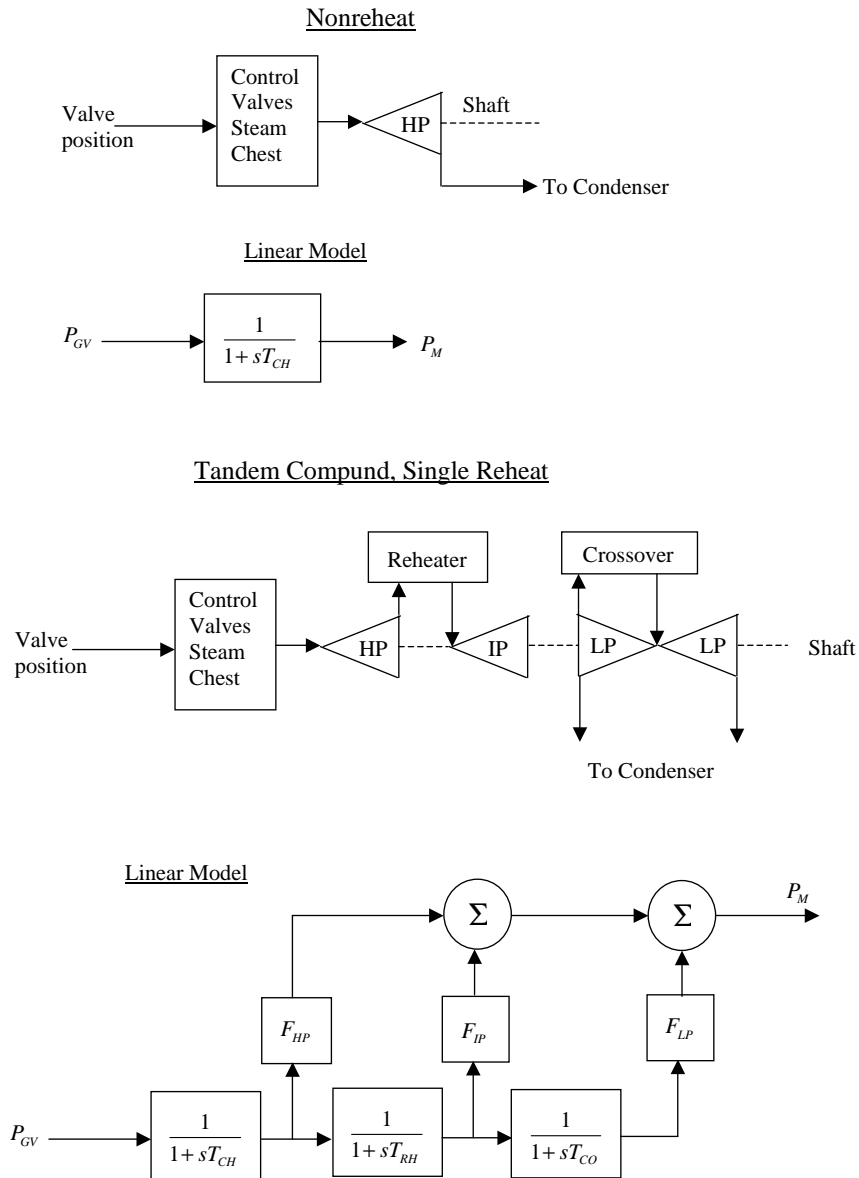


Figure 3.8. Steam turbine configurations and approximate linear models. Nonreheat and tandem compound, single reheat configurations.

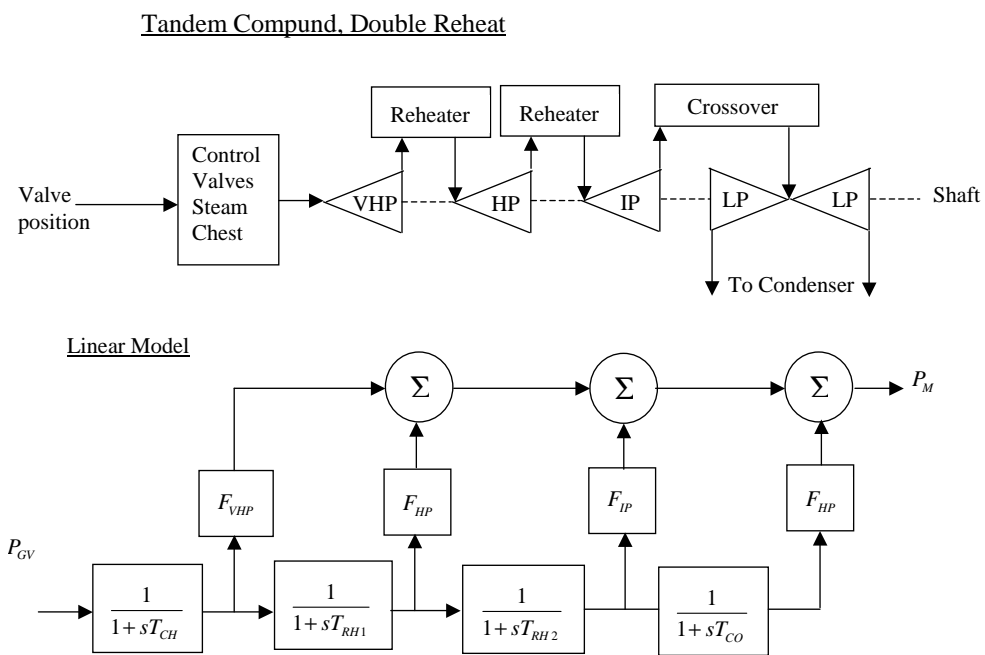


Figure 3.9. Steam turbine configurations and approximate linear models. Tandem compound, double reheat configuration.

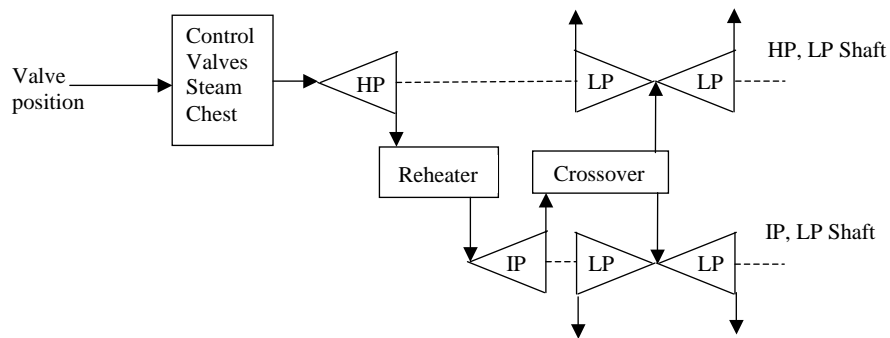
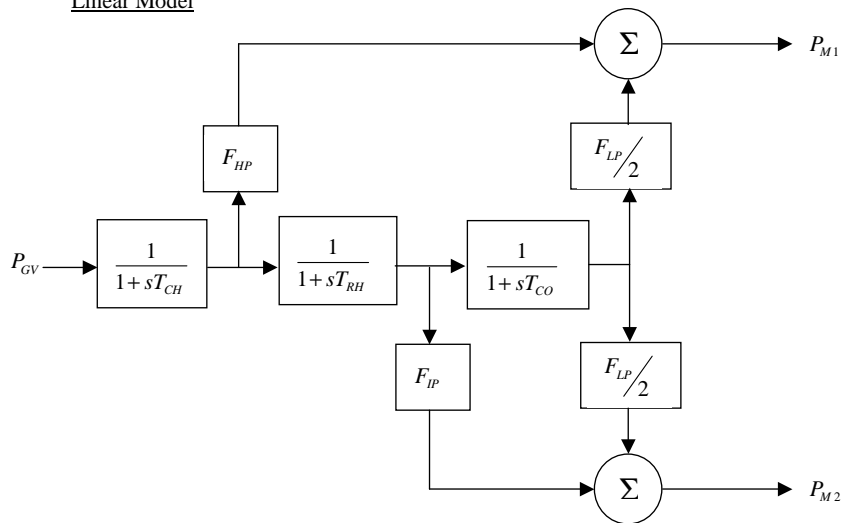
Cross Compound, Single ReheatLinear Model

Figure 3.10. Steam turbine configurations and approximate linear models. Cross compound, single reheat configuration.

Step Response To illustrate the dynamics of a steam turbine, the configuration with tandem compound, single reheat, Figure 3.8, with the following data will be studied:

$$T_{CH} = 0.1 \text{ s}, T_{RH} = 10 \text{ s}, T_{CO} = 0.3 \text{ s}$$

$$F_{HP} = 0.3, F_{IP} = 0.4, F_{LP} = 0.3$$

As $T_{CH} \ll T_{RH}$ und $T_{CO} \ll T_{RH}$, we can in an approximate analysis put $T_{CH} = T_{CO} = 0$. Then a simplified block diagram according to Figure 3.11 can be used. For this system the step response is easy to calculate, and is according to Figure 3.12.

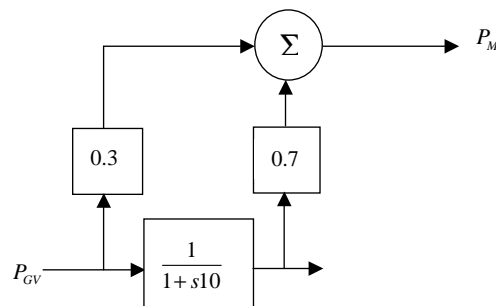


Figure 3.11. Simplified model of tandem compound, single reheat system in Figure 3.9.

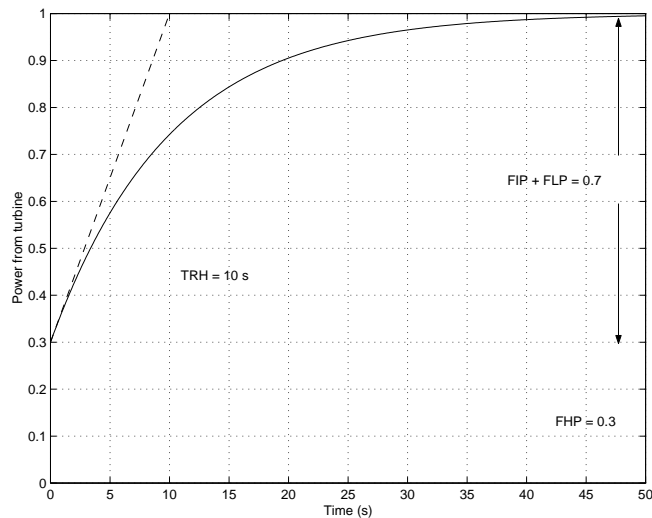


Figure 3.12. Step response of system in Figure 3.11.

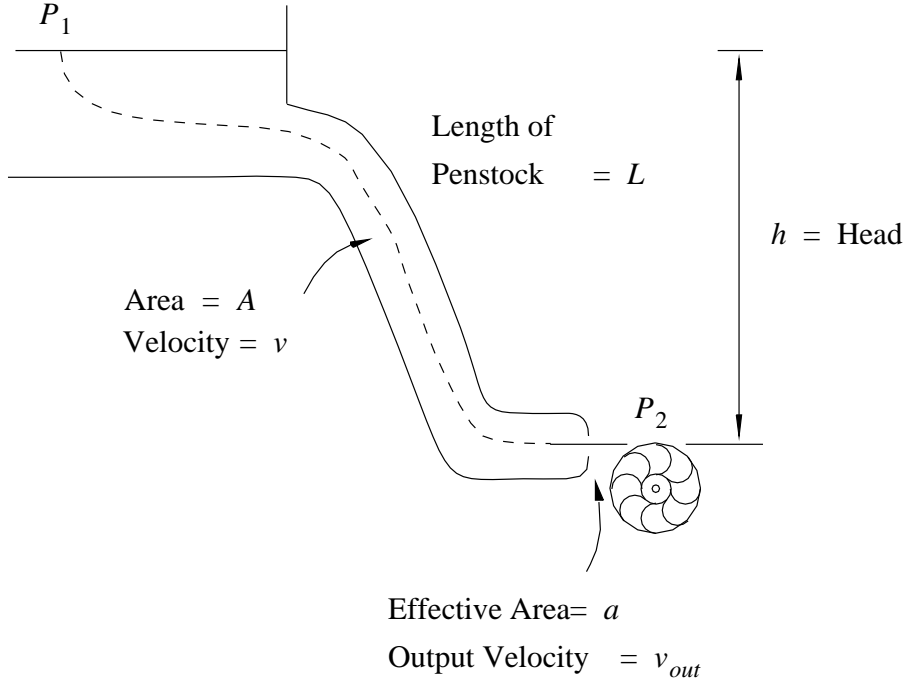


Figure 3.13. Schematic drawing of hydro turbine with water paths.

Hydro Turbines

Compared with steam turbines, hydro turbines are easier and cheaper to control. Thus, frequency control is primarily done in the hydro power plants if available. If the amount of hydro-generated power in a system is not sufficient, the steam turbines have to be included in the frequency control.

The power produced by a generator is determined by the turbine governor and the dynamic properties of the turbine. Thus, to be able to determine the frequency's dynamic behaviour, models for the turbine as well as for the turbine control are necessary.

Figure 3.13 depicts a hydro turbine with penstock and hydro reservoir and defines the notation that will be used from now on. Bernoulli's equation for a trajectory between the points P_1 and P_2 can be written as

$$\int_{P_1}^{P_2} \frac{\partial \bar{v}}{\partial t} \cdot d\bar{r} + \frac{1}{2}(v_2^2 - v_1^2) + \Omega_2 - \Omega_1 + \int_{P_1}^{P_2} \frac{1}{\rho} dp = 0 \quad (3.8)$$

The following assumptions are usually made:

- $v_1 = 0$, since the reservoir is large and the water level does not change during the time scale that is of interest here.
- The water velocity is non-zero only in the penstock.

- The water is incompressible, i.e. ρ does not change with water pressure.
- The water pressure is the same at P_1 and P_2 , i.e. $p_1 = p_2$.

Further,

$$\Omega_2 - \Omega_1 = -gh \quad . \quad (3.9)$$

The above assumptions together with eq. (3.9) make it possible to write (3.8), with $v_{out} = v_2$ and the length of the penstock L , as

$$L \frac{dv}{dt} + \frac{1}{2} v_{out}^2 - gh = 0 \quad . \quad (3.10)$$

The velocity of the water in the penstock is v . The effective opening of the penstock, determined by the opening of the turbine's control valve (guide vanes), is denoted a . If the penstock's area is A ,

$$v_{out} = \frac{A}{a} v \quad (3.11)$$

is valid and eq. (3.10) can be written as

$$\frac{dv}{dt} = \frac{1}{L} gh - \frac{1}{2L} \left(\frac{A}{a} v \right)^2 \quad . \quad (3.12)$$

The maximum available power at the turbine is

$$P = \frac{1}{2} \rho a v_{out}^3 = \frac{1}{2} \rho \frac{A^3 v^3}{a^2} \quad . \quad (3.13)$$

To get the system into standard form,

$$\begin{cases} x = v \ , \\ u = \frac{a}{A} \ , \\ y = P \ , \end{cases} \quad (3.14)$$

are introduced. (Here, we have used the standard notation, i.e. x for state, u for control signal, and y for output signal.) The system now can be written as

$$\begin{cases} \dot{x} = \frac{gh}{L} - x^2 \frac{1}{2Lu^2} \ , \\ y = \rho A \frac{x^3}{2u^2} \ . \end{cases} \quad (3.15)$$

The system corresponding to eq. (3.15) can be described with the block diagram in Figure 3.14.

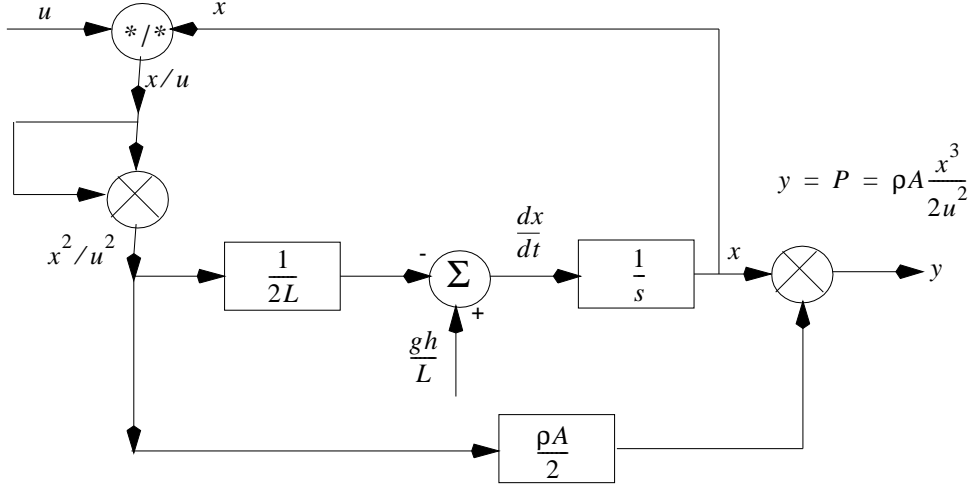


Figure 3.14. Block diagram showing model of hydro turbine.

Eq. (3.15) is nonlinear and a detailed analysis is beyond the scope of these lecture notes. To get an idea of the system's properties, the equations are linearised, and small variations around an operating point are studied. In steady state, $\dot{x} = 0$, and the state is determined by x_0 , u_0 , and y_0 , which fulfils

$$\begin{cases} x_0 = u_0 \sqrt{2gh} , \\ y_0 = \frac{\rho A x_0^3}{2u_0^2} . \end{cases} \quad (3.16)$$

Small deviations Δx , Δu , and Δy around the operating point satisfy

$$\begin{cases} \Delta \dot{x} = -2x_0 \frac{1}{2Lu_0^2} \Delta x + \frac{2x_0^2}{2Lu_0^3} \Delta u , \\ \Delta y = 3\rho \frac{Ax_0^2}{2u_0^2} \Delta x - 2\rho \frac{Ax_0^3}{2u_0^3} \Delta u , \end{cases} \quad (3.17)$$

which, using eqs. (3.16), can be written as

$$\begin{cases} \Delta \dot{x} = -\frac{\sqrt{2gh}}{u_0 L} \Delta x + \frac{2gh}{u_0 L} \Delta u , \\ \Delta y = \frac{3y_0}{u_0 \sqrt{2gh}} \Delta x - \frac{2y_0}{u_0} \Delta u . \end{cases} \quad (3.18)$$

The quantity $L/\sqrt{2gh}$ has dimension of time, and from the above equations it is apparent that this is the time it takes the water to flow through the

penstock if $a = A$. That time is denoted T :

$$T = L/\sqrt{2gh} . \quad (3.19)$$

If eqs. (3.18) are Laplace-transformed, Δx can be solved from the first of the equations, leading to

$$\Delta x = \frac{L/T}{1 + su_0T} \Delta u , \quad (3.20)$$

which, when inserted in the lower of eqs. (3.18) gives

$$\Delta y = \frac{y_0}{u_0} \cdot \frac{1 - 2u_0Ts}{1 + u_0Ts} \Delta u . \quad (3.21)$$

$u_0T = a_0T/A$ also has dimension of time and is denoted T_w . That makes it possible to write eq. (3.21) as

$$\Delta y = \frac{y_0}{u_0} \cdot \frac{1 - 2T_ws}{1 + T_ws} \Delta u . \quad (3.22)$$

It is evident that the transfer function in eq. (3.22) is of non–minimum phase, i.e. not all poles and zeros are in the left half plane. In this case, one zero is in the right half plane. That is evident from the step response to eq. (3.22), depicted in Figure 3.15.

The system has the peculiar property to give a lower power just after the opening of the control valve is increased before the desired increased power generation is reached. The physical explanation is the lower pressure appearing after the control valve is opened, so that the water in the penstock can be accelerated. When the water has been accelerated, the generated power is increased as a consequence of the increased flow. That property of water turbines places certain demands on the design of the control system for the turbines.

3.2.2 Turbine Controllers

It is the task of the turbine governor to control the control valve such that the desired power is produced by the generator in question. That power is partly determined by the set value for the produced power and partly by a contribution originating from the frequency control. In this context, the latter is of interest.

There is a number of different turbine governors for steam turbines. A quite general model that can describe most controllers in a satisfying way is depicted in Figure 3.16. The gain K determines here the speed droop characteristics of the controller, i.e. $S = 1/K$.

A model of controller of a hydro turbine is given in Figure 3.17. The control servo is here represented simply by a time constant T_p . The main

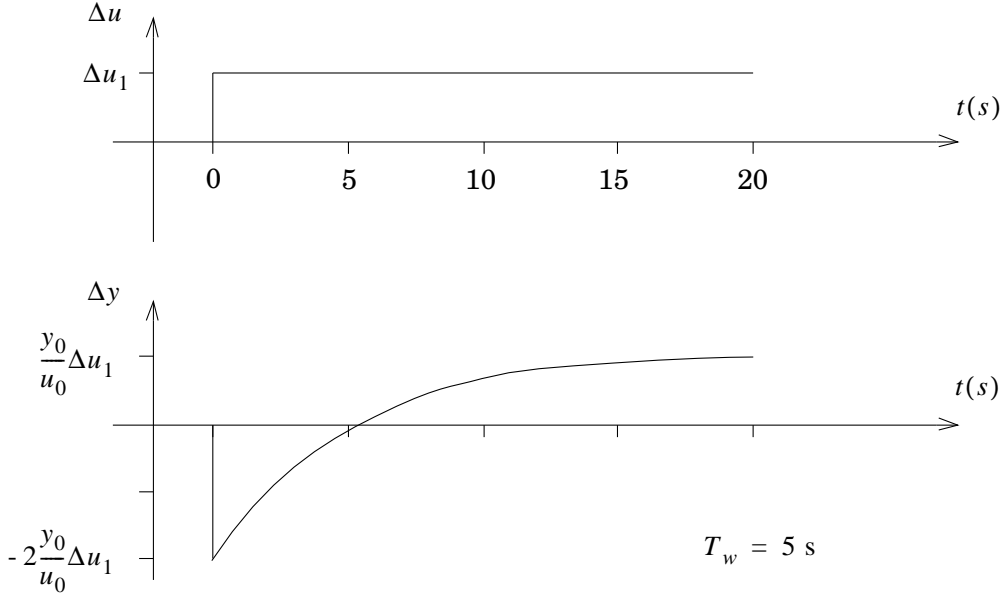


Figure 3.15. The variation of the produced power, Δy , after a step change in the control valve.

servo, i.e. the guide vane, is represented by an integrator with the time constant T_G . Typical values for these parameters are given in Table 3.1. Limits for opening and closing speed as well as for the largest and smallest opening of the control valve are given. The controller has two feedback loops, a transient feedback loop and a static feedback loop. The transient feedback loop has the amplification δ for high frequencies. Thus, the total feedback after a frequency change is $-(\delta + \sigma)$. In steady state, the transient feedback is zero, and the ratio between the frequency deviation and the change in the control valve is given by

$$\Delta u = \frac{1}{\sigma} \Delta \omega \quad . \quad (3.23)$$

Parameter	Typical Values
T_R	2.5 – 7.5 s
T_G	0.2 – 0.4 s
T_p	0.03 – 0.06 s
δ	0.2 – 1
σ	0.03 – 0.06

Table 3.1. Typical values for some Parameters of the turbine controller for hydro power.

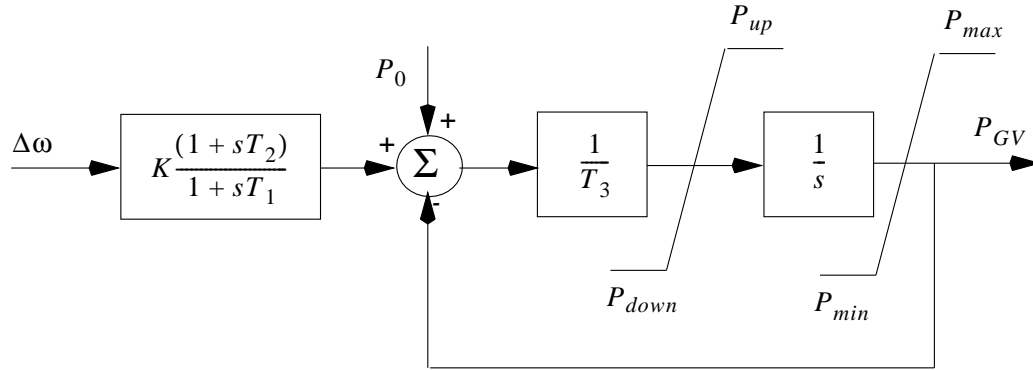


Figure 3.16. General Model of Turbine Controller for Steam Turbine.

Using eq. (3.22), the stationary change of power is obtained as

$$\Delta P = \frac{1}{\sigma} \frac{P_0}{u_0} \Delta \omega . \quad (3.24)$$

Thus, the speed droop for generator i , S_i , is

$$S_i = \frac{1}{\sigma_i} \frac{P_{0i}}{u_{0i}} , \quad (3.25)$$

and the total speed droop, S , in the system is given by

$$S = \sum_i S_i . \quad (3.26)$$

The transient feedback is needed since the water turbine is a non–minimum phase system as discussed above. If the transient feedback is left out or made too small, the system can become unstable. The transient feedback causes the system to be slower; the transient frequency deviations become considerably larger since the initial total feedback can be about ten times larger than the static feedback, i.e. the speed droop is initially lower than its stationary value.

3.3 Role of Speed Droop

It is of particular interest to study the actions of the frequency control in steady state. Under the assumption that the turbine power controller has an integrating character ($\varepsilon \rightarrow 0$ when $t \rightarrow \infty$ in Figure 3.18), it follows that in steady state

$$(f_0 - f) \cdot \frac{1}{S} + (P_0 - P) = 0 (= \varepsilon) \quad (3.27)$$

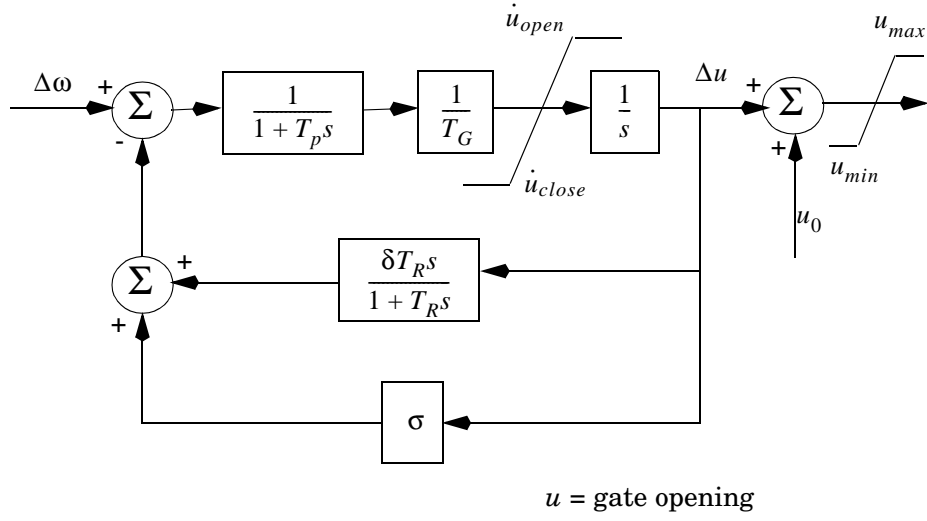


Figure 3.17. Model of turbine governor for hydro turbine.

which can be written as

$$S = -\frac{f_0 - f}{P_0 - P} = -\frac{f - f_0}{P - P_0} \text{ Hz/MW} \quad (3.28)$$

or in per unit

$$S = -\frac{\frac{f - f_0}{f_0}}{\frac{P - P_0}{P_0}} \quad (3.29)$$

(Eq.(3.29) is equivalent with eq. (3.6) with $S = 1/K$.)

The speed droop characteristic, Figure 3.19, gives all possible operating points (P, f) of the turbine. The position and slope of the straight line can be fixed by the parameters P_0 , f_0 and S . We have chosen to label the horizontal axis with the power P with for small deviations of the frequency around the nominal value is identical with the torque T . In the literature the speed droop characteristics is sometime also described by ω instead of by f .

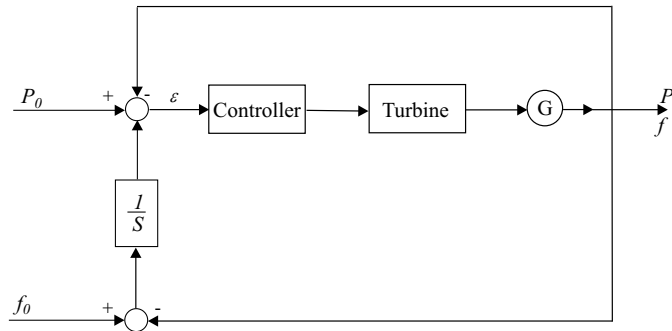


Figure 3.18. Schematic block diagram of system of controller, turbine, generator, and power system.

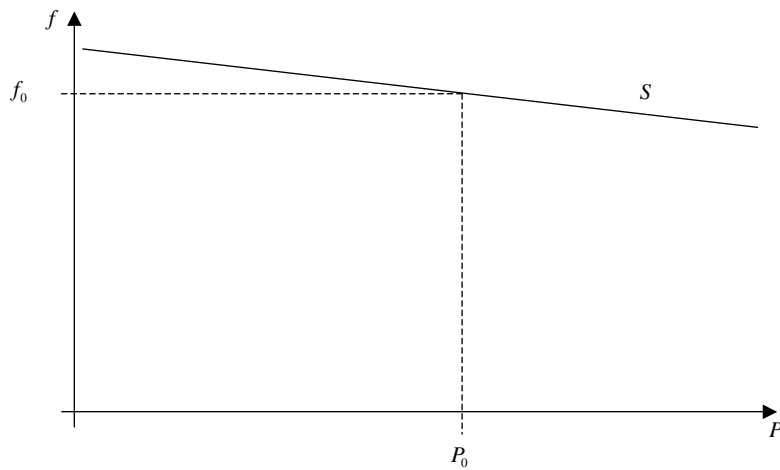


Figure 3.19. Speed droop characteristic of turbine control.

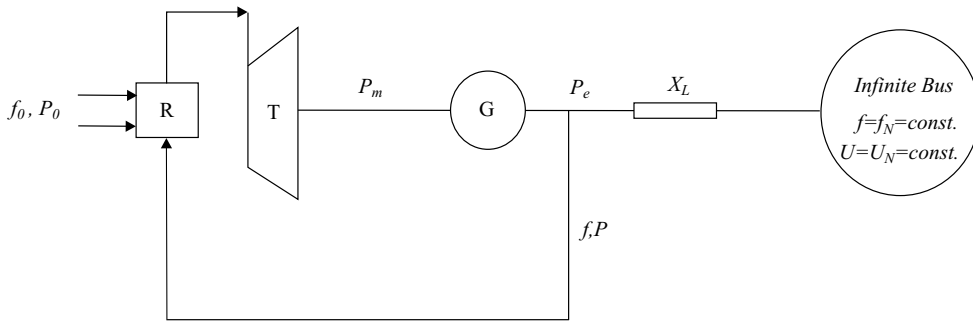


Figure 3.20. Generator operating in a large interconnected system.

We will now study how the frequency control of a generator will act in three different situations. Firstly, when the generator is part of a large interconnected system, and secondly when the generator is in islanded operation feeding a load. The third system to be studied is a two machine system.

Generator in large system If a generator is embedded in a large interconnected system, it can with a very good approximation be modelled as connected to an infinite bus as shown in Figure 3.20

In steady state the frequency is given by the one of the infinite bus, f_N . From the speed droop characteristics, Figure 3.19, the power produced by the generator can then be determined. The turbine controller controls thus only the power, not the frequency, see Figure 3.21.

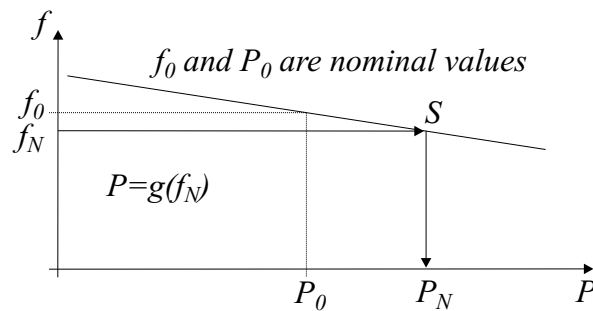


Figure 3.21. Speed droop characteristics for the case when the generator is connected to an infinite bus (large system).

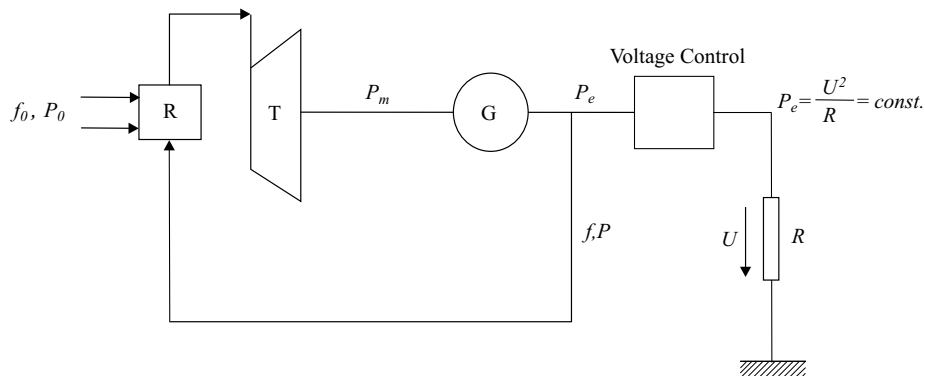


Figure 3.22. Generator in islanded operation.

Islanded Operation In islanded operation the generator feeds a load, which here is assumed to be a resistance load, Figure 3.22. By a voltage controller the voltage U is kept constant and thus also P . In this case the turbine controller will control the frequency, not the power. The resulting frequency can also here be determined from the speed droop characteristics, Figure 3.23.

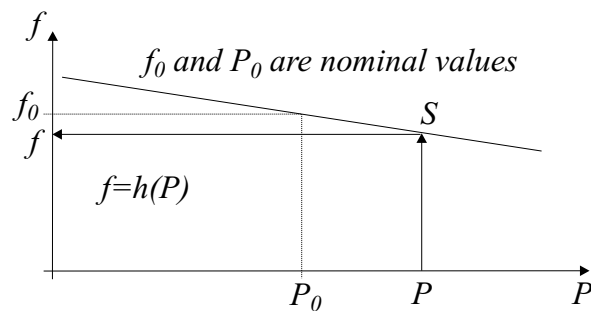


Figure 3.23. Speed droop characteristics for the case when the generator is in islanded operation.

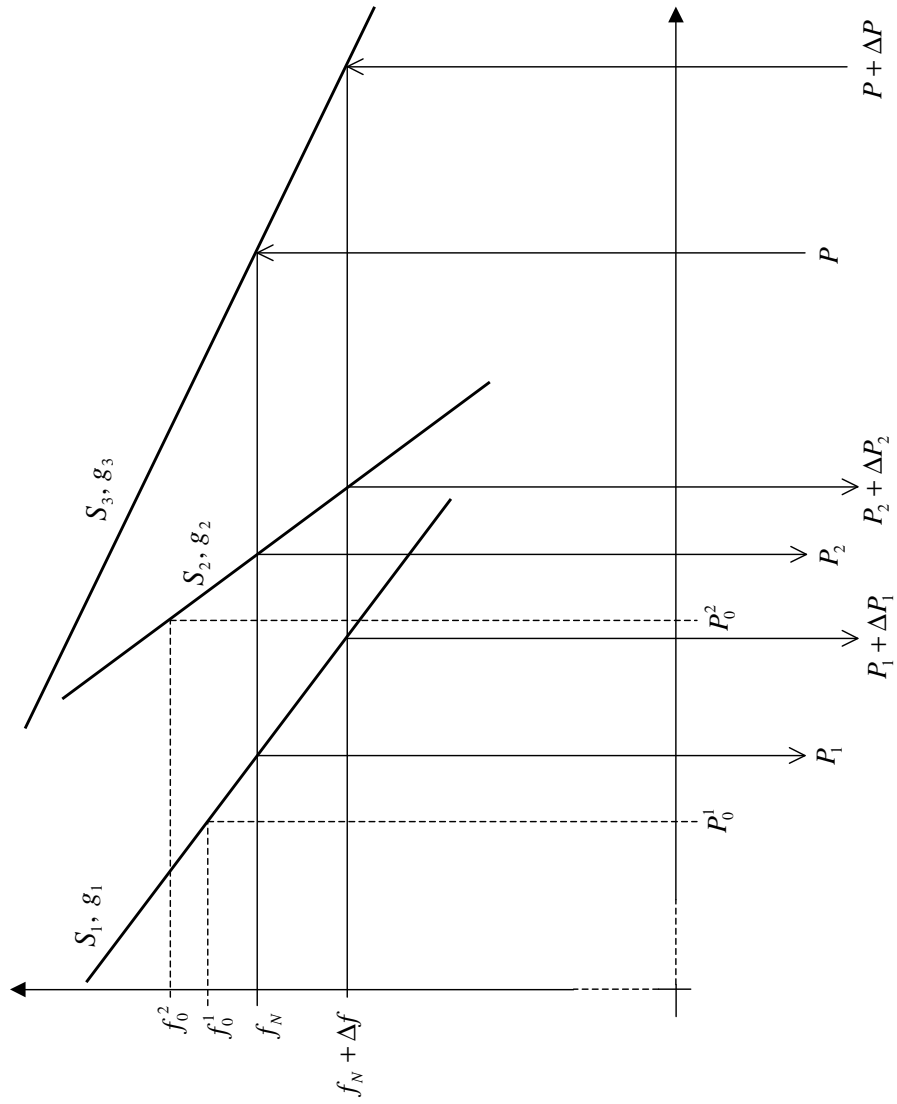


Figure 3.25. Speed droop characteristics for a two machine (subsystem) system.

4

Load Frequency Control

In this chapter the secondary, or load-frequency, control of power systems will be discussed. Simple models that enable the simulation of the dynamic behaviour during the action of frequency controllers will also be derived and studied.

In the previous chapters the role of the primary frequency control was dealt with. It was shown that after a disturbance a static frequency error will persist unless additional control actions are taken. Furthermore, the primary frequency control might also change the scheduled interchanges between different areas in an interconnected system, see the Two Machine example in section 3.3. To restore the frequency and the scheduled power interchanges additional control actions must be taken. This is done through the *Load-Frequency Control* (LFC). The LFC can be done either manually through operator interaction or automatically, in which latter case it is often called *Automatic Generation Control* (AGC). The characteristics of AGC will be studied in the subsequent sections, both during steady state and dynamic conditions.

4.1 Automatic Generation Control - Static Model

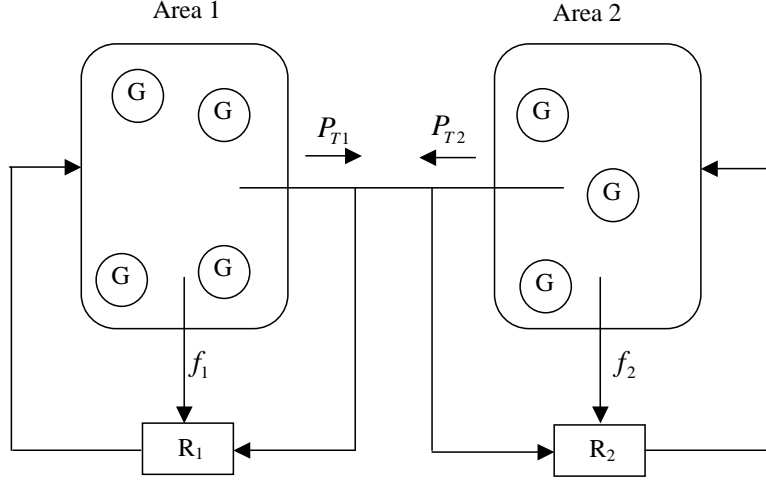
The overall goal of the LFC is to

- Keep the frequency in the interconnected power system close to the nominal value.¹
- Restore the scheduled interchanges between different areas, e.g. countries, in an interconnected system.

How this is achieved by the use of AGC will now be demonstrated.

Consider a two area system as depicted in Figure 4.1. The two controllers, R_1 and R_2 , will send new reference values of the power to the

¹In many systems deviations of up to ± 0.1 Hz from the nominal value (50 or 60 Hz) is deemed as acceptable in steady state. In some systems, North America, even tighter tolerance bands are applied, while recently in UK the tolerance band has been relaxed somewhat.



$$P_{T1} = \text{Tie-line power for Area 1} = \sum_{j_i} P_{T1}^{j_i} = \text{Sum over all tie-lines}$$

Figure 4.1. Two area system with AGC.

generators participating in the AGC. In a n area system there are n controllers R_i , one for each area i . A block diagram of such a controller is given in Figure 4.2. A common way is to implement this as a PI-controller:

$$\Delta P_{ci} = -\left(C_{pi} + \frac{1}{sT_{Ni}}\right)\Delta e_i \quad (4.1)$$

where $C_{pi} = 0.1 \dots 1.0$ and $T_{Ni} = 30 \dots 200$ s. The error Δe_i is called *Area Control Error*, ACE_i for area i .

We will now set $n = 4$, and from this it will be clear how this could be extended to any $n \geq 2$. The $ACEs$ are in this case:

$$ACE_i = \left(\sum_{j_i} P_{Ti,ref} - P_{Ti}^{j_i}\right) + B_i(f_{ref,i} - f) \quad i = 1, 2, 3, 4 \quad (4.2)$$

$$ACE_i = \Delta P_{Ti} + B_i \Delta f_i \quad i = 1, 2, 3, 4 \quad (4.3)$$

The constants B_i are called *frequency bias factors* [MW/Hz]. All $f_{ref,i}$ are the same in the different areas, and f is also the same in steady state. The goal is to bring all $ACE_i \rightarrow 0$.

The variables are thus $\sum_{j_i} P_{Ti}^{j_i}$ (four variables) and f , i.e. in total five variables. Since we have four equations ($ACE_i = 0$), we need one more

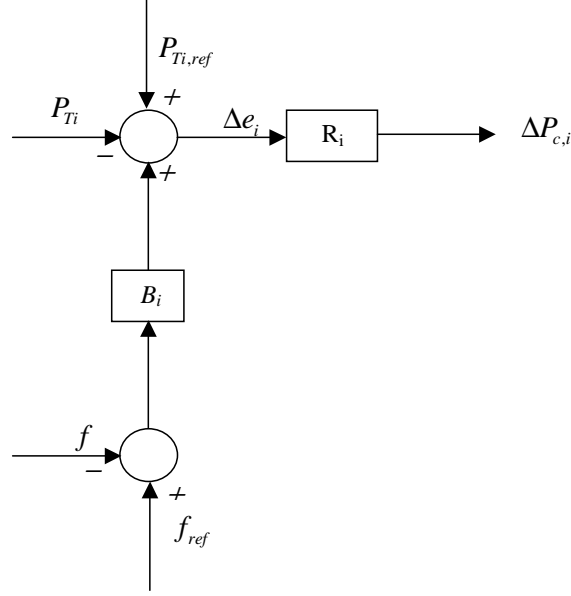


Figure 4.2. Controller for AGC ($\Delta e_i = \text{Error} = ACE_i = \text{Area Control Error for area } i$)

equation. As fifth equation we have the power balance:

$$\sum_{j_1} P_{T1}^{j_1} + \sum_{j_2} P_{T2}^{j_2} + \sum_{j_3} P_{T3}^{j_3} + \sum_{j_4} P_{T4}^{j_4} = 0 \quad (4.4)$$

and consequently a solution can be achieved.

In steady state is f identical for all areas, and we assume that the frequency is controlled back to the reference value, i.e. $f_{ref} = f$. If the sum of the reference values of the tie line powers $P_{Ti,ref}$ is 0, then the system will settle down to a operating point where $P_{Ti,ref} = \sum_{j_i} P_{Ti}^{j_i}$ for all tie line powers.

Selection of Frequency Bias Factors

Consider the two area system in Figure 4.1. The load is now increased with ΔP_l in area 2. If the tie line power should be kept the same, the generation must be increased in area 2, which means that $ACE_1 = 0$.

In this case the speed droop characteristics are according to Figure 3.25, which implies

$$\begin{aligned} \Delta f &= -S\Delta P_l, & \Delta f &= -S_1\Delta P_{T1}, \\ \Delta f &= -S_2(\Delta P_l - \Delta P_{T1}) \text{ and } \Delta P_{T1} = -\Delta P_{T2} \end{aligned} \quad (4.5)$$

The AGC controller forms now an *ACE*:

$$ACE_1 = \Delta P_{T1} + B_1 \Delta f = \Delta P_{T1} + B_1(-S_1 \Delta P_{T1}) = \Delta P_{T1}(1 - B_1 S_1) \quad (4.6)$$

which means that $ACE_1 = 0$ if $B_1 = 1/S_1$. This means the no action is taken by controller, and this is called *Non Interactive Control*. In area 2 we have

$$\begin{aligned} ACE_2 = \Delta P_{T2} + B_2 \Delta f = \Delta P_{T2} + B_2(-S_2(\Delta P_l - \Delta P_{T1})) = \\ \Delta P_{T2}(1 - B_2 S_2) - B_2 S_2 \Delta P_l \end{aligned} \quad (4.7)$$

and if $B_2 = 1/S_2$ this implies

$$ACE_2 = -\Delta P_l \quad (4.8)$$

This means that only controller 2 reacts in steady state and the load increase ΔP_l is compensated for in area 2, cf eq. (4.1).

4.2 Dynamic Model

Up to now we have mostly studied the static part of the frequency control, i.e. what can be concluded from the speed droop characteristics of the system. In this section we will study the dynamic behaviour during the action of the frequency controllers. Two cases will be analyzed. The first case corresponds to a system where all the generators and loads are strongly coupled to each other, which is the case in a highly meshed system. In this case we can model the system by a one node system, where all the generators and loads are connected at the same node. Secondly, we will study a two area system with a tie line between the two areas. This latter case will be studied with and without AGC implemented.

4.2.1 One Node System

For the individual generator the swing equation applies:

$$2H_i S_{B_i} \frac{d(\omega_i/\omega_0)}{dt} = P_{t_i} - P_{e_i}, \quad i = 1, \dots, n \quad (4.9)$$

Assuming that the generators are strongly coupled ($\omega_i = \omega$), gives

$$2\left(\sum_i H_i S_{B_i}\right) \frac{d(\omega/\omega_0)}{dt} = \sum_i (P_{t_i} - P_{e_i}) \quad (4.10)$$

$$2HS_B \frac{d(\omega/\omega_0)}{dt} = P_t - P_e \quad (4.11)$$

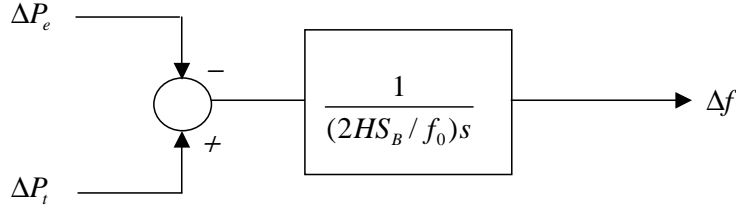


Figure 4.3. A block diagram for the dynamics of n generators connected at one node.

where

$$S_B = \sum_i S_{B_i} \quad \text{Total rating} \quad (4.12)$$

$$H = \frac{\sum_i H_i S_{B_i}}{\sum_i S_{B_i}} \quad \text{Total inertia constant} \quad (4.13)$$

$$P_t = \sum_i P_{t_i} \quad \text{Total turbine power} \quad (4.14)$$

$$P_e = \sum_i P_{e_i} \quad \text{Total generator power} \quad (4.15)$$

from $\omega/\omega_0 = (2\pi f)/(2\pi f_0) = f/f_0$ it follows that

$$\frac{2HS_B}{f_0} \frac{df}{dt} = P_t - P_e \quad (4.16)$$

As these differential equations are linear, they are also valid for the quantities

$$\begin{aligned} \Delta P_t &= P_t - P_{t_0} \\ \Delta P_e &= P_e - P_{e_0} \end{aligned} \quad (4.17)$$

$$\Delta f = f - f_0 \quad (4.18)$$

and consequently

$$\frac{2HS_B}{f_0} \frac{d\Delta f}{dt} = \Delta P_t - \Delta P_e \quad (4.19)$$

A block diagram of eq. (4.19) is given in Figure 4.3.

Turbine and Controller Consider the block diagram in Figure 4.4. From this figure it follows that

$$P_t(s) = \frac{G_t(s)}{G_t(s) + \frac{1}{K}s} [P_{t_0} - \frac{1}{S}(f - f_0)] \quad (4.20)$$

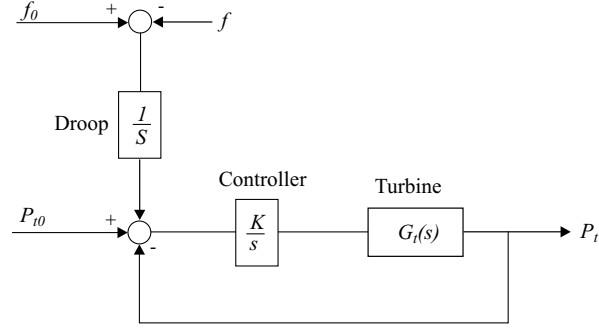


Figure 4.4. Block diagram of the dynamics for turbine and turbine control.

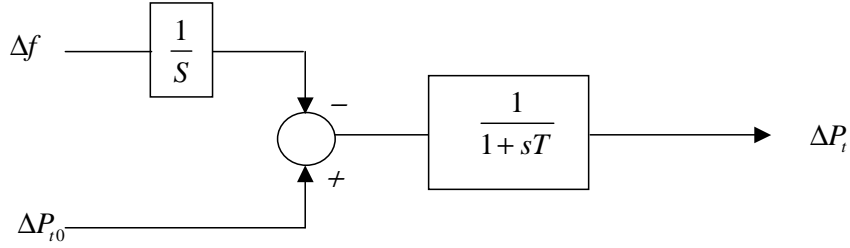


Figure 4.5. Block diagram of the system when the dynamics of the turbine is neglected.

If the dynamics of the turbine is neglected ($G_t(s) = 1$), one obtains

$$P_t = \frac{1}{1+sT} [P_{t0} - \frac{1}{S}(f - f_0)] \quad T = \frac{1}{K} \quad (4.21)$$

This equations is also valid for the Δ quantities:

$$\Delta P_t = \frac{1}{1+sT} [\Delta P_{t0} - \frac{1}{S}\Delta f] \quad (4.22)$$

and the block diagram in Figure 4.5 is valid.

In steady state we have

$$\Delta P_t = -\frac{1}{S}\Delta f \quad (\Delta P_{t0} = 0) \quad (4.23)$$

and for the case of several controllers

$$\Delta P_{t_i} = -\frac{1}{S_i}\Delta f \quad i = 1, \dots, n \quad (4.24)$$

$$\sum_i \Delta P_{t_i} = -\sum_i \frac{1}{S_i}\Delta f \quad (4.25)$$

where

$$\Delta P_t = \sum_i \Delta P_{t_i} \quad \text{Total change in the turbine power} \quad (4.26)$$

By defining

$$\frac{1}{S} = \sum_i \frac{1}{S_i} \quad (4.27)$$

we thus have

$$\Delta P_t = -\frac{1}{S} \Delta f \quad (4.28)$$

Loads The loads are either frequency dependent or frequency independent. Furthermore, kinetic energy can be stored (rotating masses in motors). A load model that captures this is given by

$$P_V - P_{V_0} = \Delta P_V = K_V \Delta f + g(\Delta \dot{f}) \quad (4.29)$$

where

- P_{V_0} : Load power when $f = f_0$
- K_V : Frequency dependency
- $g(\Delta \dot{f})$: Function the models the load with rotating masses

The function $g(\Delta \dot{f})$ will now be derived. The rotating masses have the following kinetic energy:

$$W(f) = \frac{1}{2} J (2\pi f)^2 \quad (4.30)$$

The change in the kinetic energy is given by

$$P_M = \frac{dW}{dt} \quad (4.31)$$

and

$$\Delta P_M = \frac{d\Delta W}{dt} \quad (4.32)$$

ΔW can be approximated by

$$\begin{aligned} W(f_0 + \Delta f) &= 2\pi^2 J (f_0 + \Delta f)^2 = \\ W_0 + \Delta W &= 2\pi^2 J f_0^2 + 2\pi^2 J 2f_0 \Delta f + 2\pi^2 J (\Delta f)^2 \\ &= W_0 + \frac{2W_0}{f_0} \Delta f + \frac{W_0}{f_0^2} (\Delta f)^2 \\ \Rightarrow \Delta W &\approx \frac{2W_0}{f_0} \Delta f \\ \Rightarrow \Delta P_M &\approx \frac{2W_0}{f_0} \frac{d\Delta f}{dt} = \frac{2W_0}{f_0} \Delta \dot{f} \end{aligned} \quad (4.33)$$

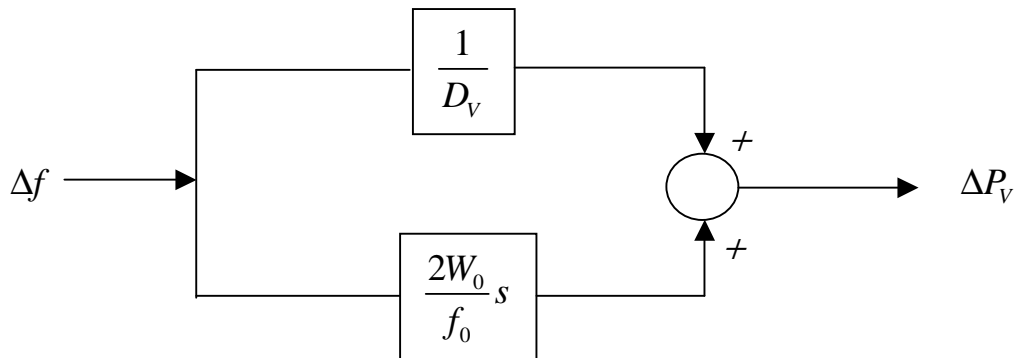


Figure 4.6. Block diagram of the dynamic load model.

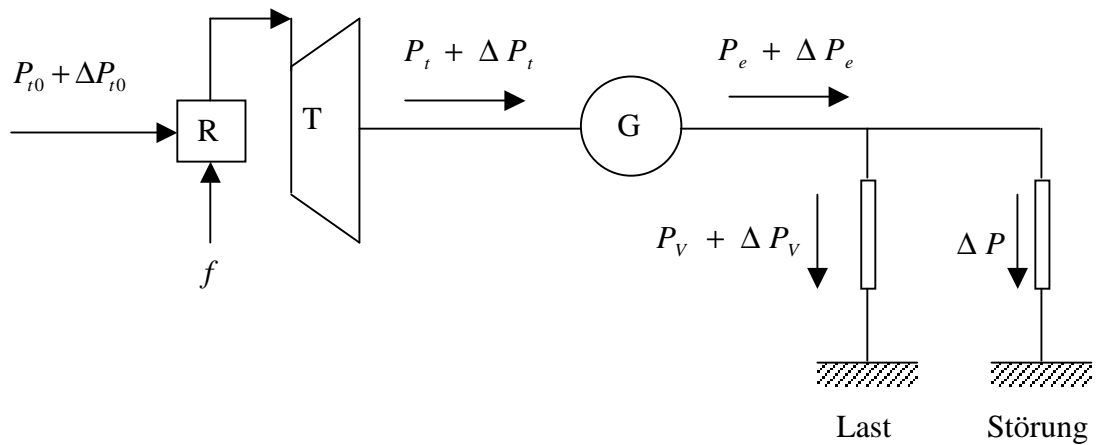


Figure 4.7. System with all generators and loads connected to one node.

The frequency dependency is given by

$$\frac{\partial P_V}{\partial f} \Delta f = \frac{1}{D_V} \Delta f = K_V \Delta f \quad (4.34)$$

The block diagram in Figure 4.6 describes the load model.

Total System The system in Figure 4.7 can now be described by the block diagram in Figure 4.8.

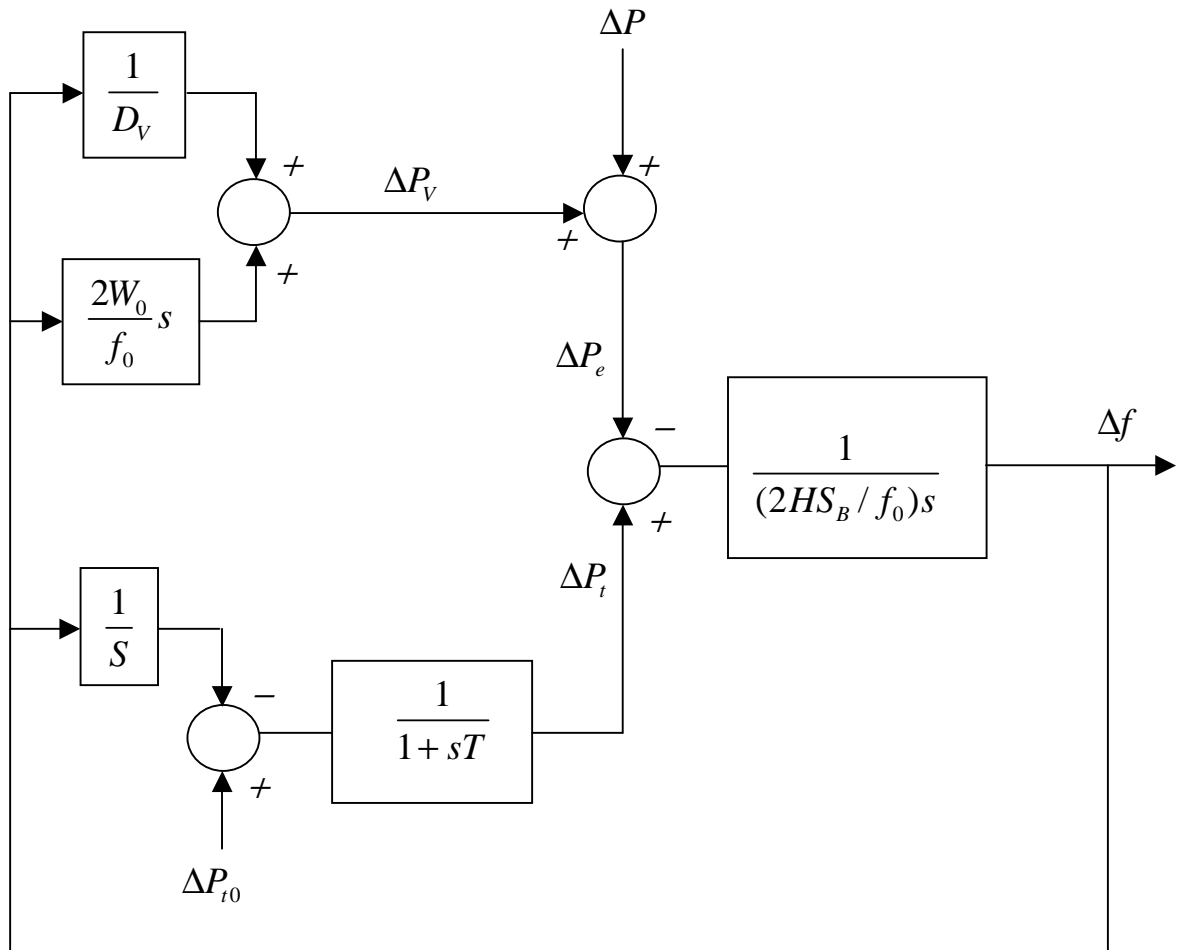


Figure 4.8. Block diagram of the system in Figure 4.7.

Dynamic Behaviour From the block diagram in Figure 4.8 it is straightforward to derive the transfer function between ΔP and Δf ($\Delta P_{t_0} = 0$):

$$\Delta f = -\frac{1 + sT}{\frac{1}{S} + \frac{1}{D_V}(1 + sT) + \left(\frac{2W_0}{f_0} + \frac{2HS_B}{f_0}\right)s(1 + sT)}\Delta P \quad (4.35)$$

The step response for

$$\Delta P(s) = \frac{\Delta z}{s} \quad (4.36)$$

is given in Figure 4.9. The frequency deviation in steady steady state is

$$\Delta f_\infty = \lim_{s \rightarrow 0}(s \cdot \Delta f) = \frac{-\Delta z}{\frac{1}{S} + \frac{1}{D_V}} = \frac{-\Delta z}{\frac{1}{D_R}} = -\Delta z \cdot D_R \quad (4.37)$$

with

$$\frac{1}{D_R} = \frac{1}{S} + \frac{1}{D_V} \quad (4.38)$$

In order to calculate an equivalent time constant, T_f , T is put to 0. This can be done since for realistic systems

$$T \ll T_M = \frac{f_0}{S_B} \left(\frac{2W_0}{f_0} + \frac{2HS_B}{f_0} \right) \quad (4.39)$$

This means that the transfer function in eq. (4.35) can be approximated by a first order function

$$\Delta f = \frac{-\Delta P}{\frac{1}{D_R} + T_M \frac{S_B}{f_0} s} = \frac{-1}{1 + T_M D_R \frac{S_B}{f_0} s} D_R \Delta P \quad (4.40)$$

or

$$\Delta f = \frac{1}{1 + T_M D_R \frac{S_B}{f_0} s} \Delta f_\infty \quad (4.41)$$

with

$$T_f = T_M D_R \frac{S_B}{f_0} \quad (4.42)$$

as the equivalent time constant.

$$T_M = \frac{f_0}{S_B} \left(\frac{2W_0}{f_0} + \frac{2HS_B}{f_0} \right) \quad (4.43)$$

with

$$\frac{1}{D_R} = \frac{1}{S} + \frac{1}{D_V} \quad (4.44)$$

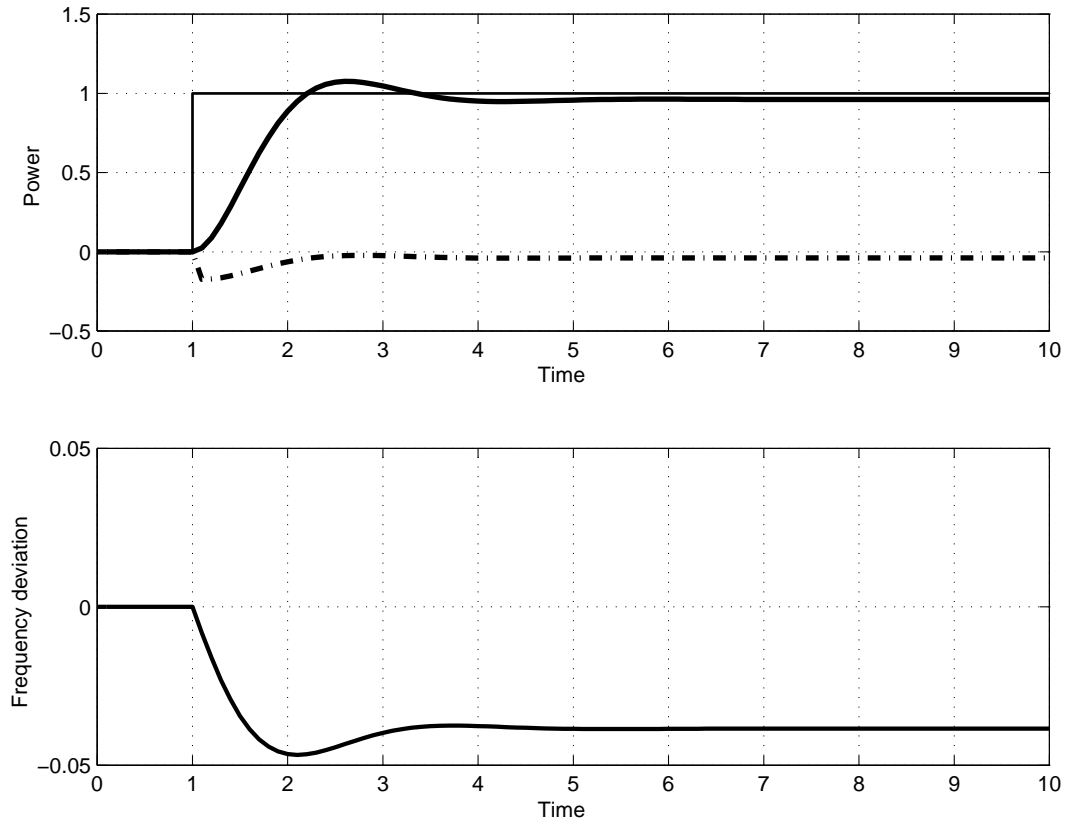


Figure 4.9. The step response for a one node system. The upper diagram shows the step function, the increase in turbine power (solid), and the load variation (dashed). The lower diagram shows the frequency deviation.

Example

- $S_B = 4000$ MW
- $f_0 = 50$ Hz
- $S = 4\% = 0.04 \frac{f_0}{S_B} = \frac{0.04 \cdot 50}{4000}$ Hz/MW
- $D_V = \frac{50}{4000}$ Hz/MW
- $\Delta z = 400$ MW
- $T_M = 10$ s

Then follows

$$\Delta f_\infty = -\frac{1}{\frac{4000}{2} + \frac{4000}{50}} 400 = -0.192 \text{ Hz} \quad (4.45)$$

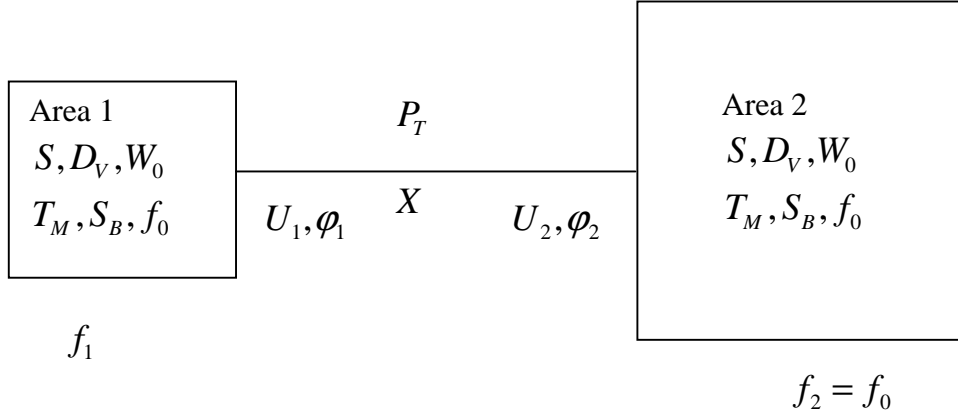


Figure 4.10. Model of a two area system. System 1 is much smaller than system 2.

and

$$T_f = 10 \frac{1}{\frac{4000}{2} + \frac{4000}{50}} \frac{4000}{50} = 0.38\text{s} \quad (4.46)$$

4.2.2 Two Area System

We will now study the behaviour in a two area system. Each area could be modelled as in the previous subsection. The two areas are connected with a tie line over which power can be exchanged.

We will first consider the case without AGC. It is further assumed that one of the areas is much smaller than the other. The bigger of the two areas can then be regarded as an infinite bus in our analysis. It will now be studied the behaviour after a load change in the smaller system, system 1. The system to be studied, with notation, is depicted in Figure 4.10.

The tie line power is given by

$$P_T = \frac{U_1 U_2}{X} \sin(\varphi_1 - \varphi_2) \quad (4.47)$$

where X is the (equivalent) reactance of the tie line. For small deviations one gets (U_1 and U_2 are constant)

$$\Delta P_T = \frac{\partial P_T}{\partial \varphi_1} \Delta \varphi_1 + \frac{\partial P_T}{\partial \varphi_2} \Delta \varphi_2 = \frac{U_1 U_2}{X} \cos(\varphi_{10} - \varphi_{20}) (\Delta \varphi_1 - \Delta \varphi_2) \quad (4.48)$$

or

$$\Delta P_T = \hat{P}_T (\Delta \varphi_1 - \Delta \varphi_2) \quad (4.49)$$

with

$$\hat{P}_T = \frac{U_1 U_2}{X} \cos(\varphi_{10} - \varphi_{20}) \quad (4.50)$$

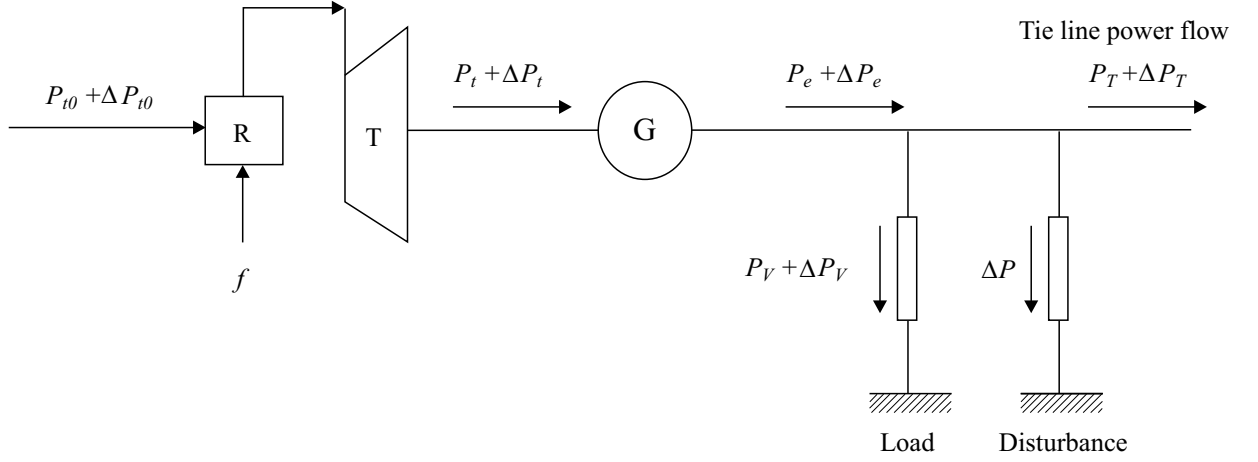


Figure 4.11. Power flow in Area 1 of the two area system.

As system 2 is very big (infinite bus) it follows that

$$\left(\frac{T_M S_B}{f_0}\right)_2 \gg \left(\frac{T_M S_B}{f_0}\right)_1 \Rightarrow f_2 = \text{constant} \Rightarrow \Delta\varphi_2 = 0 \quad (4.51)$$

and consequently

$$\Delta P_T = \hat{P}_T \Delta\varphi_1 = 2\pi \hat{P}_T \int \Delta f_1 dt \quad (4.52)$$

Figure 4.11 shows the power flow and Figure 4.12 the block diagram of the system.

Without secondary frequency control (AGC), i.e. $\Delta P_{t0} = 0$, the following transfer functions apply

$$\Delta f = \frac{-s}{2\pi \hat{P}_T + \left(\frac{1}{D_V} + \frac{1}{S(1+sT)}\right)s + \frac{T_M S_B}{f_0} s^2} \Delta P \quad (4.53)$$

$$\Delta P_T = \frac{2\pi \hat{P}_T}{s} \Delta f \quad (4.54)$$

$$\Delta P_T = \frac{-2\pi \hat{P}_T}{2\pi \hat{P}_T + \left(\frac{1}{D_V} + \frac{1}{S(1+sT)}\right)s + \frac{T_M S_B}{f_0} s^2} \Delta P \quad (4.55)$$

The response for

$$\Delta P(s) = \frac{\Delta z}{s} \quad (4.56)$$

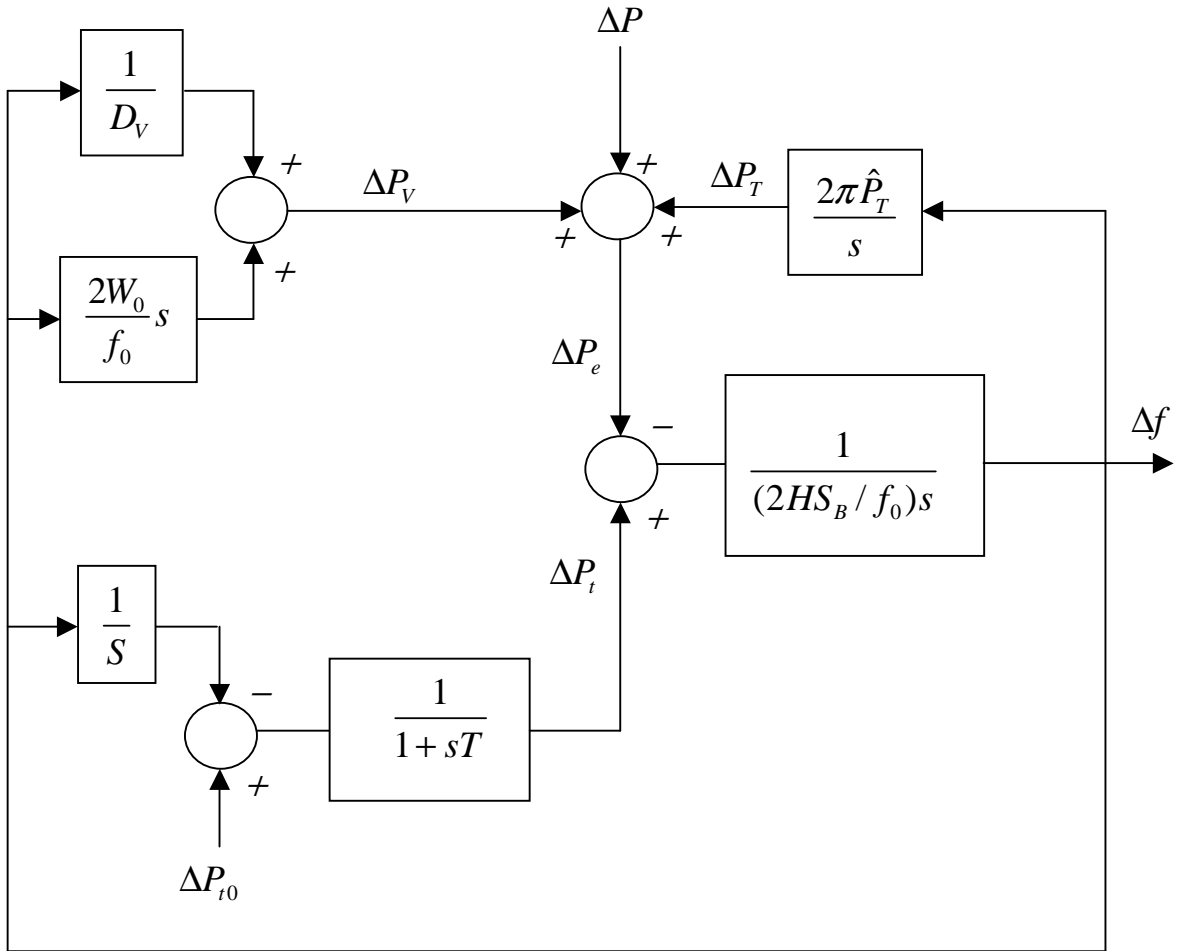


Figure 4.12. Block diagram of Area 1 of the two area system.

is shown in Figure 4.13. The steady state frequency deviation is

$$\Delta f_{\infty} = \lim_{s \rightarrow 0} (s \cdot \Delta f) = 0 \quad (4.57)$$

and the steady state deviation of the tie line power is

$$\Delta P_{T\infty} = \lim_{s \rightarrow 0} (s \cdot \Delta P_T) = -\Delta z \quad (4.58)$$

The infinite bus brings the frequency deviation Δf back to zero, by increasing the tie line power so the load increase is fully compensated.

With secondary control (AGC) one obtains the step response in Figure 4.14. The load increase is in this case fully compensated by the generators in Area 1.

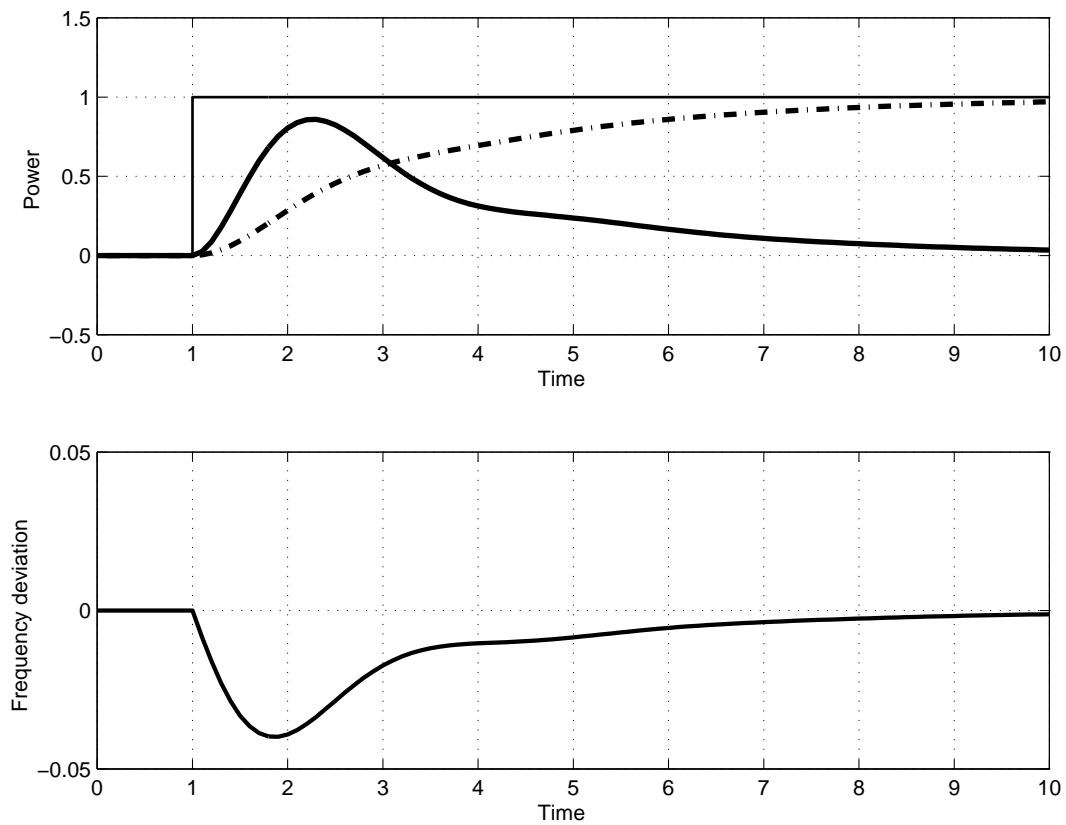


Figure 4.13. Step response for the system in Figure 4.11 without AGC. The upper diagram shows the step in load, the turbine power (solid) and the tie line power (dashed). The lower diagram shows the frequency deviation.

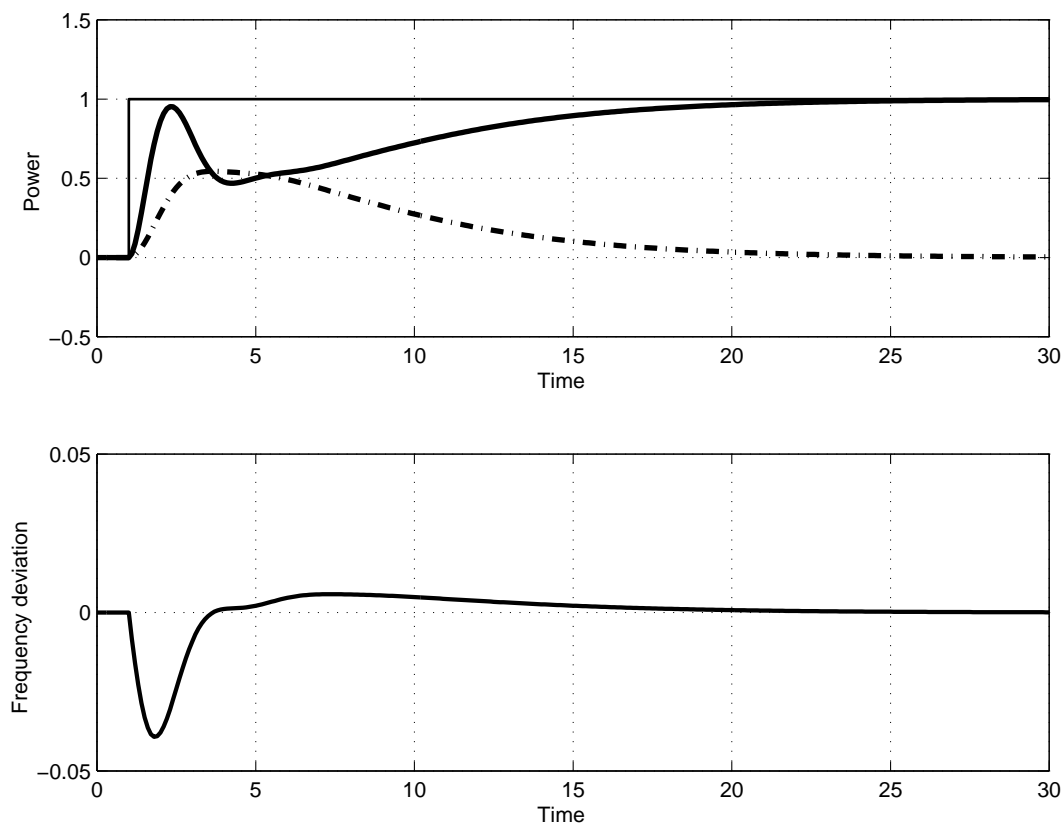


Figure 4.14. Step response for the system in Figure 4.11 with AGC. The upper diagram shows the step in load, the turbine power (solid) and the tie line power (dashed). The lower diagram shows the frequency deviation.

5

Model of the Synchronous Machine

Almost all energy consumed by various loads in an electric power system is produced by synchronous machines, or, more correctly, the conversion from the primary energy sources, like water energy, nuclear energy, or chemical energy, to electrical energy is done in synchronous machines with a mechanical intermediate link, the turbine. This is true in larger power systems, but not always in smaller systems like isolated islands, power supply of equipment in deserts, or other smaller systems. In these systems, the energy can come from asynchronous generators, for example in wind generation units, batteries, or some other source of electrical energy. In systems with synchronous generators, these have an extremely important part in many dynamic phenomena. Thus, it is very important to develop usable and realistic models of the synchronous machines. In the previous chapters, mainly the mechanical properties of the synchronous machines have been modelled using the swing equation, while a very simplistic model of the electrical properties of the synchronous machine has been used. In this chapter, a more general, detailed model of the electric parts of the synchronous machine will be derived. The simple models used earlier will be justified. It should be emphasized that the description here aims towards the development of models usable for studying dynamic phenomena in the power system. It is not the purpose of these models to give a detailed and deep understanding of the physical functions of the synchronous machine. Of course, it is desirable to have a good insight into the physics of the synchronous machine to be able to derive appropriate models. For a detailed discussion of these aspects, books and courses dealing with the theory of electrical machines should be studied.

5.1 Park's Transformation

Park's transformation is a phase transformation (coordinate transformation) between the three physical phases in a three phase system and three new phases, or coordinates, that are convenient for the analysis of synchronous machines. This transformation is also known as the dq-transformation or Blondel's transformation. A reason why the transformation is suitable can be derived from Figure 5.1.

It is obvious that the phase quantities in the a-, b-, and c-phases will vary periodically in steady state. Further, the self and mutual inductances between stator circuits and rotor circuits will vary with the rotor position. Instead of performing all computations in the fixed stator system, the stator

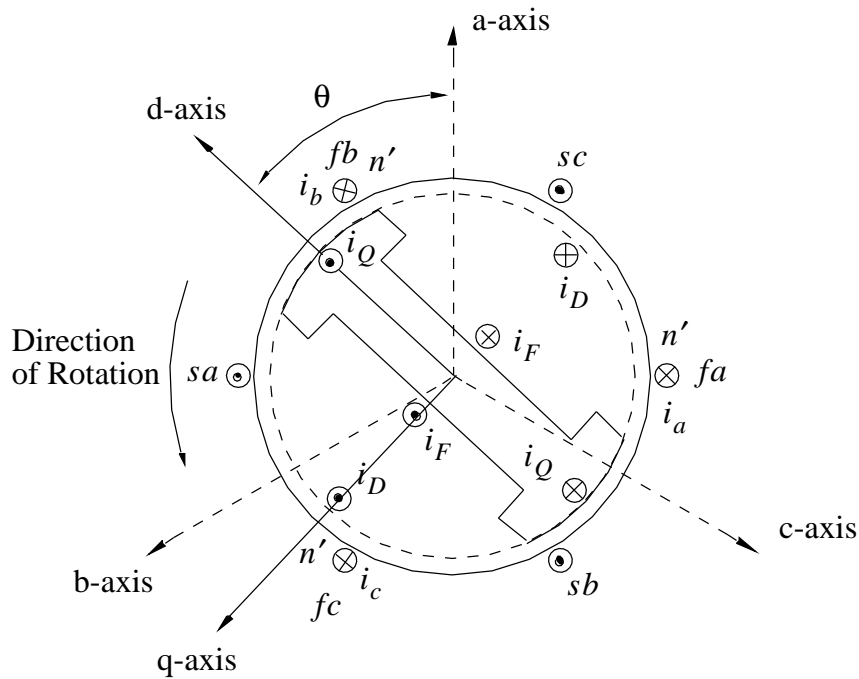


Figure 5.1. Definition of Quantities in Park's Transformation.

quantities voltages, currents, and fluxes can be transformed to a system that rotates with the rotor. Thus, two orthogonal axes are defined as shown in Figure 5.1: One along the axis in which the current in the rotor windings generates a flux, and one in an axis perpendicular to this. The first is the direct axis (d-axis), and the other is the quadrature axis (q-axis). From now on, the denominations d-axis and q-axis will be used. To make the system complete, a third component corresponding to the zero sequence must be defined.

Figure 5.1 is a simplified picture of a synchronous machine and should only be viewed as an intuitive basis for the transformation given below. The machine in Figure 5.1 has one pole pair, but Park's transformation can, of course, be applied to machines with an arbitrary number of pole pairs.

Park's transformation is, as a consequence of the reasoning above, time dependent, and the connection between the phase currents and the trans-

formed currents is given by

$$\begin{cases} i_d = \sqrt{\frac{2}{3}} \left[i_a \cos \theta + i_b \cos \left(\theta - \frac{2\pi}{3} \right) + i_c \cos \left(\theta + \frac{2\pi}{3} \right) \right] , \\ i_q = \sqrt{\frac{2}{3}} \left[-i_a \sin \theta - i_b \sin \left(\theta - \frac{2\pi}{3} \right) - i_c \sin \left(\theta + \frac{2\pi}{3} \right) \right] , \\ i_0 = \sqrt{\frac{1}{3}} (i_a + i_b + i_c) . \end{cases} \quad (5.1)$$

If the a-axis is chosen as reference,

$$\theta = \omega t + \theta_0 \quad (5.2)$$

is obtained and the time dependence in the transformation is obvious. It should be pointed out that i_a , i_b , and i_c are the real physical phase currents as functions of time and not a phasor representation of those. Now,

$$\begin{aligned} x_{abc} &= (x_a, x_b, x_c)^T \\ x_{0dq} &= (x_0, x_d, x_q)^T \end{aligned} \quad (5.3)$$

can be defined. x can here be an arbitrary quantity, like voltage, current, or flux. With this notation, Park's transformation can be written as

$$x_{0dq} = P x_{abc} \quad (5.4)$$

with

$$P = \sqrt{\frac{2}{3}} \begin{pmatrix} 1/\sqrt{2} & 1/\sqrt{2} & 1/\sqrt{2} \\ \cos \theta & \cos(\theta - \frac{2\pi}{3}) & \cos(\theta + \frac{2\pi}{3}) \\ -\sin \theta & -\sin(\theta - \frac{2\pi}{3}) & -\sin(\theta + \frac{2\pi}{3}) \end{pmatrix} . \quad (5.5)$$

The inverse transformation is then given by

$$x_{abc} = P^{-1} x_{0dq} , \quad (5.6)$$

and it can easily be shown that

$$P^{-1} = P^T . \quad (5.7)$$

A mnemonic for Park's transformation can be obtained from Figure 5.1 by projecting the a-, b-, and c-axes onto the d- and q-axes in the figure.

Equation (5.7) implies that Park's transformation is an orthonormal transformation. This is reflected in the expression for the momentary power that is produced in the stator windings

$$\begin{aligned} p &= u_a i_a + u_b i_b + u_c i_c = u_{abc}^T i_{abc} = \\ &= (P^{-1} u_{0dq})^T P^{-1} i_{0dq} = (P^T u_{0dq})^T P^{-1} i_{0dq} = \\ &= u_{0dq}^T P P^{-1} i_{0dq} = u_{0dq}^T i_{0dq} = \\ &= u_0 i_0 + u_d i_d + u_q i_q . \end{aligned} \quad (5.8)$$

Here, Equations (5.6) and (5.7) have been used. Equation (5.8) can therefore be written as

$$p = u_a i_a + u_b i_b + u_c i_c = u_0 i_0 + u_d i_d + u_q i_q . \quad (5.9)$$

Equation (5.9) shows that the introduced transformation is power invariant, which is a consequence of Equation (5.7).

It should be pointed out that there are several different variants of Park's transformation appearing in literature. They can differ from the form presented here by the direction of the q-axis and by constants in the transformation matrix. When using equations from some book or paper, it is thus important to make sure that the definition of Park's transformation used is the same as one's own. Otherwise, wrong results might be obtained.

The rotor windings produce a flux linkage that mainly lies in the direction of the d-axis. That flux evokes an emf, E , which is lagging by 90° , hence in the direction of the negative q-axis. For generator operation, the phasor for E leads by an angle δ before the phasor for the terminal voltage U . At $t = 0$, the negative q-axis thus leads by an angle δ before the phasor for the voltage along the a-axis, cf. Figure 5.1. For $t > 0$, the d- and q-axes have moved by an angle ωt with the angular speed of the rotor ω . The rotor's d-axis will hence be in position

$$\theta = \omega t + \delta + \frac{\pi}{2} . \quad (5.10)$$

It is particularly of interest to study how zero sequence, negative sequence, and positive sequence quantities are transformed by Park's transformation. It is comparatively easy to show that a pure zero sequence quantity only leads to a contribution in x_0 with $x_d = x_q = 0$. A pure positive sequence quantity

$$x_{abc}(+) = \sqrt{2}x \begin{pmatrix} \sin(\theta + \alpha) \\ \sin(\theta + \alpha - \frac{2\pi}{3}) \\ \sin(\theta + \alpha + \frac{2\pi}{3}) \end{pmatrix} \quad (5.11)$$

is transformed to

$$x_{0dq}(+) = \sqrt{3}x \begin{pmatrix} 0 \\ \sin(\alpha) \\ -\cos(\alpha) \end{pmatrix} , \quad (5.12)$$

i.e. pure DC-quantities (time independent) in the dq-system with the zero sequence component equal zero. A pure negative sequence quantity gives rise to quantities in d- and q-directions that vary with the angular frequency 2ω . The zero sequence component vanishes also in this case. (Show this!)

5.2 The Inductances of the Synchronous Machine

In the following, a synchronous machine with one damper winding in d– and one in q–axis and, of course, a field winding is considered. Quantities related to these windings are denoted with the indices D, Q, and F, respectively. The flux linkages in the stator windings and in the windings F, D, and Q depend on the currents in these windings according to

$$\begin{pmatrix} \Psi_{abc} \\ \Psi_{FDQ} \end{pmatrix} = \begin{pmatrix} L_{abc,abc} & L_{abc,FDQ} \\ L_{FDQ,abc} & L_{FDQ,FDQ} \end{pmatrix} \begin{pmatrix} i_{abc} \\ i_{FDQ} \end{pmatrix}. \quad (5.13)$$

$L_{abc,abc}, \dots, L_{FDQ,FDQ}$ are 3×3 matrices with self and mutual inductances as matrix elements. These matrices will depend on the rotor position, hence they are time dependent. It can be shown that the inductances in these matrices can be approximated by

$L_{abc,abc}$:

$$\begin{cases} L_{aa} = L_s + L_m \cos 2\theta, \\ L_{bb} = L_s + L_m \cos(2\theta - \frac{4\pi}{3}), \\ L_{cc} = L_s + L_m \cos(2\theta + \frac{4\pi}{3}), \\ L_{ab} = L_{ba} = -M_s - L_m \cos(2\theta + \frac{\pi}{3}), \\ L_{bc} = L_{cb} = -M_s - L_m \cos(2\theta + \pi), \\ L_{ac} = L_{ca} = -M_s - L_m \cos(2\theta + \frac{5\pi}{3}). \end{cases} \quad (5.14)$$

$L_{abc,FDQ}$ and $L_{FDQ,abc}$:

$$\begin{cases} L_{aF} = L_{Fa} = M_F \cos \theta, \\ L_{bF} = L_{Fb} = M_F \cos(\theta - \frac{2\pi}{3}), \\ L_{cF} = L_{Fc} = M_F \cos(\theta + \frac{2\pi}{3}), \\ \\ L_{aD} = L_{Da} = M_D \cos \theta, \\ L_{bD} = L_{Db} = M_D \cos(\theta - \frac{2\pi}{3}), \\ L_{cD} = L_{Dc} = M_D \cos(\theta + \frac{2\pi}{3}), \\ \\ L_{aQ} = L_{Qa} = -M_Q \sin \theta, \\ L_{bQ} = L_{Qb} = -M_Q \sin(\theta - \frac{2\pi}{3}), \\ L_{cQ} = L_{Qc} = -M_Q \sin(\theta + \frac{2\pi}{3}). \end{cases} \quad (5.15)$$

$L_{FDQ,FDQ}$:

$$\begin{cases} L_{FF} = L_F, \\ L_{DD} = L_D, \\ L_{QQ} = L_Q, \\ \\ L_{FD} = L_{DF} = M_R, \\ L_{FQ} = L_{QF} = 0, \\ L_{DQ} = L_{QD} = 0. \end{cases} \quad (5.16)$$

All inductances with only one index in Equations (5.14)–(5.16) are constants and depend on the design of the synchronous machine. The resulting inductances are of course, as mentioned before, not quite exact. They can be called exact in an ideal machine, where spatial harmonics and other unsymmetries are neglected. For a real synchronous machine, the approximations are usually very good and lead to fully acceptable results for the computations and analyses treated here. It should be emphasized that the model developed here is for use in computations where the synchronous machines are part of a larger system. The model is not primarily aimed at studies of the internal quantities in the generator.

It is now natural to transform the abc-components in Equation (5.13) to 0dq-components. For this, an extended transformation given by

$$P_{ex} = \begin{pmatrix} P & 0 \\ 0 & I \end{pmatrix}, \quad (5.17)$$

with P according to (5.5) and a 3×3 unit matrix I is used. The result is

$$\begin{pmatrix} \Psi_{0dq} \\ \Psi_{FDQ} \end{pmatrix} = \begin{pmatrix} L_{0dq,0dq} & L_{0dq,FDQ} \\ L_{FDQ,0dq} & L_{FDQ,FDQ} \end{pmatrix} \begin{pmatrix} i_{0dq} \\ i_{FDQ} \end{pmatrix}, \quad (5.18)$$

with the inductance matrix given by

$$\begin{pmatrix} L_{0dq,0dq} & L_{0dq,FDQ} \\ L_{FDQ,0dq} & L_{FDQ,FDQ} \end{pmatrix} = \begin{pmatrix} P & 0 \\ 0 & I \end{pmatrix} \begin{pmatrix} L_{abc,abc} & L_{abc,FDQ} \\ L_{FDQ,abc} & L_{FDQ,FDQ} \end{pmatrix} \begin{pmatrix} P^{-1} & 0 \\ 0 & I \end{pmatrix}. \quad (5.19)$$

The virtue of the Park's transformation is apparent in the following equation, where the inductance matrix in (5.18) is computed

$$L_{0dq,0dq} = \begin{pmatrix} L_0 & 0 & 0 \\ 0 & L_d & 0 \\ 0 & 0 & L_q \end{pmatrix}, \quad (5.20)$$

with

$$\begin{cases} L_0 = L_s - 2M_s, \\ L_d = L_s + M_s + \frac{3}{2}L_m, \\ L_q = L_s + M_s - \frac{3}{2}L_m, \end{cases} \quad (5.21)$$

and

$$L_{0dq,FDQ} = \begin{pmatrix} 0 & 0 & 0 \\ kM_F & kM_d & 0 \\ 0 & 0 & kM_q \end{pmatrix}, \quad (5.22)$$

where

$$k = \sqrt{\frac{3}{2}} \quad (5.23)$$

and, of course,

$$L_{FDQ,0dq} = L_{0dq,FDQ}^T. \quad (5.24)$$

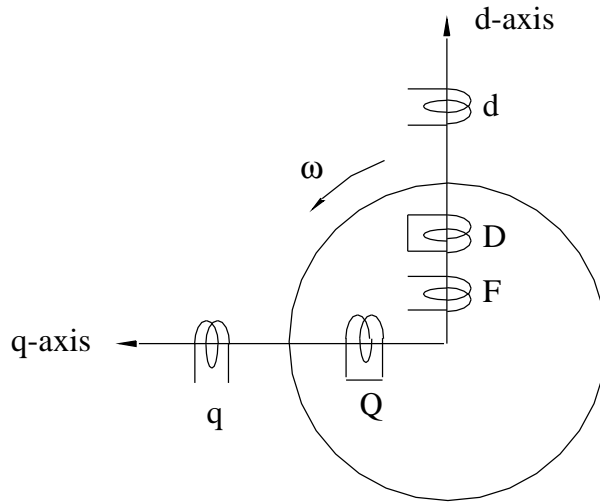


Figure 5.2. Schematic Picture of the Transformed System. (One Damper Winding in the d-Axis and One in the q-Axis.)

$L_{FDQ,FDQ}$ has, of course, not changed, but for completeness it is repeated here.

$$L_{FDQ,FDQ} = \begin{pmatrix} L_F & M_R & 0 \\ M_R & L_D & 0 \\ 0 & 0 & L_Q \end{pmatrix}. \quad (5.25)$$

Two important observations can be made from Equations (5.20)–(5.25):

- The inductances in the inductance matrix in Equation (3.18) are not dependent on time.
- The quantities in d- and q-directions are decoupled. (The induction matrix is block diagonal: one 2×2 matrix and one 1×1 matrix.)

The second observation above leads to a picture of the transformed system according to Figure 5.2.

5.3 Voltage Equations for the Synchronous Machine

For the three stator circuits and the three rotor circuits the following relations can be written:

$$\begin{cases} u_a = -r_a i_a - \dot{\Psi}_a, \\ u_b = -r_b i_b - \dot{\Psi}_b, \\ u_c = -r_c i_c - \dot{\Psi}_c, \end{cases} \quad (5.26)$$

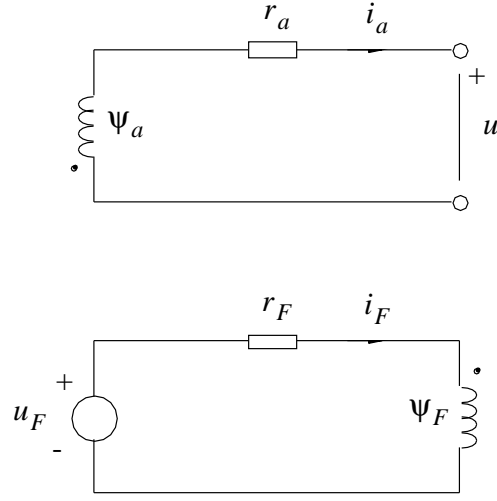


Figure 5.3. Sign Convention for Stator and Rotor Circuits.

and

$$\begin{cases} u_F = r_F i_F + \dot{\Psi}_F , \\ 0 = r_D i_D + \dot{\Psi}_D , \\ 0 = r_Q i_Q + \dot{\Psi}_Q . \end{cases} \quad (5.27)$$

Equations (5.26) and (5.27) can be written more compactly in vector form,

$$\begin{pmatrix} u_{abc} \\ u_{FDQ} \end{pmatrix} = - \begin{pmatrix} R_{abc} & 0 \\ 0 & R_{FDQ} \end{pmatrix} \begin{pmatrix} i_{abc} \\ i_{FDQ} \end{pmatrix} - \begin{pmatrix} \dot{\Psi}_{abc} \\ \dot{\Psi}_{FDQ} \end{pmatrix} . \quad (5.28)$$

The vector u_{FDQ} is defined as

$$u_{FDQ} = (-u_F, 0, 0)^T , \quad (5.29)$$

while the other vectors are defined as before. R_{abc} and R_{FDQ} are diagonal 3×3 matrices.

If Equation (5.28) is multiplied by P_{ex} according to Equation (5.17), all quantities are transformed to the dq-system, i.e.

$$\begin{pmatrix} u_{0dq} \\ u_{FDQ} \end{pmatrix} = - \begin{pmatrix} PR_{abc}P^{-1} & 0 \\ 0 & R_{FDQ} \end{pmatrix} \begin{pmatrix} i_{0dq} \\ i_{FDQ} \end{pmatrix} - \begin{pmatrix} P\dot{\Psi}_{abc} \\ \dot{\Psi}_{FDQ} \end{pmatrix} . \quad (5.30)$$

The matrix $PR_{abc}P^{-1}$ is denoted R_{0dq} , and if $r_a = r_b = r_c = r$, which in most cases is true,

$$R_{0dq} = R_{abc} = rI \quad (5.31)$$

is valid.

To get Equation (5.30) expressed solely in dq-quantities, also the last term on the right hand side must be expressed in these. Since P is time dependent, it is important to remember that

$$\dot{P} \neq 0 , \quad (5.32)$$

which leads to

$$\dot{\Psi}_{0dq} = \frac{d}{dt}(P\Psi_{abc}) = \dot{P}\Psi_{abc} + P\dot{\Psi}_{abc} , \quad (5.33)$$

and thus

$$P\dot{\Psi}_{abc} = \dot{\Psi}_{0dq} - \dot{P}\Psi_{abc} = \dot{\Psi}_{0dq} - \dot{P}P^{-1}\Psi_{0dq} . \quad (5.34)$$

Equation (5.30) can hence be written as

$$\begin{pmatrix} u_{0dq} \\ u_{FDQ} \end{pmatrix} = - \begin{pmatrix} R_{0dq} & 0 \\ 0 & R_{FDQ} \end{pmatrix} \begin{pmatrix} i_{0dq} \\ i_{FDQ} \end{pmatrix} - \begin{pmatrix} \dot{\Psi}_{0dq} \\ \dot{\Psi}_{FDQ} \end{pmatrix} + \begin{pmatrix} \dot{P}P^{-1}\Psi_{0dq} \\ 0 \end{pmatrix} . \quad (5.35)$$

Some trivial computations show that the matrix $\dot{P}P^{-1}$ can be expressed as

$$\dot{P}P^{-1} = \begin{pmatrix} 0 & 0 & 0 \\ 0 & 0 & \omega \\ 0 & -\omega & 0 \end{pmatrix} . \quad (5.36)$$

The voltage equations in the dq-system can thus be written in component form as

$$\begin{cases} u_0 = -ri_0 - \dot{\Psi}_0 , \\ u_d = -ri_d - \dot{\Psi}_d + \omega\Psi_q , \\ u_q = -ri_q - \dot{\Psi}_q - \omega\Psi_d , \end{cases} \quad (5.37)$$

and

$$\begin{cases} u_F = -r_F i_F - \dot{\Psi}_F , \\ 0 = -r_D i_D - \dot{\Psi}_D , \\ 0 = -r_Q i_Q - \dot{\Psi}_Q . \end{cases} \quad (5.38)$$

In the previous section, expressions for the dependencies of the flux linkages on the currents in the different windings were derived. To further simplify the expressions that were obtained, the per unit system for the different windings is now introduced so that all mutual inductances in the d-axis are equal, and all in the q-axis are equal. (In our case, only one damping winding in the q-axis was considered, but in a more general case several damper windings can be considered.) We introduce

$$\begin{aligned} \sqrt{\frac{3}{2}}M_F &= \sqrt{\frac{3}{2}}M_D = M_R = L_{AD} , \\ \sqrt{\frac{3}{2}}M_Q &= L_{AQ} . \end{aligned} \quad (5.39)$$

The different fluxes can then be written as

$$\begin{cases} \Psi_0 = L_0 i_0 , \\ \Psi_d = L_d i_d + L_{AD}(i_F + i_D) , \\ \Psi_q = L_q i_q + L_{AQ} i_Q , \end{cases} \quad (5.40)$$

and

$$\begin{cases} \Psi_F = L_F i_F + L_{AD}(i_d + i_D) , \\ \Psi_D = L_D i_D + L_{AD}(i_d + i_F) , \\ \Psi_Q = L_Q i_Q + L_{AQ} i_q . \end{cases} \quad (5.41)$$

Equations (5.37) and (5.38) together with Equations (5.40) and (5.41) now describe the electrical dynamics of a synchronous machine completely. These equations together with a description of the external system unequivocally determine the behaviour of the synchronous machine during different disturbances. In Figure 5.4, a graphical description of these equations is given.

In Equation (5.37), we observe that the emf in d- and q-direction consists of two terms: one that is a time derivative of the absolute value of the flux linkage and one that arises because the field winding is rotating. The first of these is usually called stator transient and the other rotational emf. In steady state, the first of these vanishes, and the whole emf is created by the rotation of the field winding. It can be shown that the terms $\dot{\Psi}_d$ and $\dot{\Psi}_q$ are in most applications much smaller than $\omega\Psi_d$ and $\omega\Psi_q$, which justifies that the first ones are often neglected.

5.4 Synchronous, Transient, and Subtransient Inductances, and Time Constants.

The complete description of the synchronous machine given in the previous section can be simplified and made more physical if a number of new parameters that can be expressed in the already defined ones are introduced. In steady state and a sufficiently long time after a disturbance, the currents in the damper windings vanish, and the inductances treated in this section describe how the currents are linked with the fluxes directly after a disturbance and in steady state. Further, the time constants that specify how fast the currents in the damper windings decay are derived. Earlier, the synchronous inductances L_d and L_q were defined. They are repeated here for completeness.

$$\begin{cases} L_d = L_s + M_s + \frac{3}{2}L_m \\ L_q = L_s + M_s - \frac{3}{2}L_m \end{cases} \quad (5.42)$$

These inductances describe the synchronous machine in steady state. For a synchronous machine with salient poles, like a hydro power generation unit, $L_m > 0$ and thus $L_d > L_q$, while $L_m \approx 0$ for machines with round rotor leading to $L_d \approx L_q$.

5.4. Synchronous, Transient, and Subtransient Inductances, and Time Constants.67

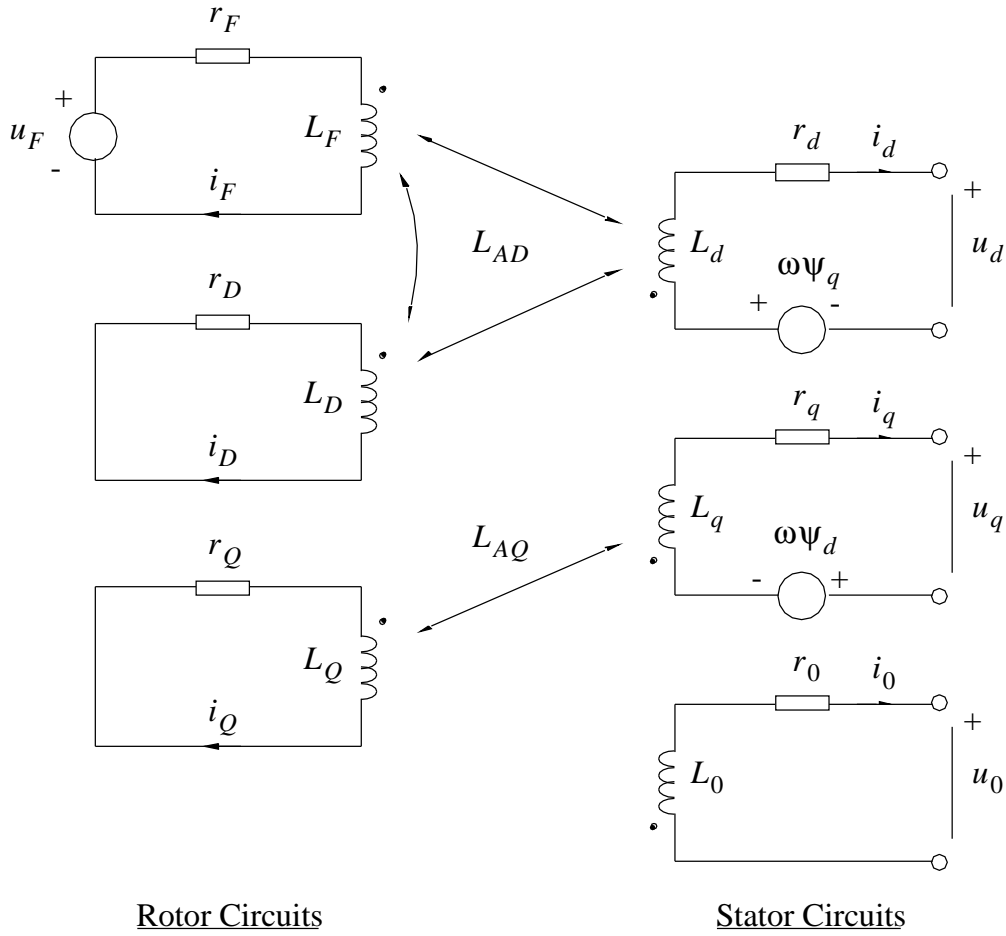


Figure 5.4. Graphical Description of the Voltage Equations and the Linkage between the Equivalent Circuits.

If all rotor windings are short circuited, and a symmetrical three phase voltage is applied on the machine's terminals, the flux linkage in the d-axis initially depends on the subtransient inductance and after a couple of periods on the transient reactance. A voltage is applied to the stator windings,

$$\begin{pmatrix} u_a \\ u_b \\ u_c \end{pmatrix} = \sqrt{2}U \begin{pmatrix} \cos \theta \\ \cos(\theta - \frac{2\pi}{3}) \\ \cos(\theta + \frac{2\pi}{3}) \end{pmatrix} c(t) , \quad (5.43)$$

with a step function $c(t)$, i.e. $c(t) = 0$ for $t < 0$ and $c(t) = 1$ for $t > 0$. If the voltage vector in Equation (5.43) is Park-transformed,

$$\begin{pmatrix} u_0 \\ u_d \\ u_q \end{pmatrix} = \sqrt{3}U \begin{pmatrix} 0 \\ c(t) \\ 0 \end{pmatrix} \quad (5.44)$$

is obtained. For $t = 0+$, that is, directly after the voltage is applied on the terminals, the flux linkages Ψ_F and Ψ_D are still zero, since they cannot change instantly:

$$\begin{cases} 0 = L_F i_F + L_{AD}(i_d + i_D) \\ 0 = L_D i_D + L_{AD}(i_d + i_F) \end{cases} \quad (5.45)$$

From (5.45), i_D and i_F can now be expressed in i_d ,

$$\begin{cases} i_D = -\frac{L_F L_{AD} - L_{AD}^2}{L_F L_D - L_{AD}^2} i_d , \\ i_F = -\frac{L_D L_{AD} - L_{AD}^2}{L_F L_D - L_{AD}^2} i_d . \end{cases} \quad (5.46)$$

The expression for i_D and i_F can be related to Ψ_d in (5.40), giving

$$\Psi_d = \left(L_d - \frac{L_D L_{AD}^2 + L_F L_{AD}^2 - 2L_{AD}^3}{L_F L_D - L_{AD}^2} \right) i_d = L_d'' i_d , \quad (5.47)$$

with the subtransient inductance L_d'' in the d-axis

$$L_d'' = L_d - \frac{L_D + L_F - 2L_{AD}}{L_F L_D / L_{AD}^2 - 1} . \quad (5.48)$$

The subtransient inductance in the d-axis, L_d'' , is thus defined as the initial flux linkage of the stator current in per unit, when all rotor windings are short-circuited and with no current flowing in them before the disturbance.

If there is no damper winding in the d-axis, or if the current in the damper winding has decayed to zero, i.e. $i_D = 0$, the same reasoning and the same computations as above lead to

$$\Psi_d = \left(L_d - \frac{L_{AD}^2}{L_F} \right) i_d = L_d' i_d , \quad (5.49)$$

with the transient inductance in the d-axis, L_d' , defined as

$$L_d' = L_d - \frac{L_{AD}^2}{L_F} . \quad (5.50)$$

Show this!

The transient inductance in the d-axis, L_d' , is thus defined as the flux linkage in the d-axis in per unit of the stator current with the assumptions above. For a machine with damper windings, that is the flux some periods after the “disturbance” when the current in the damper winding has vanished. The time constant for this is derived later.

An equivalent analysis to that above can be performed for the q-axis, but, since no field winding exists in the q-axis, the terminology is somewhat

5.4. Synchronous, Transient, and Subtransient Inductances, and Time Constants.69

different. For a machine with salient poles and damper winding in the q-axis, the effective inductance after the current in the damper winding has decayed is practically equal to the synchronous inductance. Hence it is sometimes said that, for machines with salient poles, the transient and synchronous inductances in the q-axis are equal.

If the reasoning above is repeated with the modification that $\cos \theta$ in Equation (5.43) is changed to $\sin \theta$ etc., one obtains that

$$L_q'' = L_q - \frac{L_{AQ}^2}{L_Q} \quad (5.51)$$

for a synchronous machine with an equivalent damper winding in the q-axis. According to the reasoning above,

$$L_q' = L_q \quad . \quad (5.52)$$

If one additional damper winding is introduced into the q-axis, a value of L_q' can be defined that is different from L_q . In general, for the inductances defined,

$$\begin{aligned} L_d'' &< L_d' < L_d \quad , \\ L_q'' &< L_q' < L_q \quad . \end{aligned} \quad (5.53)$$

(For the derivation of relationships defining L_q' and L_q'' if more than one damper winding in the q-axis is modelled, we refer to books on the theory of electrical machines.)

The time constants that determine how fast transients in the rotor windings decay after a disturbance are easiest to compute if it is assumed that the stator circuits are open, i.e. $i_a = i_b = i_c = 0$, or equivalently $i_0 = i_d = i_q = 0$. This is not consistent with the derivation above, but the obtained results can be used to compute the time constants that are valid when the generator is connected to a network. The time constants that will be derived here are those normally specified by the manufacturer of the generator and are easily obtained by measurements.

Suppose now that the stator windings are open and look at a step in the field voltage at the time $t = 0$, i.e. $u_F = U_F c(t)$.

$$\begin{cases} r_f i_f + \dot{\Psi}_F = U_F c(t) \\ r_D i_D + \dot{\Psi}_D = 0 \end{cases} \quad (5.54)$$

Since $i_d = 0$,

$$\begin{cases} \Psi_D = L_D i_D + L_{AD} i_F \quad , \\ \Psi_F = L_F i_F + L_{AD} i_D \quad . \end{cases} \quad (5.55)$$

At $t = 0+$, $\Psi_D = 0$ and thus

$$i_F(0+) = -\frac{L_D}{L_{AD}} i_D(0+) \quad . \quad (5.56)$$

	Round Rotor	Salient Pole
x_d (p.u.)	1.0 – 2.3	0.6 – 1.5
x_q (p.u.)	1.0 – 2.3	0.4 – 1.0
x'_d (p.u.)	0.15 – 0.4	0.2 – 0.5
x''_d (p.u.)	0.12 – 0.25	0.15 – 0.35
x'_q (p.u.)	0.3 – 1.0	—
x''_q (p.u.)	0.12 – 0.25	0.2 – 0.45
T'_{do} (s)	3.0 – 10.0	1.5 – 9.0
T''_{do} (s)	0.02 – 0.05	0.01 – 0.05
T'_{qo} (s)	0.5 – 2.0	—
T''_{qo} (s)	0.02 – 0.05	0.01 – 0.09
H (s)	3 – 5 ($n = 3000$ rpm) 5 – 8 ($n = 1500$ rpm)	1.5 – 5

Table 5.1. Typical Values for Some Parameters of Synchronous Machines.

The current $i_F(0+)$ can now be eliminated from the equations, which leads to

$$\frac{di_D}{dt} + \frac{r_D}{L_D - L_{AD}^2/L_F} i_D = -U_F \frac{L_{AD}/L_F}{L_D - L_{AD}^2/L_F} . \quad (5.57)$$

Here, it has been assumed that $r_D \gg r_F$, which generally is true. The subtransient time constant of the open circuit in the d-axis, T''_{do} , can now be defined as

$$T''_{do} = \frac{L_D - L_{AD}^2/L_F}{r_D} . \quad (5.58)$$

When i_D has vanished, i.e. when $i_D = 0$, the field current is determined solely by the upper of Equations (5.54), and the transient time constant of the open circuit, T'_{do} , is given by

$$T'_{do} = L_F/r_F . \quad (5.59)$$

Accordingly, for a synchronous machine with a damper winding in the q-axis,

$$T''_{qo} = L_Q/r_Q \quad (5.60)$$

is defined.

The quantities introduced in this section are important parameters of a machine and are usually given by the manufacturer of the machine. The reasons for this are that they are easily measured and that they are introduced in a natural way into the simplified models we will derive in the next section. In Table 5.1, typical values for some of the discussed parameters for different types and sizes of synchronous machines are given. Reactances instead of inductances are given in Table 5.1, i.e. $x_d = \omega_0 L_d$ etc., with $\omega_0 = 2\pi f_0$.

5.5 Simplified Models of the Synchronous Machine

A complete and exact model of the synchronous machine, considering the assumptions and approximations made, was presented in Sections 3.2 and 3.3. If the synchronous machine is simulated in, for example, a stability program, these are often the equations used to model the synchronous machine. Nevertheless, it is, for several reasons, often meaningful to use models that comprise more simplifications and approximations than those derived earlier. If a better insight into a problem is wanted or if a problem is analyzed without using computer simulations, simplified representations of the synchronous machine are often the only possibility. Here, such a model will be derived under the following assumptions:

- The stator transients are neglected, i.e. we set $\dot{\Psi}_d = \dot{\Psi}_q = 0$.
- The d-axis contains no damper windings.
- In the q-axis, one damper winding is modelled.

With these assumptions, the synchronous machine is described by the equations

$$\begin{cases} \Psi_d = L_d i_d + L_{AD} i_F , \\ \Psi_q = L_q i_q + L_{AQ} i_Q , \\ \Psi_F = L_F i_F + L_{AD} i_d , \\ \Psi_Q = L_Q i_Q + L_{AQ} i_q , \end{cases} \quad (5.61)$$

$$\begin{cases} u_F = r_F i_F + \dot{\Psi}_F , \\ 0 = r_Q i_Q + \dot{\Psi}_Q , \end{cases} \quad (5.62)$$

$$\begin{cases} u_d = -r i_d + \omega \Psi_q , \\ u_q = -r i_q - \omega \Psi_d . \end{cases} \quad (5.63)$$

For completeness, some relations defined above are repeated here.

$$\begin{cases} L'_d = L_d - L_{AD}^2 / L_F \\ L''_q = L_q - L_{AQ}^2 / L_Q \end{cases} \quad (5.64)$$

The goal is now to eliminate all quantities with indices F and Q , except for u_F , from the equations above to get a model that can be used to represent the synchronous machine as a component in a system. That means that the only quantities that should be present in the model are stator voltages, the stator current, and u_F , which is a control variable that can be changed by the excitation system as described in Chapter 6.

From the Equations (5.61), i_Q is eliminated, which leads to

$$\Psi_q - \frac{L_{AQ}}{L_Q} \Psi_Q = L''_q i_q . \quad (5.65)$$

Now, by defining

$$e'_d = \omega \frac{L_{AQ}}{L_Q} \Psi_Q \quad , \quad (5.66)$$

Equation (5.65) can be written as

$$\Psi_q - e'_d/\omega = L''_q i_q \quad . \quad (5.67)$$

Equivalent derivations can be done for the rotor circuit in the d-axis, i.e. for the field winding.

$$\Psi_d - \frac{L_{AD}}{L_F} \Psi_F = L'_d i_d \quad (5.68)$$

is obtained, which, using the definition

$$e'_q = -\omega \frac{L_{AD}}{L_F} \Psi_F \quad , \quad (5.69)$$

can be written as

$$\Psi_d + e'_q/\omega = L'_d i_d \quad . \quad (5.70)$$

Now, the quantities

$$\begin{cases} e_d = \omega L_{AQ} i_Q \quad , \\ e_q = -\omega L_{AD} i_F \end{cases} \quad (5.71)$$

are introduced. From the equations above, the relationships

$$\begin{cases} e_d = e'_d - (x_q - x''_q) i_q \quad , \\ e_q = e'_q + (x_d - x'_d) i_d \quad , \end{cases} \quad (5.72)$$

with $x_d = \omega L_d$ etc. can be obtained.

According to Equations (5.71) and (5.72),

$$i_Q = \frac{e'_d - (x_q - x''_q) i_q}{\omega L_{AQ}} \quad . \quad (5.73)$$

Substituting this into (5.62) gives

$$r_Q \frac{e'_d - (x_q - x''_q) i_q}{\omega L_{AQ}} + \frac{L_Q}{\omega L_{AQ}} \dot{e}'_d = 0 \quad , \quad (5.74)$$

or, assuming $\dot{\omega} = 0$,

$$T''_{qo} \dot{e}'_d + e'_d - (x_q - x''_q) i_q = 0 \quad . \quad (5.75)$$

For the rotor circuit in the d-axis, i.e. for the exciter winding, accordingly

$$T''_{do} \dot{e}'_q + e'_q + (x_d - x'_d) i_d = -\frac{\omega L_{AD}}{r_F} u_F \quad (5.76)$$

is obtained, which, using

$$e_F = \frac{\omega L_{AD}}{r_F} u_F \quad , \quad (5.77)$$

can be written as

$$T''_{do} \dot{e}'_q + e'_q + (x_d - x'_d) i_d = -e_F \quad . \quad (5.78)$$

If Equations (5.75) and (5.78) are Laplace-transformed and the voltage equation (5.63) is rewritten with the introduced quantities, we obtain

$$\begin{pmatrix} u_d \\ u_q \end{pmatrix} = \begin{pmatrix} e'_d \\ e'_q \end{pmatrix} + \begin{pmatrix} -r_d & x''_q \\ -x'_d & -r_q \end{pmatrix} \begin{pmatrix} i_d \\ i_q \end{pmatrix} \quad , \quad (5.79)$$

with e'_d given by

$$e'_d = \frac{(x_q - x''_q) i_q}{1 + sT''_{qo}} \quad (5.80)$$

and e'_q from

$$e'_q = -\frac{e_F + (x_d - x'_d) i_d}{1 + sT''_{do}} \quad . \quad (5.81)$$

This model, i.e. Equations (5.79)–(5.81), together with the swing equation, are often called the fourth order model. This model of the synchronous machine demands, with the assumptions made here, four state variables: e'_d and e'_q and the “mechanical” quantities ω and δ .

Often, also the damper winding in the q-axis can be neglected. That leads to a third order model, which can be written as

$$\begin{pmatrix} u_d \\ u_q \end{pmatrix} = \begin{pmatrix} 0 \\ e'_q \end{pmatrix} + \begin{pmatrix} -r_d & x_q \\ x'_d & -r_q \end{pmatrix} \begin{pmatrix} i_d \\ i_q \end{pmatrix} \quad , \quad (5.82)$$

with e'_q according to Equation (5.81).

6

The Excitation System of the Synchronous Machine

In this chapter, a short description of the function and design of the most common excitation systems is given. Models of these systems for implementation in simulation programs and for analytical studies are also given.

6.1 Construction of the Excitation System

The main purpose of the excitation system is to feed the field winding of the synchronous machine with direct current so that the main flux in the rotor is generated. Further, the terminal voltage of the synchronous machine is controlled by the excitation system, which also performs a number of protection and control tasks. A schematic picture of a generator with excitation system is depicted in Figure 6.1. Below, a short description of the functions of the different blocks in Figure 6.1 is given:

- **The exciter** supplies the field winding with direct current and thus comprises the “power part” of the excitation system.
- **The controller** treats and amplifies the input signals to a level and form that is suited for the control of the exciter. Input signals are pure control signals as well as functions for stabilizing the exciter system.
- **The voltage measurement and load compensation unit** measures the terminal voltage of the generator and rectifies and filters it. Further, load compensation can be implemented if the voltage in a point apart from the generator terminals, such as in a fictional point inside the generator’s transformer, should be kept constant.
- **The power system stabilizer, PSS**, gives a signal that increases the damping to the controller, cf. Chapter 7. Usual input signals for the PSS are deviations in rotor speed, accelerating power, or voltage frequency.
- **The limiter and protection** can contain a large number of functions that ensure that different physical and thermal limits, which generator and exciter have, are not exceeded. Usual functions are current limiters, over-excitation protection, and under-excitation protection. Many of these ensure that the synchronous machine does not produce or absorb reactive power outside of the limits it is designed for.

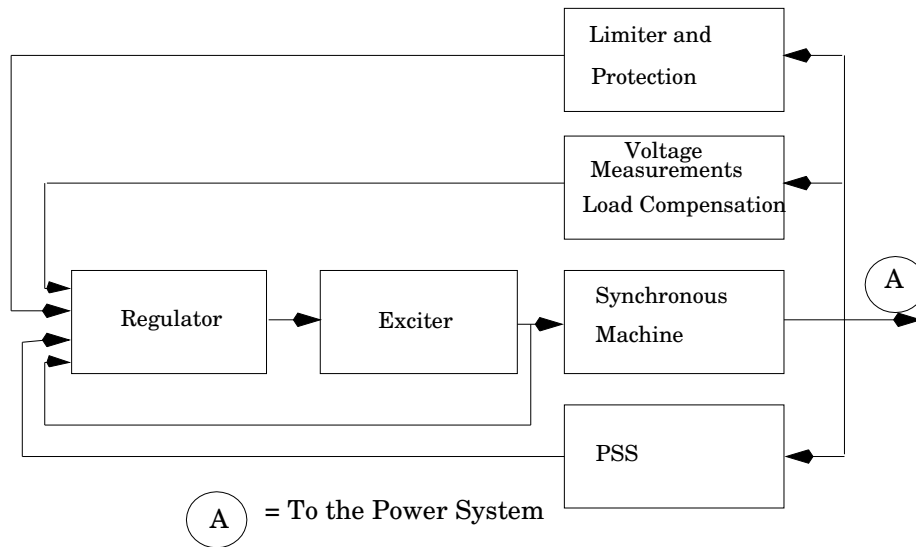


Figure 6.1. Schematic Picture of a Synchronous Machine with Excitation System with Several Control, Protection, and Supervisory Functions.

Today, a large number of different types of exciter systems is used. Three main types can be distinguished:

- **DC excitation system**, where the exciter is a DC generator, often on the same axis as the rotor of the synchronous machine.
- **AC excitation system**, where the exciter is an AC machine with rectifier.
- **Static excitation system**, where the exciting current is fed from a controlled rectifier that gets its power either directly from the generator terminals or from the power plant's auxiliary power system, normally containing batteries. In the latter case, the synchronous machine can be started against an unenergised net, "black start". The batteries are usually charged from the net.

Below, a more comprehensive treatment of some of the functions described above is given.

6.2 Compensation Equipment

Figure 6.2 shows the block diagram of a compensation circuit, consisting of a converter for measured values, a filter, and a comparator.

There are several reasons for the use of compensation in voltage control of synchronous machines. If two or more generators are connected to the

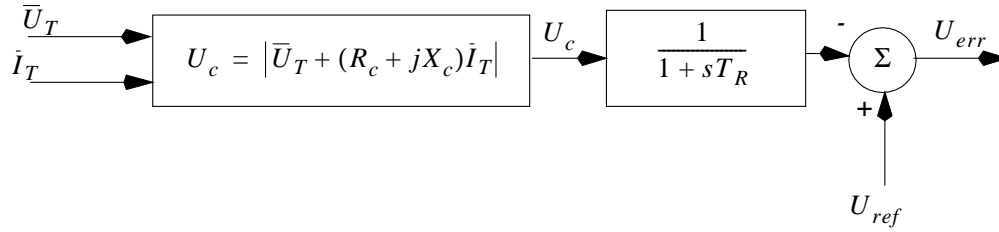


Figure 6.2. Block Diagram for Compensating Circuit.

same bus, the compensation equipment can be used to create an artificial impedance between those. That is necessary to distribute the reactive power in an appropriate way between the machines. The voltage is measured “somewhat inside” the generator, corresponding to positive values of R_c and X_c in Figure 6.2. If a machine is connected with a comparatively large impedance to the system, which usually is the case since the generator’s transformer normally has an impedance in the order of magnitude of 10% on basis of the machine, it can be desirable to compensate a part of this impedance by controlling the voltage “somewhat inside” of that impedance. This then corresponds to negative values of R_c and X_c . As a rule, X_c is much larger than R_c .

6.3 DC Excitation Systems

Today, hardly any DC excitation systems are being installed, but many of these systems are still in operation. Generally, it can be said that there is a large number of variants of the different excitation systems listed above. Every manufacturer uses its own design, and demands that depend on the application often lead to considerable differences in the detailed models of the devices in each group. Here, typical examples for models will be given. In reality, the models given by the manufacturers and power suppliers must be used. One example of a DC excitation system, the IEEE type DC1 system, is given in Figure 6.3. The input signal for the controller is the voltage error U_{err} from the compensation equipment. The stabilizing feedback U_F is subtracted, and sometimes a signal from the PSS is added. Both these signals vanish in steady state. The controller is mainly described by the dominating time constant T_A and the amplification K_A . The limits can represent saturation effects or limitations of the power supply. The time constants T_B and T_C can be used to model internal time constants in the controller. These are often small and can then usually be neglected.

The output signal from the voltage controller, U_R , controls the exciter. The exciter consists of a DC machine that can be excited independently or shunt excited. For shunt excited machines, the parameter K_E models the

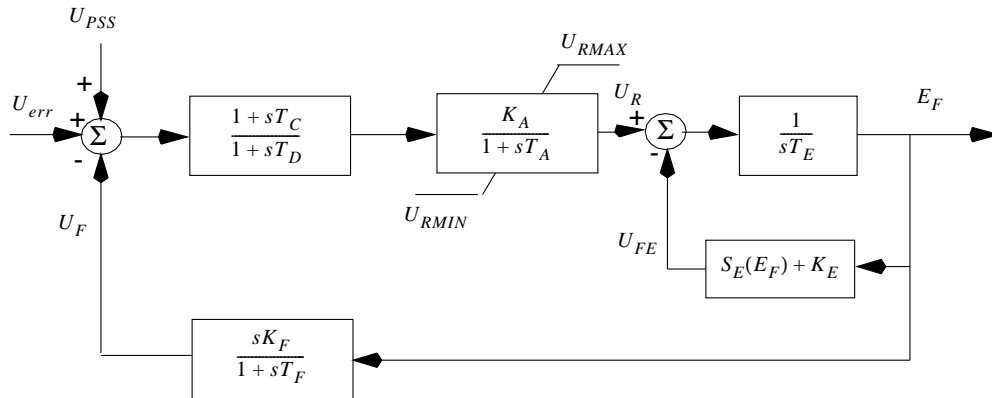


Figure 6.3. Model of DC Exciter System (IEEE Type DC1).

setting of the field regulator. The term S_E represents the saturation of the exciter and is a function of the exciter's output voltage, E_F . If saturation is neglected, that is $S_E = 0$, the effective time constant of the exciter becomes T_E/K_E , and its effective amplification is $1/K_E$.

6.4 AC Excitation Systems

For AC excitation systems, the exciter consists of a smaller synchronous machine that feeds the exciter winding through a rectifier. The output voltage of the exciter is in this case influenced by the loading. To represent these effects, the exciter current is used as an input signal in the model. In Figure 6.4, an example of a model of AC exciter systems is shown (IEEE type AC1). The structure of the model is basically the same as for the DC excitation system. Some functions have been added. The rectifier of the exciter prevents (for most exciters) the exciter current from being negative. The feedback with the constant K_D represents the reduction of the flux caused by a rising field current I_F . That constant depends on the synchronous and transient reactances of the exciter. The voltage drop inside the rectifier is described by the constant K_C , and its characteristic is described by F_{EX} , which is a function of the load current.

DC and AC excitation systems are sometimes called rotating exciters, since they contain rotating machines. That distinguishes them from static excitation systems, which are described in Section 6.5.

6.5 Static Excitation Systems

In static excitation systems, the exciter winding is fed through a transformer and a controlled rectifier. By far most exciter systems installed today are of

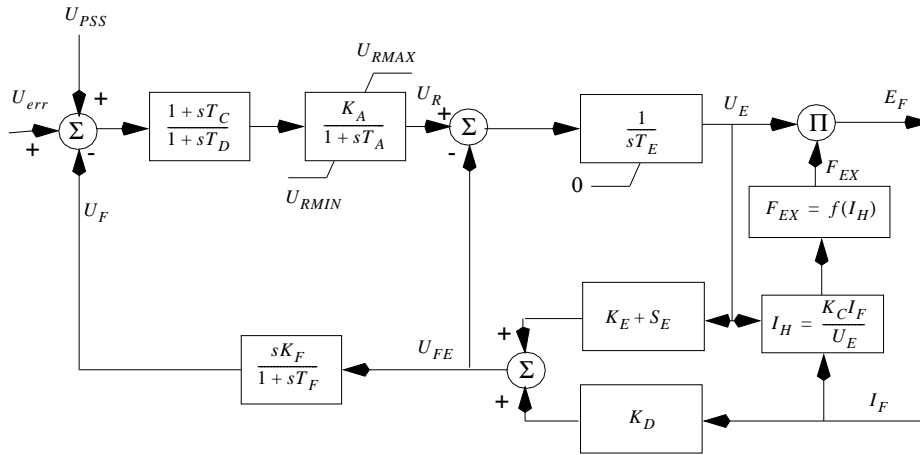


Figure 6.4. Model of an AC Exciter System (IEEE Type AC1).

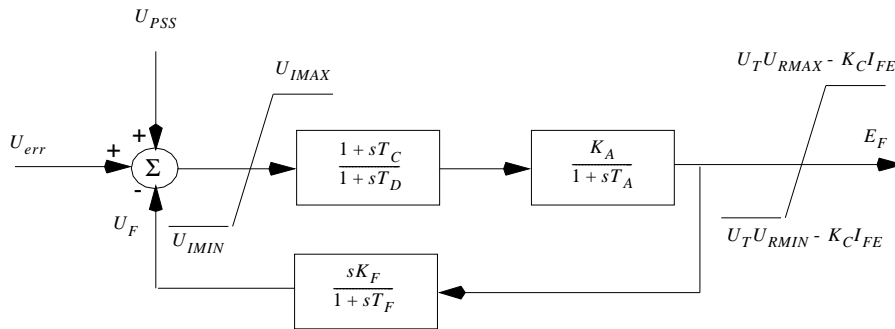


Figure 6.5. Model of a Static Exciter System.

that type, and a large number of variants exists. The primary voltage source can be a voltage transformer that is connected to the generator terminals, but even a combination of voltage and current transformers can be found. With the latter arrangement, an exciter current can be obtained even if the voltage at the generator terminals is low, for example during a ground fault in or near the power plant. Sometimes, it is possible to supplement these voltage sources by using the auxiliary power of the power plant as voltage source. That makes it possible to start the generator in an unenergised net. An example of a model of a static exciter system is shown in Figure 6.5.

Static excitation systems can often deliver negative field voltage and even negative field current. However, the maximum negative field current is usually considerably lower than the maximum positive field current.

The time constants are often so small that a stabilizing feedback is not needed. The constant K_F can then be set to zero. Since the exciter system

is normally supplied directly from the generator bus, the maximum exciter voltage depends on the generator's output voltage (and possibly its current). This is modelled by the dependency of the limitations of the exciter output on the generator's output voltage. The constant K_C represents the relative voltage drop in the rectifier.

7

Damping in Power Systems

In this chapter, a short introduction to damping in a power system is given. Different sources of positive and negative damping are discussed, and methods to improve the damping are given.

7.1 General

What damping in the context of electro–mechanical oscillations in a power system means is quite self–evident. Normally, two different kinds of electrical torques appear at a generator rotor that is oscillating: a synchronizing torque ΔT_s and a damping torque ΔT_d . The synchronizing torque ΔT_s is in phase with the deviation in rotor angle $\Delta\theta$, whereas the damping torque ΔT_d is in phase with the deviation in rotor speed $\Delta\omega$. The synchronizing torque, also called the synchronizing power, strives, if it is positive, to bring the rotor back to the stable equilibrium in which the mechanical power is equal to the electrical power. When the generator has reached an operating point where the synchronizing power no longer can return the system to the stable equilibrium, the generator will fall out of phase. The variation of the synchronizing torque with the rotor angle determines, together with the machine’s moment of inertia the frequency of rotor oscillations. The partitioning into synchronizing and damping torque is shown in Figure 7.1.

Damping is neglected in the classical model. Therefore, the system will, after a disturbance, either fall out of phase (instability) or oscillate with unchanged amplitude. This is not realistic, since real systems contain damping. The damping torque depends on the time derivative of the rotor angle in such a way that the oscillation is damped. Normally, the damping torque is rather small and thus influences the oscillation frequency only marginally. It mainly influences the amplitude. In a synchronous machine, the main contributors to damping are the damper windings and the field winding.

If the modes of oscillation in a system are determined by computing the eigenvalues of the linearised system’s Jacobian matrix, changes in the synchronizing and damping torques will become apparent as follows: An increase of the synchronizing torque moves the eigenvalue parallel to the imaginary axis towards larger values. This corresponds to an increase in the spring constant in a mechanical analogy. If the damping torque is increased instead, the eigenvalue will move parallel to the real axis to the left. In the classical model, all eigenvalues will be situated on the imaginary axis.

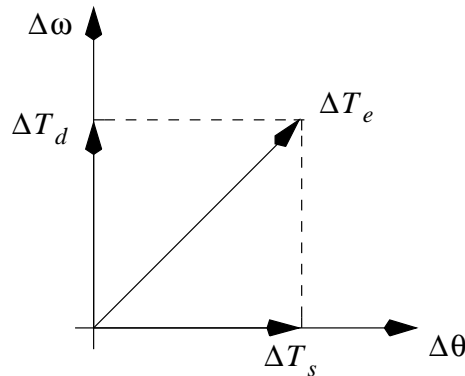


Figure 7.1. Partitioning of Electrical Torque in Synchronizing and Damping Components.

Necessary for stability is that no eigenvalues are situated in the right half plane. This corresponds to positive ΔT_s as well as positive ΔT_d in Figure 7.1.

7.2 Causes of Damping

As mentioned earlier, the internal damping of a generator comes from the windings in the rotor circuit. That damping is determined by phases and amplitudes of the oscillating torques caused by induced currents in exciter winding and damping windings. Further, some loads contribute with positive damping. These contributions originate from the frequency dependency of the loads, but also their voltage dependency contributes.

Generally, the inner damping of the generators decreases with decreasing frequency of the oscillations. The currents in the damping windings decay, and hence, for very slow oscillations, their contribution is small.

Low or negative damping in a power system can lead to spontaneous appearance of large power oscillations. This can, in the worst case, necessitate tripping of lines and it must be avoided. That type of instability is called small signal instability or instability caused by low damping. (Earlier, that type of instability was called dynamic instability.)

A common reason for low damping is the use of voltage controllers with high gain. That was experienced in generators feeding a strong net through a line. Such a configuration can also be analyzed comparably easily. It can be shown that an eigenvalue with positive real part can occur when large amounts of power are transmitted and voltage controllers with high gains are used. Before the reason behind this phenomenon was known, the problem was solved by operating the generator with manual voltage control, or by making the voltage controller slower or decreasing its gain.

To explain that mechanism in detail is beyond the scope of this com-

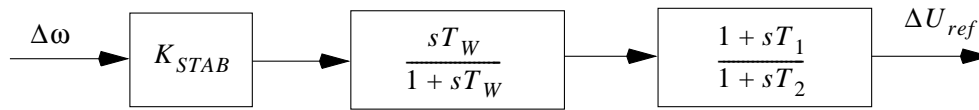


Figure 7.2. Block Diagram of a Simple PSS.

pendium, but in summary, it can be said that the rotor angle influences the generator voltage, which through the voltage controller influences the transient emf, which influences the electrical torque. Now it turns out that, when the load on the machine is high, the phase angle can be such that a contribution with negative damping is obtained. If the amplification in the voltage controller is high, that negative contribution can be significant.

7.3 Methods to Increase Damping

Several methods for increasing the damping in a power system are available. The simplest and usually cheapest way is the installation of power system stabilizers, PSS, in the generators. The operating principle for these is very simple. To increase the damping in the system, a signal is added to the reference voltage of the generator's voltage controller. The phase of this signal should of course be such that it results in a positive contribution to the damping. Thus, the same physical mechanism in the system of generator and voltage controller that above resulted in negative damping is used to obtain positive damping.

Such a power system stabilizer usually utilizes the rotor deviation from the synchronous frequency $\Delta\omega$ as input signal. Sometimes, other signals that contain the same information can be used, like P_e or T_e . A diagram illustrating the principle mode of operation of a PSS is given in Figure 7.2. The input signal, in this case $\Delta\omega$, first passes a high-pass filter to ensure that permanent frequency deviations do not contribute. The next filter shifts the phase appropriately for the critical oscillation frequency so that a positive contribution to damping is obtained. The constant K_{stab} determines the size of that contribution. That constant should of course not be chosen larger than necessary to obtain the needed damping, since this could lead to undesired side effects.

Other possibilities for increasing the damping in a system are different types of controllable equipment that may be installed in the system, such as HVDC (High Voltage Direct Current) or SVC (Static Voltage Condensers). These components can often give large contributions to damping, but they are usually too expensive to install them only to increase the damping, and the existing equipment is not always located optimally for damping purposes.

8

Load Modelling

Since, neglecting losses, an equal amount of power is consumed in the loads in the system as is generated in the generators, the load characteristics are on principle just as important for the system properties as the generators. That is, however, not reflected in the level of detail and the accuracy usually used in load models for analyzing system stability. This chapter discusses briefly how load characteristics influence the system stability and which problems arise in the derivation of appropriate load models. The most common load models are presented.

8.1 The Importance of the Loads for System Stability

The characteristics of the loads influence the system stability and dynamics in many different ways. The voltage characteristics of the loads have a direct influence on the accelerating power for generators nearby and are thus very important for the behaviour during the first oscillation after a fault. It has been shown in section 2.2.1 that the frequency dependency of the loads influences directly how large the frequency deviation after different system disturbances will become. The frequency dependency of the loads also influences the system damping. The same is true for their voltage dependency since it influences the voltage control.

This compendium concentrates on what is usually called angular stability, or synchronous stability, that is, the ability of the generators to stay synchronized after disturbances. Another important property of a power system is the ability to keep the voltages in the system within acceptable limits during disturbances. This is a measure for the voltage stability of the system. Voltage stability is highly dependent on the balance of reactive power in the system, but also the active power has some influence here. It is obvious that the voltage dependency of the loads is of high importance for the system's voltage stability.

It is for several reasons difficult to derive good load models. (Of course, deriving models for single load objects is formally not very difficult. Loads here are, however, lumped loads as they are perceived from a bus in the high voltage grid.) First, it is difficult to estimate the composition of the loads, since it varies during the day as well as during the year. Further, this composition varies from bus to bus. Thus, sometimes different load models have to be used at different buses, depending on the composition of the loads, for example industrial loads, domestic loads, and rural loads.

8.2 Load Models

For studies of angular stability, loads are usually modelled with static models. Sometimes, large induction motors have to be represented individually by special models to obtain the correct dynamic behaviour. Dynamic load models for lumped loads have begun to be used during the last few years, especially for studying voltage stability, but those are expected to be used in the future more widely and even for other types of studies. The frequency dependency is generally modelled according to Section 4.2, page 47.

8.2.1 Static Load Models

For traditional stability studies, where the investigated time frame is at most around 10 s after the disturbance, the most commonly used model types are static models. They are called static since they describe the load using only algebraic equations. The modelled load dynamics are in these cases so fast that they can be considered instantaneous compared with other phenomena, like rotor oscillations, that are modelled. The most common model for voltage dependency is

$$\begin{aligned} P &= P_0 \left(\frac{U}{U_0} \right)^\alpha, \\ Q &= Q_0 \left(\frac{U}{U_0} \right)^\beta. \end{aligned} \tag{8.1}$$

However, the load can also be modelled as an arbitrary polynomial in (U/U_0) ,

$$P = P_0 \sum_i k_i \left(\frac{U}{U_0} \right)^{\alpha_i}. \tag{8.2}$$

In Equations (8.1) and (8.2), U_0 is the nominal voltage at nominal load, P_0 and Q_0 . In Equations (8.1), the voltage exponents α and β are often different.

If $\alpha = 0$, the load is called constant power load; if $\alpha = 1$, it is called constant current load; and if $\alpha = 2$, it is a constant impedance load. It is very common to model the (active) load for stability studies as consisting of these three parts. Usually, a somewhat larger voltage exponent is used for the reactive load.

Some examples for the voltage exponents of different loads are:

Electric heating: $\alpha = 2$, $Q = 0$.

Light bulbs: $\alpha \approx 1, 6$, $Q = 0$.

Fluorescent tubes: $\alpha \approx 0, 9$, $\beta \approx 2$.

To be able to include active and reactive losses in the underlying distribution grid, the above models have to be modified.

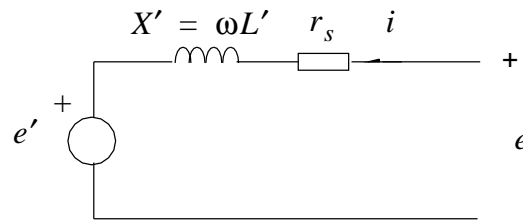


Figure 8.1. Representation of Induction Motor.

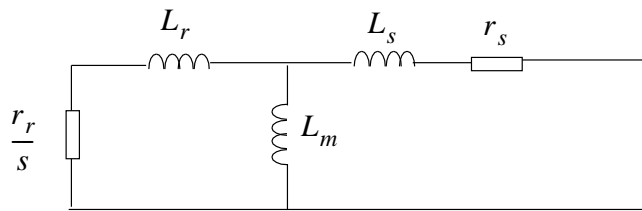


Figure 8.2. Equivalent Circuit for Induction Motor.

8.2.2 Motor Loads

Around half of all electric power used by the industry is used for operation of motors. Sometimes, the load in certain nodes is dominated by electric motors. It can then be justified to model those explicitly.

For small changes in voltage, a motor load behaves approximately like a constant power load. For larger voltage changes, it can be necessary to use a more accurate representation. Synchronous machines are then modelled according to the models derived in Chapter 5, with the mechanical part P_m depending on the characteristic of the mechanical load. A large part of the motor load consists of induction motors that can be modelled as follows: An induction motor is basically a synchronous machine with short-circuited exciter coil. If the exciter coil rotates with an angular speed different from the rotating fluxes generated by the three phase coils, a current that generates a flux is induced in the exciter coil. Between the rotating synchronous flux generated in the phase windings and the flux from the exciter winding, energy is exchanged. This is the basis for the function of the induction motor.

The induction motor can, according to Figure 8.1, be described by a voltage source behind an impedance. The value of L' can be obtained from the equivalent circuit of the induction motor shown in Figure 8.2.

In Figure 8.2

r_s and L_s are the stator resistance and inductance,

L_m is the magnetizing inductance,

r_r and L_r are rotor resistance and inductance.

The slip s is defined by

$$s = \frac{\omega_0 - \omega}{\omega_0} \quad (8.3)$$

and thus L' is given by

$$L' = L_s + \frac{L_m L_r}{L_m + L_r} . \quad (8.4)$$

The dynamics are described by

$$\frac{de'}{dt} = \frac{1}{\tau'_0} (e' - j\omega_0(L_s + L_m - L')i) + j\omega_0 s e' , \quad (8.5)$$

$$i = \frac{e - e'}{r_s + j\omega_0 L'} , \quad (8.6)$$

$$\frac{d\omega}{dt} = \frac{1}{2H_m} (T_e - T_l) , \quad (8.7)$$

$$T_e = \Re(e' \cdot i^*) . \quad (8.8)$$

Here,

ω is the machine's angular speed,

ω_0 is the system's angular speed,

T_l is the load torque,

$\tau'_0 = (L_r + L_m)/r_r$ are no load operation constants.

8.2.3 Equivalent Dynamic Loads

The load models presented above are, as mentioned, valid for studying phenomena that do not last longer than about ten seconds after a disturbance. If phenomena taking place in a longer time frame should be studied, slow dynamics in the system have to be accounted for. These dynamics originate mainly from two different sources: The tap changers installed at lower voltage levels that try to restore the voltage to the desired value and the controllers installed at the loads.

The control of tap changers can be done in several different ways, but common to most systems are that tap changers are stepped, typically in intervals of some tens of seconds, until the voltage is restored. Since this control exists at different voltage levels (cascade coupled controllers), undesirable overshoots in the control can occur if the control loops are not coordinated. Generally, the control has to be slower the lower the voltage level is.

In Sweden, a large part of the load, at least in winter, consists in many areas of heating loads. The changes in this type of load are determined by thermostats. Hence, it takes some time until, for example, a voltage drop

becomes apparent. That time is determined by the thermal time constants for what is heated, such as houses, and by the design of the thermostats.

Summarizing, it can be said that the dynamics determined by tap-changer control and load dynamics are highly complicated. Measurements are needed to get reliable results. Measurements of load characteristics have during the last few years become very important, and much work is being done in many utilities to investigate load characteristics under different loading conditions.

A typical example of a load behaviour after a voltage drop is shown in Figure 8.3. It is clearly visible how the load drops momentarily, as described by the load models from Section 8.2.1, to recover later to a considerably higher level. A rather general description is given by

$$T_p \frac{dP_r}{dt} + P_r = P_s(U) - P_t(U) \quad , \quad (8.9)$$

$$P_l(t) = P_r + P_t(U) \quad , \quad (8.10)$$

where

$P_r(t)$ is a state variable,

$P_s(U)$ is a static model for the long term load behaviour,

$P_t(U)$ is a static model for the transient load behaviour,

$P_l(t)$ is the value of the active load at the time t .

Of course, $U = U(t)$ in the equations above.

For the reactive load, similar behaviour and equations are valid.

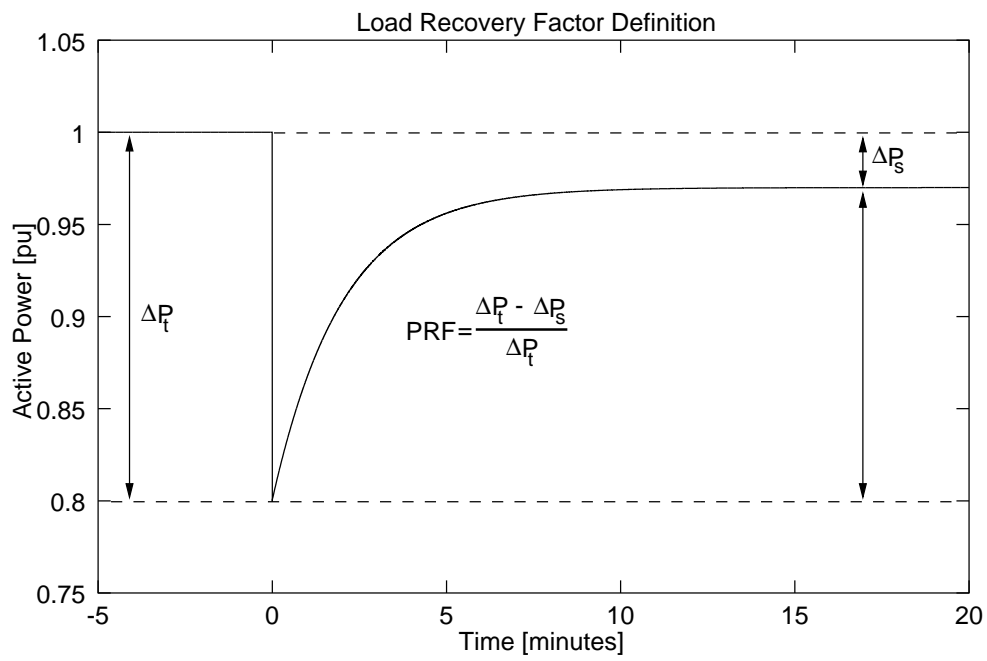


Figure 8.3. The Transient Behaviour of the Load in Equations (8.9) and (8.10) after a Step in the Voltage.

References

- [1] P. Kundur, *Power System Stability and Control*, McGraw-Hill Inc., New York, 1994 (ISBN 0-07-035958-X)
- [2] Dynamic Models for Steam and Hydro Turbines in Power System Studies, *IEEE Trans. Power Appar. Syst.* 1904-1915, Nov./Dec. 1973
- [3] G. Andersson, *Modelling and Analysis of Electric Power Systems*, ETH, 2003
- [4] G. Andersson, *Dynamic Phenomena in Electric Power Systems*, KTH, 2000

Appendix A

Connection between per unit and SI Units for the Swing Equation

If nothing else is given after a quantity, that quantity is in SI-units. If a quantity is expressed in per unit, p.u. is given in brackets after the quantity (p.u.). For simplicity, it is assumed that the nominal electrical and mechanical frequencies are equal, (rad/s).

In SI-units,

$$J \frac{d^2\theta}{dt^2} = \Delta T \quad , \quad (\text{A.1})$$

with

J = moment of inertia for rotor turbine (kgm^2),

θ = angle (rad),

ω = angular velocity (rad/s),

ΔT = effective torque on the rotor turbine (Nm).

When using electrical degrees, Equation (A.1) is usually written as

$$\frac{M}{\omega_0} \cdot \frac{d^2\theta}{dt^2} = \Delta T \quad , \quad (\text{A.2})$$

with

M = moment of inertia = $J\omega_0 \frac{180}{\pi}$ (Js/el°).

The H -factor, or constant of inertia, for synchronous machine i is defined by

$$H_i = \frac{\frac{1}{2}J\omega_0^2}{S_i} \quad , \quad (\text{A.3})$$

with

H_i = constant of inertia for synchronous machine i (s),

S_i = rated power of synchronous machine.

The per unit base for torques at synchronous machine i , $T_{bas,i}$, is given by

$$T_{bas,i} = \frac{S_i}{\omega_0} \quad , \quad (\text{A.4})$$

leading to

$$\Delta T = \Delta T(p.u.) \frac{S_i}{\omega_0} \quad . \quad (\text{A.5})$$

Using (A.3) and (A.5), (A.1) can be written as

$$\frac{2H_i S_i}{\omega_0^2} \cdot \frac{d^2\theta}{dt^2} = \frac{S_i}{\omega_0} \Delta T(p.u.) \quad , \quad (\text{A.6})$$

or

$$\frac{d^2\theta}{dt^2} = \frac{\omega_0}{2H_i} \Delta T(p.u.) . \quad (\text{A.7})$$

Equation (A.7) can also be written as

$$\frac{d}{dt}(\dot{\theta}) = \frac{\omega_0}{2H_i} \Delta T(p.u.) , \quad (\text{A.8})$$

which is the same as

$$\frac{d}{dt}(\omega) = \frac{\omega_0}{2H_i} \Delta T(p.u.) , \quad (\text{A.9})$$

or

$$\frac{d}{dt}(\omega(p.u.)) = \frac{\Delta T(p.u.)}{2H_i} . \quad (\text{A.10})$$

Generally,

$$P = T\omega_m , \quad (\text{A.11})$$

with the actual mechanical angular speed of the rotor ω_m that, according to the assumptions, is equal to the electrical angular speed ω . With the equations above, this gives

$$P(p.u.) = T(p.u.)\omega(p.u.) . \quad (\text{A.12})$$

Equation (A.10) now becomes

$$\dot{\omega}(p.u.) = \frac{\Delta P(p.u.)}{2H_i} \cdot \frac{1}{\omega(p.u.)} . \quad (\text{A.13})$$

For rotor oscillations, $\omega(p.u.) \approx 1$ and (A.13) can be approximated by

$$\dot{\omega}(p.u.) = \frac{\Delta P(p.u.)}{2H_i} , \quad (\text{A.14})$$

or

$$\dot{\omega} = \frac{\omega_0}{2H_i} \Delta P(p.u.) . \quad (\text{A.15})$$

The most common equations in literature are (A.9), (A.10), (A.14), and (A.15). Of these, (A.9) and (A.10) are exact if ω is the actual angular frequency. Equations (A.14) and (A.15) are good approximations as long as $\omega \approx \omega_0$. That is valid for “normal” oscillations in power systems.

Appendix B

Influence of Rotor Oscillations on the Curve Shape

If the relative movement between the field winding of a synchronous machine and its phase windings is a purely rotating motion with constant angular speed, the resulting induced voltages in the phase windings will be shaped ideally like a sinusoid. From now on, it is assumed that the field winding is in the rotor, while the phase windings are on the stator, but since the relative motion determines the voltage in the phase windings, it is even possible to think of stationary field windings and rotating phase windings. In all modern larger synchronous machines, the field winding is on the rotor, so the assumption above does have a practical background. However, almost all relationships and conclusions are independent of this assumption.

For simplicity, consider a single phase synchronous machine according to Figure B.1. A three phase machine has two more phase windings shifted $\pm 120^\circ$ relative to the phase winding in the figure. The phase winding and the exciter winding are arranged so that the flux linkage through the phase winding is sinusoidally shaped as a function of the angle θ_m in Figure B.1:

$$\Phi(t) = \Phi_0 \cos \theta_m = \Phi_0 \cos \omega_0 t \quad , \quad (\text{B.1})$$

with the angular speed of the rotor ω_0 according to the system's electrical frequency. That flux induces a voltage in the phase winding that is given by

$$U(t) = \frac{d\Phi}{dt} = -\Phi_0 \omega_0 \sin \omega_0 t = -\hat{U} \sin \omega_0 t \quad . \quad (\text{B.2})$$

Now, we shall study how the flux linkage through the phase windings will be influenced when rotor oscillations appear in the system. If the balance between power into the generator and power from the generator, i.e. between mechanical torque and electrical power, is disturbed, the rotor will start to oscillate relative to an undisturbed reference rotor that continues to rotate with the angular speed ω_0 . The rotor position can generally be described by

$$\theta_m(t) = \omega_0 t + \theta(t) \quad , \quad (\text{B.3})$$

where $\theta(t)$ is a solution of the swing equation. It has earlier been mentioned that stable solutions of the swing equation for a synchronous machine connected to a strong grid consist of oscillations that are nearly sinusoidal with frequencies on the order of magnitude of some tenths of a Hertz to some

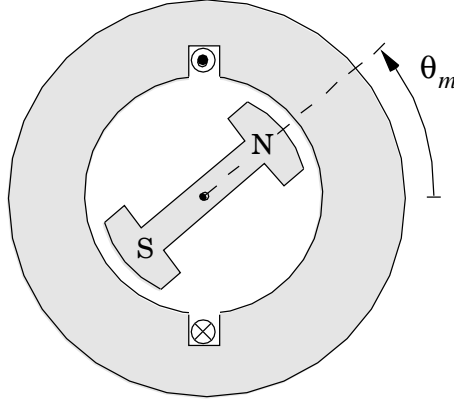


Figure B.1. Schematic Picture of Single Phase Synchronous Machine.

Hertz. To investigate how the linked flux, and thus the voltage and the current, look during an oscillatory movement, a rotor motion according to

$$\theta_m(t) = \omega_0 t + \mu \sin(\omega_r t + \theta_r) , \quad (\text{B.4})$$

with the angular speed ω_r corresponding to the oscillation frequency and the amplitude of the oscillatory movement μ , is assumed. The flux linkage can now be written as

$$\Phi(t) = \Phi_0 \cos \theta_m(t) = \Phi_0 \cos(\omega_0 t + \mu \sin(\omega_r t + \theta_r)) , \quad (\text{B.5})$$

which implies that the oscillatory movement contains a phase-angle modulation of the flux linkage. The momentary angular frequency, $\Omega(t)$, is defined for $\Psi(t)$ as

$$\Omega(t) = \frac{d}{dt}(\omega_0 t + \mu \sin(\omega_r t + \theta_r)) \quad (\text{B.6})$$

and varies between $\omega_0 + \mu\omega_r$ and $\omega_0 - \mu\omega_r$. It can be shown (cf. text books on modulation theory) that Equation (B.5) can be written as

$$\Phi(t) = \Phi_0 \sum_{n=-\infty}^{n=\infty} J_n(\mu) \cos((\omega_0 + n\omega_r)t + n\theta_r) . \quad (\text{B.7})$$

$J_n(\mu)$ is a Bessel function of the first kind with the argument μ and degree n , as given by

$$J_n(\mu) = \frac{1}{\pi} \int_{-\pi}^{\pi} \cos(\mu \sin x - nx) dx . \quad (\text{B.8})$$

An important property of $J_n(\mu)$ that will be used later is

$$J_{-n}(\mu) = (-1)^n J_n(\mu) . \quad (\text{B.9})$$

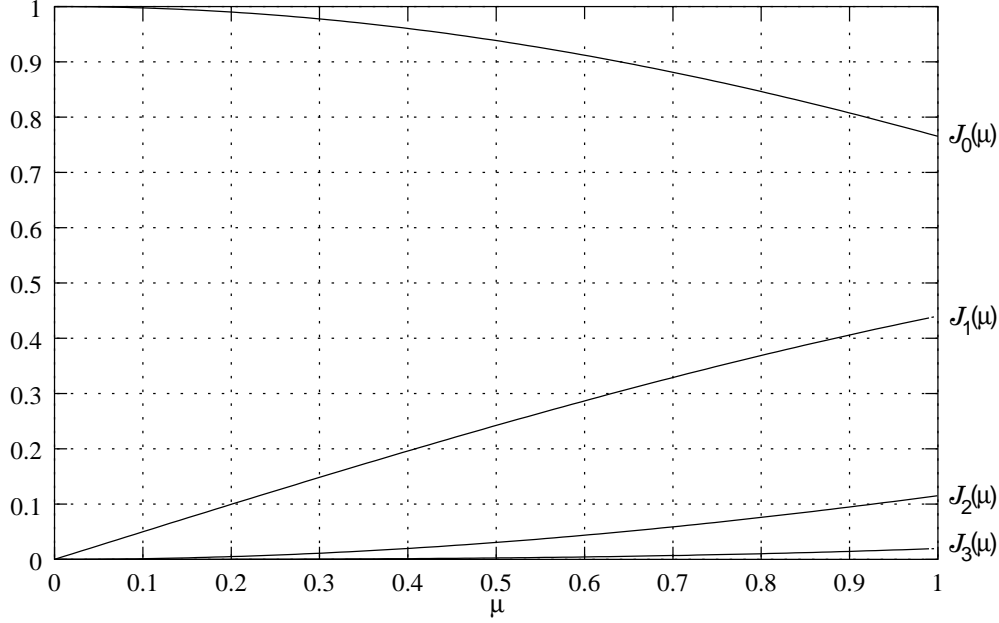


Figure B.2. Bessel Functions of the First Kind of Order 0 to 3.

From Equation (B.7) follows that, in spite of that the momentary angular frequency for $\Phi(t)$ is between $\omega_0 + \mu\omega_r$ and $\omega_0 - \mu\omega_r$, $\Phi(t)$ will have infinitely many side bands with the frequencies $\omega_0 \pm n\omega_r$ beside the fundamental frequency ω_0 . A relevant question is how large the amplitude of these side bands is. Generally, the coefficients $J_n(\mu)$ decay rapidly when the order n becomes larger than the argument μ . In Figure B.2, values for the first four Bessel functions are shown for the argument μ between 0 and 1. It should be observed that μ is measured in radians, so that 1 corresponds to approximately 57° , which in this context is quite a large amplitude. Figure B.2 shows that side bands with $n = 3$ and larger can be neglected even for amplitudes as large as $\mu = 1$. $\Phi(t)$ can thus be approximated quite accurately by

$$\Phi(t) \approx \Phi_0 \sum_{n=-2}^{n=2} J_n(\mu) \cos((\omega_0 + n\omega_r)t + n\theta_r) . \quad (\text{B.10})$$

Typical oscillation frequencies are, in most cases considerably, lower than 3 Hz, so that practically the whole energy spectrum for $\Phi(t)$ lies in the frequency area $f_0 \pm 6$ Hz, i.e. $50(60) \pm 6$ Hz. This justifies the usual representation of the grid with the traditional phasor model with a constant frequency corresponding to f_0 .

If the amplitude is very small, say less than $\mu \approx 0.2$, corresponding to an amplitude of approximately 10° , side bands with $n = 2$ and higher can

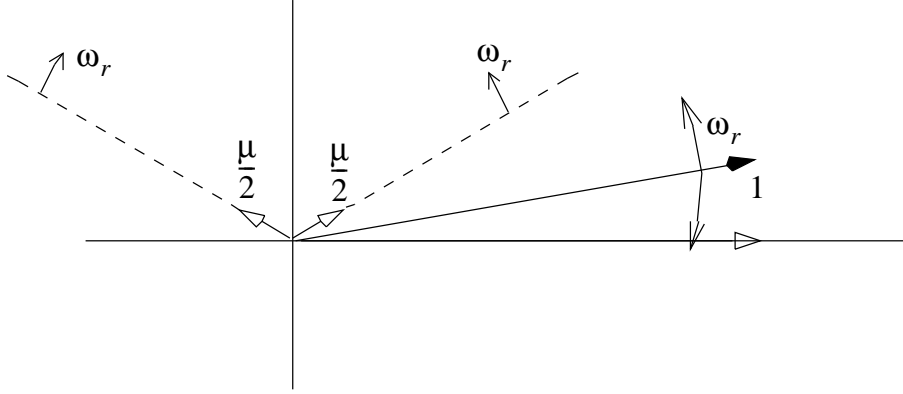


Figure B.3. Vector with Superimposed Oscillation, According to the Text.

be neglected, see Figure B.2. Further, it can be shown that, if μ is small,

$$J_0(\mu) \approx 1 - \frac{\mu^2}{4} , \quad (\text{B.11})$$

$$J_1(\mu) \approx \frac{\mu}{2} ,$$

are valid, and $\Phi(t)$ can be written as

$$\Phi(t) \approx \Phi_0 \left(\left(1 - \frac{\mu^2}{4}\right) \cos \omega_0 t + \frac{\mu}{2} \cos((\omega_0 + \omega_r)t + \theta_r) - \frac{\mu}{2} \cos((\omega_0 - \omega_r)t - \theta_r) \right) . \quad (\text{B.12})$$

Equation (B.9) has here been used. That approximation is used even in a context of power system analysis other than rotor oscillations, namely when studying so-called subsynchronous oscillations, SSO. If there is a resonance phenomenon at a subsynchronous frequency it is called subsynchronous resonance, SSR. The most common cause of SSO are torsional oscillations on the axis connecting the turbine(s) and the generator rotor. The frequencies of the natural oscillations on that axis are typically 5 Hz and higher. (For an axis with n distinct “masses”, including generator rotor and, maybe, exciter, there are $n - 1$ different eigenfrequencies.) For the side band in Equation (B.12), i.e. for $\omega_0 \pm \omega_r$, the frequency can deviate significantly from the nominal frequency, so that it is normally not possible to look only at the component with nominal frequency. Since the electrical damping for the lower side band, the subsynchronous frequency, can be negative, due to, for example, series compensation, the partitioning according to Equation (B.12) has to be kept. The damping in the upper side band, the supersynchronous frequency, is almost always positive.

To increase the understanding for the partitioning in Equation (B.12), a more intuitive derivation than the stringent mathematical one using Bessel

functions can be given. Consider a vector with amplitude 1 that performs small oscillations with an angular frequency ω_r and amplitude μ . This can be illustrated geometrically according to Figure B.3. The vector with filled arrowhead oscillates symmetrically around the horizontal axis with the frequency ω_r and the amplitude μ . That vector can now be partitioned into the three vectors with unfilled arrowheads. One vector does not move and lies along the horizontal axis. Two vectors with amplitude $\mu/2$ rotate with the angular frequency $\pm\omega_r$ according to Figure B.3. It is easily observed that the sum of the vectors with hollow arrowhead is at all times equal to the vector with filled arrowhead. Since the vectors rotate with the angular frequency ω_0 with respect to a stationary system, Equation (B.12) is obtained directly from the projection of the vectors on to the horizontal axis, with the modification that the factor for the fundamental frequency is one.